NOVA SCHOOL OF SCIENCE & TECHNOLOGY

DEPARTAMENT OF CONSERVATION AND RESTORATION

LAURA-CASSANDRA VĂLEAN

BSc in Conservation and Restoration

A MULTI-ANALYTICAL CHARACTERISATION OF ILFORD AND KODAK SAMPLE SETS:

CONTRIBUTION TO THE STUDY OF FIBRE-BASED DEVELOPING-OUT-PAPERS

MASTER IN CONSERVATION AND RESTORATION, SPECIALISATION IN CONSERVATION SCIENCE

NOVA University Lisbon

September, 2024

NOVA SCHOOL OF SCIENCE & TECHNOLOGY

DEPARTAMENT OF CONSERVATION AND RESTORATION

A MULTI-ANALYTICAL CHARACTERISATION OF ILFORD AND KODAK SAMPLE SETS:

CONTRIBUTION TO THE STUDY OF FIBRE-BASED DEVELOPING-OUT-PAPERS

LAURA-CASSANDRA VĂLEAN

BSc in Conservation and Restoration

Adviser: Doctor Élia Catarina Tavares Costa Roldão
Assistant Professor, NOVA University Lisbon

Co-advisers: Doctor Sílvia Oliveira Sequeira
Paper Conservator, Laboratório José de Figueiredo and Museus e Monumentos de Portugal

Doctor Susana França de Sá
Assistant Professor, NOVA University Lisbon

Examination Committee:

Chair: Doctor Joana Lia Ferreira
Assistant Professor, NOVA University Lisbon

Member: Doctor William Wei,
Senior Conservation Scientist

Adviser: Doctor Élia Catarina Tavares Costa Roldão
Assistant Professor, NOVA University Lisbon

MASTER IN CONSERVATION AND RESTORATION, SPECIALISATION IN CONSERVATION SCIENCE

NOVA University Lisbon
September, 2024

A Multi-analytical Characterisation of Ilford and Kodak Sample Sets: Contribution to the Study of Fibre-based Developing-out-papers

Copyright © Laura-Cassandra Vălean, NOVA School of Science and Technology, NOVA University Lisbon.

The NOVA School of Science and Technology and the NOVA University Lisbon have the right, perpetual and without geographical boundaries, to file and publish this dissertation through printed copies reproduced on paper or on digital form, or by any other means known or that may be invented, and to disseminate through scientific repositories and admit its copying and distribution for non-commercial, educational or research purposes, as long as credit is given to the author and editor.

To my family

ACKNOWLEDGMENTS

I would like to start by expressing my gratitude to my thesis supervisor, Professor Élia Roldão. From the very first day, researching this topic sparked my curiosity, but working under your guidance truly fuelled my enthusiasm and motivation. Thank you for managing all the problems with patience and kindness, always coming up with new ideas and bringing a smile to my face whenever needed. It was great to have you as my research supervisor and mentor in my journey to becoming a Photo Conservator. I am also immensely grateful to my co-supervisors, for constantly bringing clarity and valuable insights into this research. To Professor Sílvia Oliveira Sequeira, for all the assistance in understanding paper history, production and degradation, and conducting the fibre identification analysis. To Professor Susana Sá, for all the support during the analytical process, prompt feedback and very clear explanations.

To the Department of Conservation and Restauration (DCR) for giving me the opportunity to study here. Over these two years, I have evolved immensely, learning something new every day. I am also thankful for providing all the resources and academic environment necessary to complete this research.

To Professor Márcia Gomes Vilarigues for all the support provided throughout this research and to *projeto PRR RE-C04-i01 e PRR medida 6 - STEAM e Impulso Adulto na UNL* for the equipment used during photo-documentation.

To Dr. Isabel Nogueira from Instituto Superior Técnico, Universidade de Lisboa, for the help in conducting the SEM-EDS analysis.

To Lénia Oliveira Fernandes for sharing here Kodak sample book, an important part of this research, and for always bringing new perspectives and suggestions.

To all my faculty colleagues for welcoming and helping me adjust to the new environment, catching up with all the knowledge I was missing, and sharing so much about Portuguese culture. Special thanks to Raquel Sousa and Carla Garcia for always being there when I needed support and for helping me create many wonderful memories.

Finally, to my family, for raising me with so much love, for all the sacrifices made so I could follow my dreams, and for always being proud of all my little victories.

A photograph is usually looked at – seldom looked into
(Ansel Adams)

ABSTRACT

By understanding the significant role of physical features and chemical composition in the way photographs are admired and conserved, this study highlights the necessity of understanding these elements for accurate dating, authentication, and well-informed conservation decisions.

The present work explores photographic prints' materiality, focusing on fibre-based developing-out-papers (DOPs). This type of photographic paper was mainly commercially produced throughout the 20th century. Its complex structure consists of multiple layers containing organic and inorganic matter. By using different materials and following various manufacturing techniques, the producing companies were able to obtain papers with a wide range of base tints, surface features, thicknesses, and gelatine emulsions with different light sensitivities, image tones, speeds, and tonal ranges. In this sense, commercial sample sets of already printed photographic papers represent valuable research materials. They were distributed by the manufacturers at the time to professional photographers and amateurs to show the range of papers available.

The complexities of DOPs are addressed through the multi-analytical characterisation of three sample sets: two from Ilford, produced around 1950, and one from the U.S. company Kodak, dating to 1972. By doing so, the study aims to complement the knowledge on fibre-based DOPs, by bringing new information about European manufacturing of photographic paper, specifically the one produced by Ilford.

To achieve this goal, the present research began by examining the main steps in production. This initial phase uncovered important details about print compositions, which helped in interpreting the analysis results.

Prior to prints' analysis, a survey of recurrent analytical techniques used for DOPs' characterization was conducted in order to establish an effective methodology. Emphasizing non-invasive techniques applicable to artworks, this study includes methods like photo-documentation, microscopy, thickness and weight measurements, colourimetry, micro energy dispersive X-ray fluorescence (μ–EDXRF), external reflection Fourier transform infrared (ER-FTIR), and Raman spectroscopies. These techniques allow for a detailed examination of surface characteristics, stratigraphy, and chemical composition. The study also includes sampling techniques for fibre and pulp identification and scanning electron microscopy

with energy dispersive spectroscopy (SEM-EDS) analysis to deepen understanding of papers' stratigraphy and elemental attribution for each layer. This comprehen-sive analysis offered valuable information to support conservation decision-making and historical understanding of fibre-based DOPs.

Keywords: fibre-based DOPs, photographic paper manufacturing, XRF, SEM-EDS, Raman spectroscopy, ER-FTIR.

RESUMO

Ao compreender o papel significativo das características físicas e da composição química na forma como as fotografias são admiradas e conservadas, este estudo realça a necessidade de compreender estes elementos para uma datação exata, autenticação e decisões de conservação bem informadas.

O presente trabalho explora a materialidade das impressões fotográficas, centrando-se nos papéis de revelação à base de fibras (DOPs). Este tipo de papel fotográfico foi maioritariamente produzido comercialmente ao longo do século XX. A sua estrutura complexa é constituída por várias camadas contendo matéria orgânica e inorgânica. Utilizando diferentes materiais e seguindo várias técnicas de fabrico, as empresas produtoras conseguiram obter papéis com uma vasta gama de tonalidades de base, caraterísticas de superfície, espessuras e emulsões de gelatina com diferentes sensibilidades à luz, tons de imagem, velocidades e gamas tonais. Neste sentido, os conjuntos de amostras comerciais de papéis fotográficos já impressos representam valiosos materiais de investigação. Foram distribuídos pelos fabricantes da altura a fotógrafos profissionais e amadores para mostrar a gama de papéis disponíveis.

As complexidades dos DOPs são abordadas através da caraterização multi-analítica de três conjuntos de amostras: dois da Ilford, produzidos por volta de 1950, e um da empresa americana Kodak, datado de 1972. Ao fazê-lo, o estudo pretende complementar o conhecimento sobre os DOPs à base de fibras, trazendo novas informações sobre o fabrico europeu de papel fotográfico, especificamente o produzido pela Ilford.

Para atingir este objetivo, a investigação começou por compreender os principais passos da produção. Durante esta fase, foram descobertos pormenores importantes sobre a composição das impressões, o que facilitou a compreensão dos resultados da análise.

Antes da análise dos prints, foi efetuado um levantamento das técnicas analíticas recorrentes utilizadas para a caraterização dos DOP, de modo a estabelecer uma metodologia eficaz. Enfatizando técnicas não invasivas aplicáveis a obras de arte, o estudo inclui métodos como a foto-documentação, microscopia, medições de espessura e peso, colorimetria, fluorescência de raios X (XRF), espetroscopia de infravermelhos com transformada de Fourier de reflexão externa (ER-FTIR) e Raman. Estas técnicas permitem um exame porme-norizado das caraterísticas da superfície, da estratigrafia e da composição química. O estudo inclui também técnicas de amostragem para identificação de fibras e pasta e análise por

microscopia eletrónica de varrimento com espetroscopia de energia dispersiva (SEM-EDS) para aprofundar a compreensão da estratigrafia dos papéis e a atribuição elementar de cada camada. Esta análise abrangente forneceu informações valiosas para apoiar a tomada de decisões de conservação e a compreensão histórica dos DOP à base de fibras.

Palavras chave: DOPs à base de fibras, fabrico de papel fotográfico, XRF, SEM-EDS, espetroscopia Raman, ER-FTIR.

CONTENTS

1 INTRODUCTION 1

1.1 Research aims and outline 1

2 STATE OF THE ART 3

2.1 Fibre-based DOP 3

2.1.1 General aspects 3

2.1.2 Manufacturing process 4

2.2 Implications of DOPs' composition in Photography Conservation – current challenges and preservation issues 10

2.3 Analytical techniques used for fibre-based DOPs characterisation 11

2.3.1 Studies on reference DOPs and sample sets 11

2.3.2 Visual features characterisation (surface, colour, thickness and weight) 12

2.3.3 Stratigraphy and material composition 13

3 METHODOLOGY 15

3.1 Case studies 15

3.1.1 Sets format 15

3.1.2 Samples characteristics 18

3.1.3 The values of the sets 22

3.1.4 Multi-analytical characterisation 23

4 RESULTS AND DISCUSSIONS 25

4.1 Visual characteristics: base tint, surface features, thickness and weight 25

4.1.1 Base tint characterisation 25

4.1.2 Surface features 29

4.1.3 Thickness and weight measurements 33
4.2 UV-induced visible fluorescence: photo-documentation and microscopy 35
4.3 Stratigraphy and material composition: elemental and molecular approaches 38
4.3.1 Fibre and pulp identification 38
4.3.2 μ–EDXRF 40
4.3.3 SEM-EDS 43
4.3.4 Raman 46
4.3.5 ER-FTIR 47
4.4 Composition implications in the conservation of the case studies 56
4.5 Methodology proposal for material composition identification: advantages and disadvantages 56
5 CONCLUSIONS 59
BIBLIOGRAPHY 61
A METHODOLOGY 67
A.1 Details about the case studies 67
A.2 Methodology 69
B RESULTS 74
B.1 SEM-EDS – elemental composition by layer 74
B.2 Analysis summary tables 76
B.3 UV-induced visible fluorescence - verso 90

LIST OF FIGURES

Figure 2.1 Schematic cross-section of a typical baryta-coated, fibre-based DOP (© Laura-Cassandra Vălean)....4
Figure 2.2 The timeline of pulps used for the photographs' paper support throughout the 20th century, created to illustrate the results of the study described in [1] (© Laura-Cassandra Vălean)....5
Figure 2.3 Stages in Ilford paper production process: (a) *Mr Don Smith, in the Cassio plant, between the coating head and drying unit of one baryta coating machines, c.1965* [15]; (b) Emulsion coating of photographic paper at Ilford [21]....7
Figure 3.1 Small format Ilford set....16
Figure 3.2 Medium format Ilford set: (a) cover; (b) open to one sample....17
Figure 3.3 The handwritten note found in the back of IM....17
Figure 3.4 Detail from *Ilford News*, no.4....17
Figure 3.5 Kodak sample set: (a) cover; (b) paper samples....18
Figure 3.6 Alphanumeric code of the sample sets: (a) IS; (b) IM; (c) Kodak....21
Figure 4.1 Differences in base tints between the Ilford and Kodak papers....26
Figure 4.2 Three-dimensional representation of the papers L*a*b* values front and back....27
Figure 4.3 Difference between the front and back colour (ΔE value)....28
Figure 4.4 Microphotographs of the papers texture in raking light....29
Figure 4.5 Microphotographs with the texture of *Ektalure K, Portalure G, and Ektalure E* papers – from the current study (top), and *Paperbase* (bottom)....29
Figure 4.6 Microphotographs with the texture of Ilford *Matt* papers....30
Figure 4.7 Close-up details in axial specular light from IM: (a) a glossy print (*Contact C.2. 1P Glossy*); (b) a semi reflective print (*Plastika P.2.K Cream Semi Matt*); and (c) a matte print (*Bromide B.2.25 K Cream Matt*)....30
Figure 4.8 Close-up details in axial specular light from the Kodak samples with smooth texture and different sheen: (a) glossy (*Polycontrast F*), two semi reflective prints – (b) high lustre (*Medalist J*); (c) lustre (*Kodabromide A*), and (d) a matte print (*Portalure M*)....30
Figure 4.9 Glossiness characterisation through colourimetric measurements (ΔL*SCI-SCE)..31

Figure 4.10 Difference between ΔL*SCI-SCE values and gloss units from *Paperbase* for IS and Kodak sets 32
Figure 4.11 Thickness and weight measurements results 34
Figure 4.12 UV-induced visible fluorescence: (a)*IS_Bromide B.2. 5K Matt*; (b)*IS_Bromide B.2. 55K Cream Matt*; (c) *IS_Plastika T.2.K Cream Grained Half Matt*; (d) *IS_Contact C.2.25P Satin* 35
Figure 4.13 UV-induced visible fluorescence: (a)*IM_Bromide B.2. 5K Matt*; (b)*IM_Bromide B.2. 55K Cream Matt*; (c) *IM_Plastika F.2.K Grained Half Matt*; (d) *IM_Contact C.2.25P Satin* 35
Figure 4.14 UV-induced visible fluorescence: verso of (a)*IM_Bromide B.2. 5K Matt*; (b)*IM_Bromide B.2. 55K Cream Matt*; (c) *IM_Plastika F.2.K Grained Half Matt*; (d) *IM_Contact C.2.25P Satin* 36
Figure 4.15 UV-induced visible fluorescence: *IM_Bromide B.2. 23 P Light Weigh Lustre*, recto (a), and verso (b) 36
Figure 4.16 UV-induced visible fluorescence: Kodak samples (a); *Polycontrast F:* recto (b), verso (c), and microphotograph of the paper support (d) 37
Figure 4.17 UV-induced visible fluorescence: verso of *Medalist J* sample (a) and of *Ektalure X* (b) 38
Figure 4.18 Herzberg Stain on *Mural R* (200x); a possible vessel or vascular tracheid identified. 38
Figure 4.19 μ–EDXRF Spectra of *IS_Plastika B.2.K Matt*: recto (D_{max}) and verso 40
Figure 4.20 μ–EDXRF Spectra of *IM_Plastika V.2.K Cream Rayon*: recto (D_{max}) and verso 40
Figure 4.21 μ–EDXRF Spectra of *IM_Bromide B.2.23 P Light Weight Lustre:* recto (D_{max}) and verso 41
Figure 4.22 μ–EDXRF Spectra of particles identified on the back of *IM_Plastika D.2 K Semi Matt* and *IM_Plastika T.2 K Cream Grained Half Matt* 41
Figure 4.23 μ–EDXRF Spectra of *Portalure M*: recto (D_{max}) and verso 42
Figure 4.24 μ–EDXRF Spectra of *Kodabromide A*: recto (D_{max}) and verso 42
Figure 4.25 SEM-EDS cross-section of print *IM_Bromide B.2.23 P Light Weight Lustre* (a), *Kodabromide A* (b), and *Mural R* (c) 43
Figure 4.26 SEM-EDS cross-sections: variations of the baryta layer SEM-EDS cross-section of print *IS_Bromide B.2. 5K Matt* (a); *IM_Bromide B.2. 55K Cream Matt* (b); *Portalure M* (c) 44
Figure 4.27 SEM-EDS cross-sections: variations of the baryta layer 44
Figure 4.28 SEM-EDS cross-section of print *IM_Bromide B.2. 5K Matt* and *IS_Plastika R.2.K Cream Matt* 45
Figure 4.29 Raman spectrum of the yellow particle - *IS_Plastika V.2.K Cream Rayon* (paper support) 46
Figure 4.30 Raman spectrum of the *IM_Bromide B.2.23.K Light Weight Lustre* (paper support) 47
Figure 4.31 ER-FTIR spectrum of *IS_Bromide B.2.1.P Glossy* and gelatine ER-FTIR reference spectrum 48
Figure 4.32 ER-FTIR spectra of *IM_Bromide B.2.35 K Rayon* for D_{max}, D_{mid}, and D_{min} analysis . 49

Figure 4.33 ER-FTIR spectra (D_{mid}) of IM papers with different surface features 49
Figure 4.34 ER-FTIR spectra (D_{mid}) of Kodak papers with different surface features 50
Figure 4.35 ER-FTIR spectra of samples without the baryta coating 50

Figure A. 1 IM set: (a) Index page, and (b) the notes found in the back. 67
Figure A. 2 *Ilford Manual of Photography* (1945) – Details about papers' features 68
Figure A. 3 Illumination setup for (a) normal, ranking and axial specular; (b) UV-induced visible fluorescence 69
Figure A. 4 Illumination setup for raking light photo-documentation of the texture under the microscope 70
Figure A. 5 Thickness (a) and weight (b) measurements setups 71

Figure B. 1 SEM-EDS elemental composition by layer for *IM_Bromide B.2.23 P Light Weight Lustre* 74
Figure B. 2 SEM-EDS elemental composition by layer for *Kodabromide A* 75
Figure B. 3 SEM-EDS elemental composition by layer for *IM_Plastika P.2.K Cream Semi Matt* 75
Figure B. 4 SEM-EDS elemental composition by layer for *Portralure M* 75
Figure B. 5 UV-induced visible fluorescence photo-documentation of prints' verso 90

LIST OF TABLES

Table 2.1 . Kodak papers' texture – description and main production steps; table produced based on [9] 9
Table 3.1 Differences between *Bromide, Plastika* and *Contact* papers [64] 19
Table 3.2 Features of the Kodak samples [67] 19
Table 3.3 Multi-analytical characterisation: sequence, goals and samples analysed 24
Table 4.1 Results for fibre identification microchemical tests 39
Table 4.2 Elements identified with μEDXRF 42
Table 4.3 Bands attribution for the yellow particle Raman spectrum - *IS_Plastika V.2.K Cream Rayon* (paper support) 46
Table 4.4 Bands attribution in the Raman spectrum of *IM_Bromide B.2.23.K Light Weight Lustre* (paper support) 47
Table 4.5 Bands attribution in the ER-FTIR spectrum of *IS_Bromide B.2.1 P Glossy* 48
Table 4.6 Summary of the multi-analytical characterisation of the sample sets 51
Table 4.7 Advantages and disadvantages of the methodology used. 56

Table A. 1 Surfaces available in the Kodak set with their description from the *Dataguide* [67] 68
Table A. 2 Illumination setup and camera settings 69

Table B. 1 Multi-analytical characterisation results of small-format Ilford set (IS) 76
Table B. 2 Multi-analytical characterisation results of the medium-format Ilford set (IM) 81
Table B. 3 Multi-analytical characterisation results of the Kodak set 87

ACRONYMS AND SYMBOLS

ATR	Attenuated total reflection
DOP	Developing-out-paper
EDS	Energy Dispersive Spectroscopy
ER	External Reflection
FTIR	Fourier Transform Infrared Spectroscopy
MoMA	Museum of Modern Art in New York
OBA	Optical brightening agent
PCA	Principal component analysis
POP	Printing-out-paper
RC	Resin-coated
RH	Relative humidity
SCE	Specular Component Excluded
SCI	Specular Component Included
SEM	Scanning electron microscope
UV	Ultra Violet
XRF	X-Ray Fluorescence

δ	Bending vibrations
μ	Micro
ν	Stretching vibrations

1

INTRODUCTION

1.1 Research aims and outline

With the transition from analogue to digital photography, the emphasis has increasingly been placed on the images themselves, often overlooking photographs' materiality. The materials, structure, and surface characteristics of photographic prints are essential to how we perceive and experience them. This aspect is representative of photographers' and printers' preferences and illustrates which materials were available or popular in specific periods and geographic regions [1]. This context emphasizes Barbara Savedoff's observation: *[…] photographs do multiply the object's image, but they are not multipliable objects* [2].

Photographs' materiality is significant not only for aesthetic reasons but also for their preservation. Understanding the prints' composition enables conservators to better predict degradation processes and select suitable conservation treatments, packaging, housing, and environmental conditions for storage and display. Identifying the type of printing process and photographic paper is also essential for dating and authenticating prints and artworks [1]. Therefore, understanding photographs' materiality is critical in the conservation decision-making process and the curatorial and connoisseurship fields.

Photographic papers are complex objects composed of multiple layers with both organic and inorganic matter in their composition. Their diversity is influenced by the type of photographic process they were made for, the manufacturing company and the production period [1]. In this sense, fibre-based developing-out-papers (DOP) represent a particularly intricate topic. They were almost entirely commercially produced in the 20th century, a time marked by numerous technological advancements, and frequent changes in manufacturing recipes. The exact composition of these papers is often difficult to locate in companies' archives, and their analysis is further complicated by their stratigraphy [3].

For this reason, researchers can gain a deeper understanding of papers' composition, stratigraphy, and surface features, by analysing reference papers or sample sets of photographic papers where the manufacturing company and types are clearly identified. Both reference papers and sample sets are valuable, yet rare resources. The manufacturers distributed sample sets at the time to professional photographers and amateurs to show the papers

available. Therefore, they offer a wider range of papers and reflect better the desired aesthetic, as the manufacturer printed them to demonstrate optimal results. They also provide insights into how papers degrade over time. However, because they are printed, sampling and analysis can be more challenging, and their original colour and surface features might be altered by time, complicating the comparison with other papers of the same type.

While this subject has been extensively explored in U.S. studies – mostly Kodak's manufacturing process and reference papers' characteristics – there remains a significant knowledge gap concerning European photographic papers [1]. To date, only one major study is focusing mainly on European photographic materials, in this case the ones produced by the Belgian-German company Agfa-Gevaert [4]. Additionally, the consulted studies often employ different methodologies, either focusing on visual characteristics or on the material composition.

In response to these gaps, the present study aims to advance our understanding of European photographic papers, specifically those produced by the British company Ilford in the mid-20th century. A multi-analytical characterization was conducted on three sample sets: two from Ilford, produced around 1950, and one from the U.S. company Kodak, dating from 1972. This analysis aims to identify the differences in papers due to production time, manufacturer, and geographic region, correlating the visual features of the papers with their stratigraphy and composition.

The first objective of the research was gaining more information on the manufacturing process of fibre-based DOPs and reviewing the commonly used analytical techniques for their characterization. The study continued with proposing a methodology for documenting the surface features, stratigraphy, and chemical composition of the 54 samples. By establishing a clear methodology and presenting comprehensive results, this research aims to facilitate the future analysis of other photographic papers, extending knowledge and enabling the identification of these papers in artworks. The study places particular emphasis on non-sampling techniques that can be applied to artworks, such as photo-documentation under various conditions, microscopy, thickness and weight measurements, colourimetry, micro energy dispersive X-ray fluorescence (μ–EDXRF) spectrometry, external reflection Fourier transform infrared (ER-FTIR) spectroscopy, and Raman spectroscopy. However, to gain a deeper understanding of the paper support, samples were also collected for fibre and pulp identification tests. Additionally, samples were taken for scanning electron microscopy with energy dispersive spectroscopy (SEM-EDS) to provide a clearer understanding of papers' stratigraphy. While collecting samples for SEM-EDS from photographs is generally not recommended, the information obtained in this study can be correlated with case studies after the type of photographic paper has been identified using a non-sampling technique.

2

STATE OF THE ART

To thoroughly understand the case studies and potential analytical techniques for print characterisation, an extensive literature review was conducted, covering topics like the composition and stratigraphy of fibre-based DOPs, their manufacturing processes, paper production at Ilford and Kodak, conservation issues, studies on reference papers and analytical techniques for photographs characterisation.

For insights on photographic paper manufacturing history at Ilford and Kodak and to accurately date the sample sets, 20th century resources were consulted, including interviews, publications from former employees, company documents, patents, advertisements, and photography journals. These materials were often scarce and challenging to find. In contrast, the literature for DOP characterization was more accessible, comprising articles, volumes, and collection databases focused on photo conservation.

2.1 Fibre-based DOP

2.1.1 General aspects

In the early 20th century, the photographic industry transitioned from printing-out papers (POP) to fibre-based developing-out papers (DOP), requiring only brief light exposure and chemical development. DOPs offered advantages like lower costs, faster processing, no daylight requirement, and consistent image quality [5]. Another significant difference is the image colour, with DOP having a neutral black-to-grey image colour. Technological advancements allowed for more variety in weights, tints, textures, and glossiness, reaching a peak in surfaces availability by the 1930s [6]. Despite the introduction of new products like colour photography and resin-coated papers, fibre-based DOPs are still produced today [7].

The support for fibre-based DOPs is high-quality paper coated with a baryta layer, which consists of barium sulphate ($BaSO_4$) particles suspended in gelatine. On top of it rests the image layer, formed by the gelatine binder and filamentary silver, the final image material being metallic silver (Ag). Filamentary silver particles are composed of intertwined large and

irregular filaments, which absorb the light, hence the DOP's neutral black image colour [8]. Typically, DOPs include a protective topcoat of hardened gelatine over the image layer. The four typical layers of DOPs are illustrated in *Figure 2.1.* However, variations in manufacturing could exist, such as DOPs without a baryta layer.

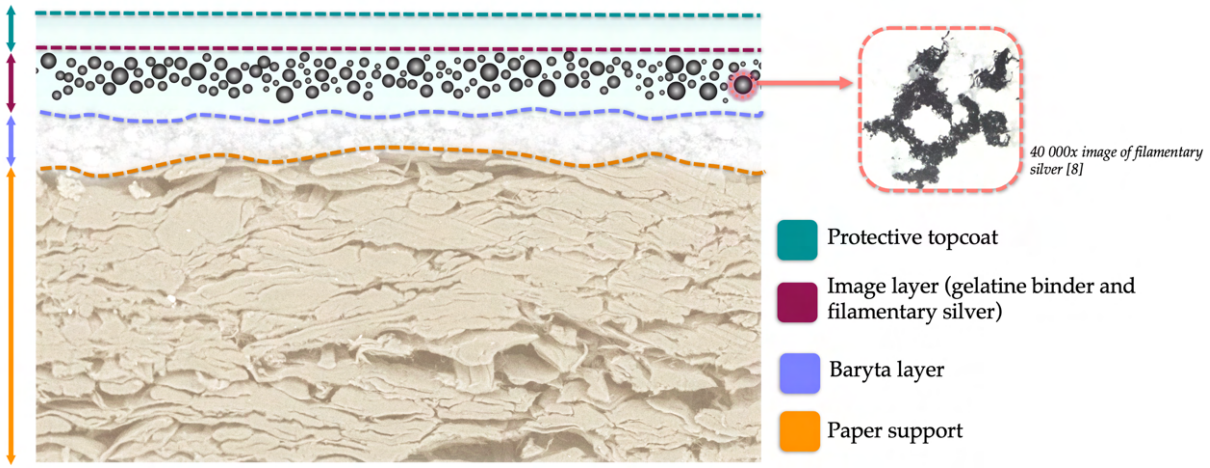

Figure 2.1 Schematic cross-section of a typical baryta-coated, fibre-based DOP (© Laura-Cassandra Vălean)

2.1.2 Manufacturing process

The study of the fibre-based DOPs manufacturing represented a fundamental step in the present research, providing context to understand prints' characteristics, the interpretation of analytical results and the identification of possible deterioration causes.

As fibre-based DOPs were almost entirely commercially produced [3], the competition among the manufacturing companies led them to protect production technologies and recipes. Archival materials that could provide more insights were periodically discarded [9]. 20th century photographic paper production was also marked by numerous changes, considering the multiple technical advancements of the time. These aspects highlight the incomplete information provided by the available resources and the need for complementary analysis conducted on 20th century photographic papers.

Although a detailed analysis of DOP manufacturing over specific timeframes or companies was not possible, general insights were gathered, mainly from former employees' publications. Kit Funderburk's work, later edited by Gawain Weaver [9], includes a description of the main stages in manufacturing, along with some details about changes in materials and technologies over the years and the struggles that came with them. The volume published by two previous Ilford workers [10] focuses mainly on the company's administrative aspects but contains a valuable list of production dates for all of Ilford's photographic materials. Additional resources included an export trade report [11], a two-part interview with a former worker in the photographic paper industry [12, 13], and Maurice Fisher's website [14], which compiles information on Ilford's history, publications and advertisements.

Paper support

The first step in the production was the paper support manufacturing. A strong emphasis was placed on the paper stock's quality, which had to be free of photoactive impurities, have a uniform and highly opaque surface, high wet strength and low chemical solutions absorption, excellent dimensional stability, and uniform moisture content [15]. The paper stock supplier for Ilford was Wiggins Teape & Alex Pirie Ltd. [10, 11, 12]. Initially, Kodak also acquired the paper stock from Europe. However, the shortages during World War I determined Kodak to find local suppliers, leading to trials conducted in 1914 in their new mill. Finding the suitable recipes, the fitting equipment and the process proved challenging. Nonetheless, with time, they got to produce photographic-grade paper support to complement the European supplies [9].

The paper support production started with **stock preparation,** where the pulp fibres were separated in water, beaten and refined. **Chemical addition** followed, where sizing agents, fillers, strength additives, or dyes were introduced into the mixture. The dirt, fibre bundles and other contaminations were removed through the **screening** process. The mixture of fibres, chemical additives, and water went through the **sheet-forming** step, removing water by drainage or suction. The paper web was formed by now and was **wet pressed** through rolls to remove the water further. The paper was then **surface treated** by applying chemicals for sizing and physical properties improvement. This step was followed by additional drying. The dried paper was **calendered**, being pressed through metal rolls that smoothened the surface and reduced the thickness. The web was **reeled** on a large spool and then slitted to the desired width to be **rewound** on a core [9].

With the advancements in production technologies, the types of pulps used have changed throughout the 20th century [16]. This fact was confirmed through a study [1] where over 2000 photographic papers from the 20th century were analysed. A trend was identified, illustrated in *Figure 2.2*. The research indicated that during the beginning of the century, rag pulp was used, but throughout the 1920s, softwood bleached sulphite pulp gradually replaced it. From the last part of the 1950s, the prevalence of the softwood and hardwood bleached sulphite pulp blend increased. In the 1970s bleached hardwood kraft pulp started being used, and mixtures of bleached softwood sulphite with alpha-grade cellulose.

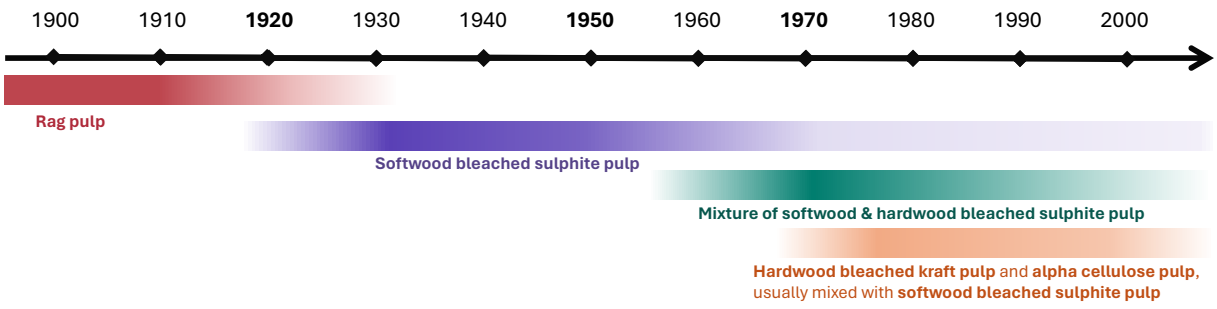

Figure 2.2 The timeline of pulps used for the photographs' paper support throughout the 20th century, created to illustrate the results of the study described in [1] (© Laura-Cassandra Vălean)

Some details were also obtained about the paper supports produced by Kodak. The data shows they started with a mixture of 30% white rags, 20% sulphite wood pulp, and 50% soda wood pulp, as 100% white rags made the paper too curly and absorbent. By 1923, Kodak adjusted the composition to 75% rag and 25% sulphite pulp. The sulphite pulp reduced the cockling problems but produced a dull colour. After 1924, Kodak replaced the 25% sulphite pulp with high-alpha pulp. By 1926, some Kodak papers utilized a mix of 50% pulp and 50% high-alpha pulp. Except for one case, all Kodak paper supports were made with 100% high-alpha pulp by 1931. It is mentioned that towards the end of the 1950s, Kodak used ten different pulps from various wood species, depending on the paper purpose. During the 1960s, small quantities of hardwood and softwood bleached sulphides were replaced by northern hardwood bleached kraft. The recipes varied depending on whether the paper was photographic grade or based on desired characteristics [9]. The Ilford references do not provide any details on this topic.

Regarding sizing, some information about Kodak paper was obtained. For wet-end sizing, where sizing materials are added before the sheet is formed, the traditional material used was rosin, added with aluminium sulphate. This mixture is known to be used around 1927-1928. By 1931, it was replaced entirely by steric acid. Another sizing process was tub-sizing, a surface treatment where the paper was immersed in a bath, typically containing a gelatin solution, and passed through rollers to remove excess and allow gelatin penetration into the fibres. To harden the gelatin, the paper was treated with formaldehyde, which was replaced by chromium chloride after the mid-1930s. During the 1940s, melamine formaldehyde was introduced as a wet-strength agent. After the 1950s, gelatine tub-sizing was gradually replaced by starch tub-sizing. It is also mentioned that during the mid-1960s, dry-strength resins started to be used for tub-sizing [9]. No information was obtained about the sizing treatments for Ilford paper.

The description of paper manufacturing at Kodak lacks details on the fillers used in the support. However, some patents from Wiggins Teape & Alex Pirie Ltd, Ilford's paper supplier, brought some insights into this matter. They mention using kaolinite [$Al_2Si_2O_5(OH)_4$] [17] or titanium dioxide (TiO_2) to make light paper opaquer [18]. It was also mentioned that iso-ascorbic acid crystals were used to overcome the iron contamination of the paper [13].

Baryta coating

The winded raw paper would further undergo the process of baryta coating. This procedure has been done at Kodak since 1900, first undertaken by brush coaters and later, from the mid-1930s, by air knife coaters. Both coaters would apply a uniform layer of baryta that would follow the paper contour. Several layers of baryta could be applied, depending on the desired surface. The binder was gelatine, usually in a 9.6:1 ratio ($BaSO_4$:gelatine), and sometimes 14:1. As hardening material, formaldehyde was used, and after the mid-1930s, chromium chloride [9].

The process began with testing and sorting the delivered paper rolls. The paper was coated with a gelatine layer and afterwards with the baryta emulsion. This was done by

transfer from a roll. The coated paper web was dried through festoon driers and wound into a roll afterwards. Ultimately, the roll went through the calendering process [9]. Ilford, on the other hand, received the paper already coated, this step being done by Cassio Photographic Paper Co. Ltd. [10] (*Figure 2.3.a)*

Emulsion coating

The following step was the emulsion and protective topcoat application. While there are not many insights about it at Kodak [9], the principal steps are described for Ilford production around 1954 [19]. In the first stage, the silver nitrate solutions and soluble halides were added to the gelatine, reacting and forming silver halide and a soluble nitrate. This solution underwent a heat treatment when the silver halide crystals grew to a size and distribution that would determine the final material features. This emulsion was then shredded or cut and washed to eliminate the by-products and reagents. A second heat treatment was conducted when the sensitivity nuclei were formed, and the maximum sensitivity was obtained. Finally, sensitizing dyes, stabilizing reagents, hardeners, and spreaders were added [19]. An interview with a former Ilford worker from around 1944 states that a vertical coating machine was used [20], fact supported by a photograph made around 1934-1939 [21] (*Figure 2.3.b).*

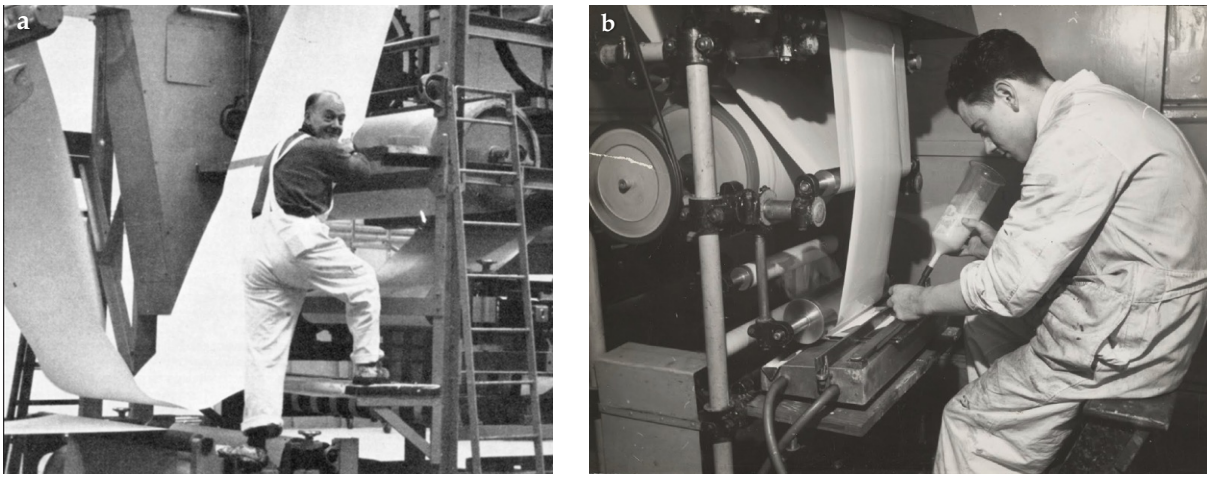

Figure 2.3 Stages in Ilford paper production process: (a) *Mr Don Smith, in the Cassio plant, between the coating head and drying unit of one baryta coating machines, c.1965* [15]; (b) Emulsion coating of photographic paper at Ilford [21]

Features of the DOPs

The manufacturing process could vary depending on the desired characteristics. Papers of different weights and thicknesses could be produced. Pigments or dyes could be added to the paper stock and baryta layer to create various base tints. However, no specific colourants were mentioned [9]. The methods used to increase paper whiteness included pulp bleaching and 'blueing' – adding blue dyes or pigments, like smalt blue or Prussian blue – to counteract the paper's yellowness. However, this last process reduces the amount of emitted light, causing a grey effect. This problem was solved by introducing the optical brightening agents (OBAs) in the photographic paper industry around the 1950s [22].

OBAs are chemical compounds that primarily absorb ultraviolet (UV) radiation and reemit it as visible light. This process enhances the brightness of the substrate, as OBAs can emit more than 100% of the incident visible light [22]. Most manufacturers used brighteners based on the cyclic compound stilbene ($C_6H_5CH{=}CHC_6H_5$) [23]. The OBAs could be integrated into the raw stock, baryta layer, photographic emulsion or processing chemicals [24]. In the case of raw stock, OBAs could be added in the beater, wet-end sizing, tub-sizing, as fillers or coatings [22]. Different fibre types in the pulp have variable degrees of dye absorption [24].

There is no clear evidence of when OBAs were introduced in the photographic industry. A survey on 1159 fibre-based DOP samples, dating from 1896 to 2004, was conducted for OBAs identification [24]. The survey showed that the first occurrence of OBAs was around the early to mid-1950s. Data on Kodak indicates that OBAs were first used only in the late 1950s [9]. However, a more recent survey for the *Paperbase* project [25] identified two Kodak papers, possibly from 1947 (*London Bromesko* and *London Bromide*) as containing OBAs.

In the interview with Albert Farnley, it is stated that in 1949, the Ilford *Bromide* paper had OBAs – *Leucophor C* fluorescent dye (4.4' diphenyl-diamino stilibene-2.2' disulphonic acid) from Sandoz in Czechoslovakia [12]. After 1961, Cassio Photographic Paper Co. Ltd switched from Leucophor C to *Blankophor BUP* [13], which had a good fibre affinity, stability in alkaline solutions and throughout the peroxide bleaching process [22].

Different adjustments to the production were made to obtain various surface characteristics. The main steps in terms of texture are described in *Table 2.1*. The papers' glossiness was dependent on the texture, and could be further changed using matting agents, such as $BaSO_4$, starch (often corn or rice starch), silica (SiO_2), or pearl (bismuth oxychloride). [9].

Table 2.1 . Kodak papers' texture – description and main production steps; table produced based on [9]

Texture & microphotographs from [9]	**Smooth**	**Tweed & Tapestry**	**Rough**	**Fine-grained**	**Silk**	**Suede**
			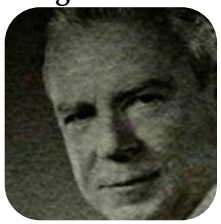			
Period	Mid-1880s-2005	1942-1987 (Tweed) 1932-1987 (Tapestry)	Mid 1880s-1966	1932-1999	1929-1980	1940-1972
Description	*No noticeable surface pattern to interfere with the rendition of fine detail.*	*Tweed/canvas appearance; minimizes the need for fine retouching; good for breaking up large surfaces.*	*Noticeable texture which tended to subdue fine details and emphasize large areas of subject.*	*A slightly pebbled surface which added richness without loss of definition.*	*Silk appearance; an attractive surface for expressing brightness in snow scenes and seascapes.*	*Smooth suede leather appearance, extremely matte surface which toned down some detail and added depth to subjects.*
Production	• Most difficult to produce. • Fibre selection and paper base very important. • Heavy calendered. • Multiple layers of baryta coating (up to six).	• Texture produced in the wet pressing by the felt marking of the formed raw sheet. • Calendering with reduced pressure to not damage the texture. • Baryta coating with lower weights; usually, only one layer.	• Texture was produced in the wet pressing step (felt marking). • Coating weights of baryta layer were low; one layer. • Not calendered afterwords.	• Texture produced in the wet pressing step, but by roll marking. • Calendering and baryta coating – same as for tweed papers.	• The paper support was smooth, baryta coated. • The final baryta calendering operation had light pressure. • The texture is embossed.	• Texture created by adding matting agents in the emulsion (ground glass).
Observations	• Glossy prints required the highest standards. • Sheen depended on the calendering and matting agents.	• A marked paper could be reproduced for years but depended on the felt and pressure used.	• The texture became less rough over years.		• Popular for wedding photography	• Reflection-free surface.

2.2 Implications of DOPs' composition in Photography Conservation – current challenges and preservation issues

Compared to the POP processes, the DOPs are inherently more stable due to the bigger size of the filamentary silver in the image layer [5]. However, sulfiding deterioration can still occur if the print was not properly washed, an exhausted fixing bath was used, or sulfiding gases are present in the atmosphere. Silver mirroring is a common degradation that commonly appears first in the maximum density (D_{max}) areas, around the edges due to the oxidative-reductive reaction of the silver [8].

Regarding the binder, gelatine is chemically stable but can cause problems in the print's physical stability. Gelatine swells considerably with increased humidity, but in dry conditions it becomes brittle. If the print goes through multiple RH fluctuations, it can become curled and cockled. Gelatine's melting point is around 30°C, which can cause the emulsion side to adhere to the surfaces in contact or change its surface characteristics ("ferrotyping"). Oxidative gases can penetrate swollen gelatine more easily, leading to silver image damage [8].

Paper's physical properties can also cause problems. Paper is a hygroscopic material, that expands mostly in the cross direction. Deformations can easily occur in an unstable climate, as each layer swells at different degrees. Paper is also prone to deterioration due to light exposure, high relative humidity (RH), elevated temperatures, mould, and air pollution [8].

The study of the manufacturing process revealed some deterioration issues caused by the production. For instance, Kodak faced challenges with 100% rag pulp paper being too cockled and absorbent. Papers from 1927-1928 had issues with rosin oxidation during sizing, which produced peroxide, leading to chemical fog in the emulsion [9]. The lack of information on the pigments and dyes used for base tints is concerning, as there is no data on their lightfastness or solubility.

The conservation treatment of the fibre-based DOPs is also challenging due to their various surface characteristics. Surface cleaning can easily scratch glossy prints, while textures can be altered during the flattening process. Silver-mirrored photographs are also difficult to treat, as surface cleaning methods might reduce the mirroring [26].

The presence of OBAs can raise further problems in exhibiting and conserving the photographs. OBAs are sensitive chemical compounds, with light being one of the main deterioration causes [27]. OBAs' lightfastness is influenced by their concentration, aggregation degree, substrate stability, application method, air pollution, humidity and temperature. OBAs' quenching (when they no longer emit light) can also be caused by the interaction with the rutile form of TiO_2 [22].

Conservation interventions on photographs with OBAs can also be challenging. Water-soluble OBAs can become mobile during aqueous treatments. A short exposure to water might cause OBAs to migrate to the air-surface interface during drying. Prolonged water exposure

can lead to tide lines, uneven surfaces, and an overall reduction of OBAs [23]. Additionally, when samples of photographic papers are washed together, cross-contamination can occur, resulting in brighter patches and blurry spots [24].

While conserving the original print is typically the goal for photo conservators, there are instances where artists specify reprinting the original [28]. For example, at the Kröller Müller Museum, it was decided to replace the damaged photographic paper in Ger van Elk's artwork; the new paper selection was based on the visual judgment of the conservator, curator, and artist. However, the author suggests that using analytical techniques could have improved the selection [4].

2.3 Analytical techniques used for fibre-based DOPs characterisation

The resources consulted to establish a methodology for fibre-based DOPs characterisation included articles, volumes, and collection databases. These resources focused on studies of sample sets and reference papers or understanding the structure and features of photographs printed on fibre-based DOPs. The main databases used for researching the articles were *Google Scholar, B-on*, and *Taylor and Francis*, searching for keywords like *multi-analytical characterisation* (or *investigation, analysis, identification, dating*) *of photographs (*or *photographic prints, gelatine silver prints, DOPs, black-and-white photographic paper*). Additionally, *Topics in Photographic Preservation* have been consulted.

2.3.1 Studies on reference DOPs and sample sets

Extensive research on reference papers has been conducted in the United States. Paul Messier was one of the pioneers in highlighting the importance of collecting and characterizing reference papers. In collaboration with other specialists, he explored trends in 20th century photographic paper production by assessing the presence of OBAs, types of fibres and pulps used in the paper support, back printing, the barium (Ba) to strontium (Sr) ratio in the baryta layer, and papers' texture [1, 24, 29]. Initially, the collection contained around 2,000 black-and-white fibre-based DOP reference papers, noting the lack of European and Asian references. Now, the collection has expanded to about 7,500 samples and forms the core of studies conducted by the Lens Media Lab [30]. Projects here include a database known as *Paperbase* [25] which comprises information and visual characteristics of DOPs samples like the brand, thickness, base colour, tone colour, texture, gloss, fluorescence, back print, and format of the sample. The platform allows for detailed observation and comparison of specific results across surveyed papers.

Two other studies dedicated to sample sets characterisation focus on a *1966 Kodak B/W Darkroom Dataguide R-20* [31] and the surface features of a 1973 Agfa set [4]. In connection with the paper produced by the Belgian-German company, Agfa-Gevaert, the *Fotomuseum* from Antwerp conducted the *Gevaert Paper Project* [32] which focused on the inventory of the papers.

These two are the only studies to date that we are aware of focusing only on researching the Euro-pean photographic paper manufacturing.

2.3.2 Visual features characterisation (surface, colour, thickness and weight)

One surface feature that characterizes photographic papers is **gloss** (sometimes referred to as *sheen*), indicating to the amount of reflected light from a surface [9]. Various methodologies have been used to depict it. These include photo-documentation with axial or oblique specular illumination, where the light source is positioned so that the camera captures the specular reflection [6, 33]. This setup was also used for the print documentation in the Graphic Atlas database as a tool for printing technique identification [34].

The glossiness can also be assessed with the gloss meter [4, 35, 36]. Another possibility is proposed in a study related to matte paint layers [37] where glossmeter measurements are compared with colourimetry values obtained by subtracting the Specular Component Excluded (SCE) L* from the Specular Component Included (SCI) L* value (ΔL*SCI-SCE). The curve obtained with the 60º gloss-meter measurement was similar to that obtained with the ΔSCI-SCE values, showing potential for application in other fields.

The surface features of photographic paper also include **texture,** which refers to the prints' physical topography [38]. To document texture, photo-documentation with raking light illumination is preferred, where the light source is placed at a low angle to enhance planar deformations and textures [6].

Based on the raking light setup, a standardised technique using a microscope was developed. This technique, combined with automatic classification methods, could allow papers to be identified solely based on their texture [29, 39, 40, 41]. The pictures are acquired with the TextureScope, a microscope system assembly described in [42].

The texture has also been documented using the polynomial texture mapping (PTM) technique [43], or edge reflection analysis [44]. However, the resolution of the surface texture calculations is 50 μm, considered low compared to the profilometer resolution [45]. The profilometer can generate three-dimensional (3D) topographic maps and two-dimensional (2D) profiles along selected lines and determine the values for the standard roughness parameters. Thes values are considered more accurate in the characterisation and identification of photographic paper surfaces [4].

Fibre-based DOPs are also characterised by their **base tint**, referring to the colour of the paper support that may be influenced by the baryta layer [9]. A normal light illumination setup for photo-documentation is ideal for accurately documenting the paper's tint [6]. Colourimetry can provide precise documentation of base tint.

It was also observed that the thickness and weight measurements could help in paper-type identification [46].

2.3.3 Stratigraphy and material composition

The most accessible way to assess the presence of OBAs in photographs is by observing the prints under long-wave UV radiation (320-380 nm). Samples containing OBAs will emit a specific fluorescent glow. However, there are cases when prints might appear bright under UV without having OBAs because of the natural fluorescence of gelatine or the fact that baryta reflects the unfiltered blue light emitted by many near-UV radiation sources. OBAs can also be hard to observe if degraded [24]. For the identification of OBA type, several analytical techniques have been tested, including fluorescence spectroscopy, FTIR, electrospray ionization mass spectrometry (ESI-MS), and matrix-assisted laser desorption ionization time-of-flight mass spectrometry (MALDI-TOF-MS) [27].

Identifying the pulp type of the paper support can provide significant insights for dating photographs. Microchemical tests have been used to study the trend in the paper pulps used for photographic paper production [1, 43]. Herzberg stain helps to distinguish between rag, groundwood, and chemical wood pulps [47], while Lofton-Merritt stain to distinguish between bleached and unbleached pulp [48]. The role of Graff "C" stain is to differentiate softwood from hardwood pulp, determine if the pulp is chemical, semi-chemical or mechanical, and if it is kraft pulp, sulphite pulp, dissolving grade sulphite or dissolving grade sulphate [49].

ATR-FTIR has often been used to characterise photographic emulsions [50, 51]. However, the technique presents the disadvantage of requiring close contact with the object. Therefore, many conservation scientists started exploring the potential of ER-FTIR spectroscopy, a non-contact technique that does not require sampling [52]. However, ER-FTIR's downsides include harder-to-read spectra and the lack of reference libraries [53].

To extend ER-FTIR usage towards photographs, a study researched the influence of image density, surface finish and layer structure on ER-FTIR spectra [52], observing which characteristics change with the image density, different layering structure, and surface characteristics. This idea was further explored by Walker [54] on a *1967 Kodak B/W Darkroom*. The study of eleven fibre-based DOP samples showed that variations in thickness, layers, materials, glossiness, and texture could lead to different spectra, highlighting the importance of analysing reference photographic papers and sample sets to understand better how these properties influence ER-FTIR spectra.

Some studies have also been found on print identification and dating with near-infrared spectroscopy (NIR) coupled with the statistical method of PCA [55, 56].

XRF provides information about the inorganic components in photographs, such as image material, the presence of a baryta layer, fillers, and impurities in the paper support. The analysis involves examining maximum and minimum image density areas (D_{max} and D_{min}) and the paper support [57], a methodology followed in numerous studies [43, 50, 51, 58, 59]. XRF was also used quantitatively in one research [1] to identify trends in the ratio between barium (Ba) and strontium (Sr) in the baryta layer. XRF has the advantage of being a contactless

technique, with no need of sampling. However, interpreting XRF spectra can be challenging since they contain information from all layers [60].

Researchers studied papers' cross-sections to gain a deeper understanding of each layer [34, 54]. However, a considerable sample is required, usually collected from a D_{max} area to differentiate the baryta layer from the emulsion [31]. Cross-sections can be observed under the microscope in two ways: in a solvent between glass slides [61, 31] or embedded in resin [62].

Further information can be obtained by studying cross-sections with SEM-EDS. This technique uses a beam of electrons instead of visible light, offering a magnification of up to 100,000 times and producing three-dimensional images. SEM equipped with energy-dispersive X-ray spectroscopy (EDS) allows for simultaneous elemental analysis [63].

3

METHODOLOGY

3.1 Case studies

Three sample sets of fibre-based DOPs were chosen to study European photographic paper production in the mid-20th century and compare it to later U.S. production. The sets, showing both similarities and differences, help to evaluate the comparison of papers from different manufacturers and periods using multi-analytical methods.

Two sets were produced by the English company Ilford, a major European photographic materials manufacturer in the 20th century. One set has a smaller format, while the other has a medium one. The third set was made by Kodak, a major U.S. photographic materials company. The Ilford sets were manufactured around 1950, while the Kodak one in the 1970s. Another significant difference is the purpose of the samples – the Ilford medium set seems dedicated to professionals, while the other two are smaller and more suitable for amateurs. All sets are part of private collections.

To facilitate the presentation of the sets and results, to each set was assigned a colour – violet for Ilford small-format set (●), red for the medium format Ilford set (●), and green for the Kodak one (●).

3.1.1 Sets format

- **Small-format Ilford set (IS)**

The small-format Ilford set (*Figure 3.1*) is a photographic paper specimen set distributed with the Ilford publication, *Printing and Enlarging* [64]. It includes 18 samples, each measuring 75x50 mm, organized within a paper envelope into three compartments based on typology (*Bromide*, *Plastika*, and *Contact*). On the exterior of the upper flap, the company name is printed in red ink, while the inside features a table with the papers' codes and characteristics.

The accompanying A5 textbook contains 43 pages of information and illustrations on material selection and printing techniques. Given its content, the size, and the everyday subjects of the images, this set was likely intended for amateur or apprentice photographers.

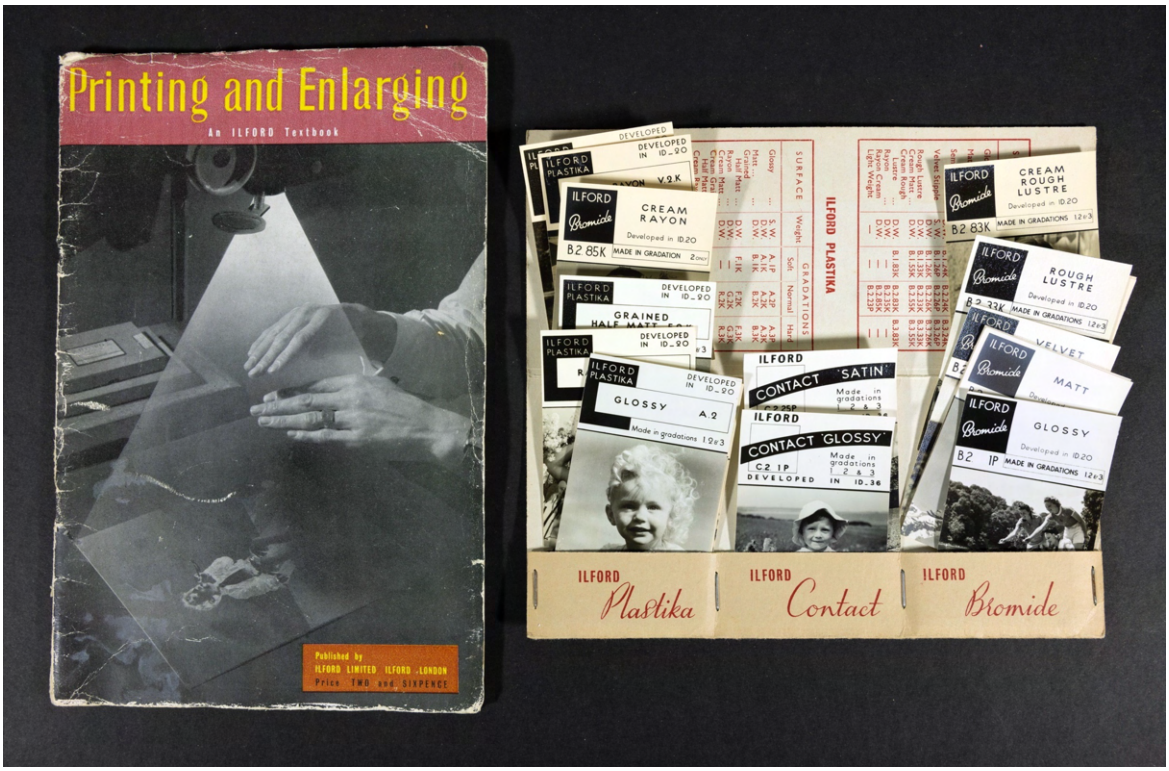

Figure 3.1 Small format Ilford set

- **Medium-format Ilford set (IM)**

The medium-format Ilford set resembles the appearance of an album (*Figure 3.2*), containing 25 prints, with a 238x176 mm format, bound by a yellow paint coated metal spiral. The cover is made of rigid boards, covered in dark-red book cloth with the company and classes of papers names embossed in a golden colour in the centre.

The paper size, professional photography topics, and rich tonal ranges suggest this set was intended for photographic studios and professional photographers. The two cards found at the back of the set support this hypothesis. One is a business card from a photographic materials shop in Porto, Portugal, and a Portuguese inscription (*Appendix A.1, Figure A.1*). The other one is a handwritten note from Mr Luiz Filipe de Arouca Pimentel (*Figure 3.3)*.

The set could also be intended for photographic societies as the alphanumeric code from the index page, *IA. 39 (Appendix A.1, Figure A.2.a)* is similar to one found in the fourth number of the *Ilford News (IA.16) (Figure 3.4)* [65].

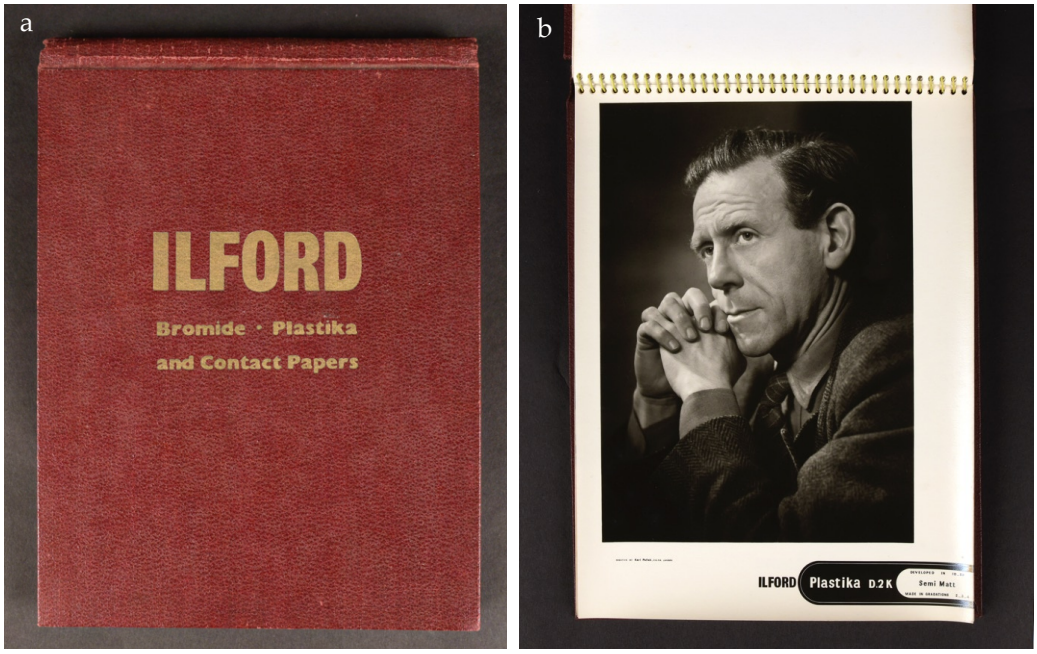

Figure 3.2 The handwritten note found in the back of IM

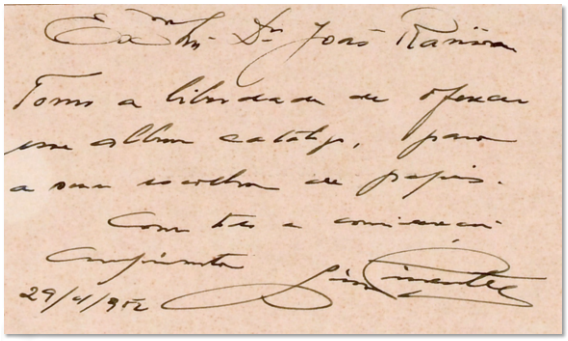

Excellency Mr. Dr. João Ramiro(?)

I took the liberty of offering a catalogue album, for your choice of papers.

With all my admiration. Compliments

29/01/1952

Figure 3.3 Medium format Ilford set: (a) cover; (b) open to one sample

ILFORD NEWS
FOR PHOTOGRAPHIC SOCIETIES

The Theory of Exposure Simply Explained

2. THE SUBJECT AND CAMERA

By G. B. Harrison, Ph.D., F.R.P.S.

ALBUMS FOR SOCIETIES

We should like all societies to have a new album of Ilford Papers before the opening of the next photographic season and we should be glad if those secretaries who wish to take advantage of this offer would send in a post card to this effect. Just write I.A.16 on the post card, sign your name and append the name of your society and the album will be sent well before your members start making their exhibition pictures for next season.

Figure 3.4 Detail from *Ilford News*, no.4

• Kodak set (K)

The Kodak papers are part of the 1972 *Kodak Master Darkroom Dataguide for Black-and-White*, 4th edition (*Figure 3.5*). This 146x223 mm spiral-bound publication offers basic information on processing, printing, enlarging, and copying. The content is divided into three sections on films, papers, and chemicals. The second section includes the 11 samples, measuring 127x90 mm, together with details about their features.

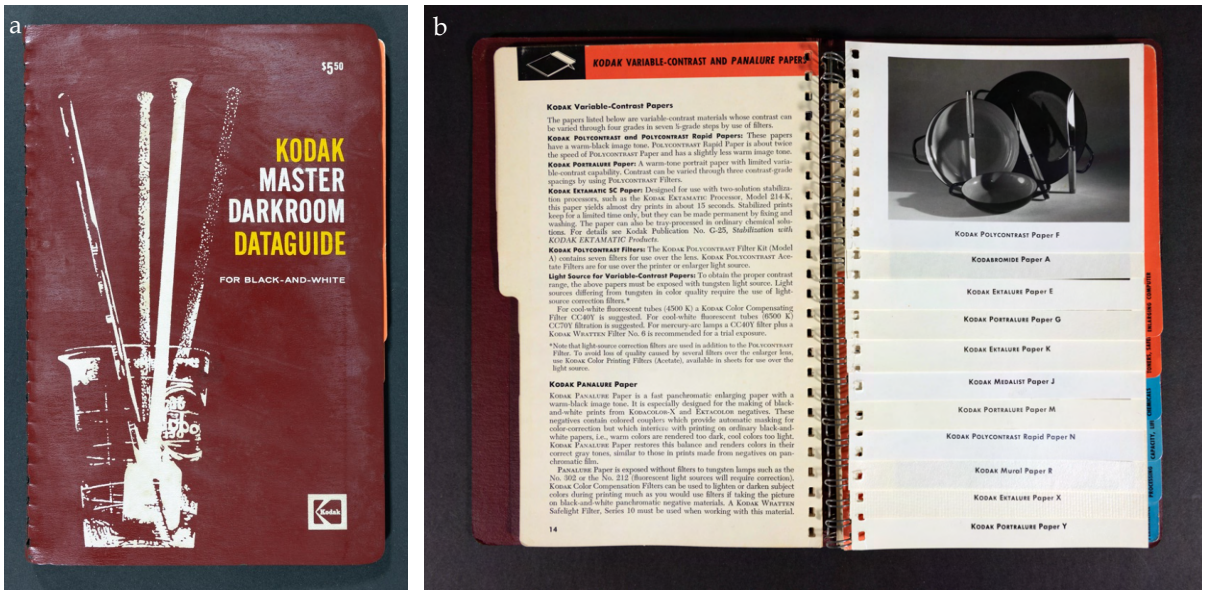

Figure 3.5 Kodak sample set: (a) cover; (b) paper samples

3.1.2 Samples characteristics

3.1.2.1 Paper classes

One of the first classifications of the samples is between different paper classes. This classification is based on the photographic emulsion type. There are two main types of DOP emulsion. The first one is gelatine silver chloride paper, also called *gaslight paper*, which required only gaslight exposure and didn't need darkroom processing. These papers were used in contact with the negative in printing frames. As negatives became smaller, there was a need for a new emulsion type suitable for enlarging and printing images from negatives onto paper. This led to a gradual shift toward bromide gelatin silver papers [5].

Other characteristics related to the emulsion are the colour sensitivity, speed, grain, gradation, type of developer recommended and developing time, image tone and recommended toners [64, 66].

• • Ilford sets

Both Ilford sets contain the same paper classes – *Bromide*, *Plastika* and *Contact*. *Bromide* paper is presented as the fastest, the best one for enlarging and rapid production. *Plastika's* main characteristic is the ability to reproduce all tones in the negative. The *Contact* paper was

previously commercialised as *Gaslight Paper*, indicating that the exposure and development could be made in a usual room [64]. Other differences highlighted in the textbooks are summarised in *Table 3.1*.

Table 3.1 Differences between *Bromide, Plastika* and *Contact* papers [64]

Paper class	Image colour	Silver salt	Contact Printing Speed	Developing time (18°C) in sec.
Bromide	Fine black	Mainly Silver Bromide *Silver chloride might be present as well	4s at 48 inches from 25-watt lamp	120
Plastika	Warm-Black	Silver chloro-bromide	10s at 48 inches from 25-watt lamp	90-120
Contact	Blue-Black	Mainly Silver Chloride *Other silver salts might be present	5s at 12 inches from 60-watt lamp	45-60

- **Kodak set**

The set includes seven classes of papers: *Polycontrast, Kodabromide, Ektalure, Portalure, Medalist, Polycontrast Rapid and Mural*. Their features are presented in the *Dataguide*, as summarised in *Table 3.2*. The Kodak set does not include papers with a gelatine silver chloride emulsion.

Table 3.2 Features of the Kodak samples [67]

Type of Paper	Image Tone	Paper Speeds							Developing time (21°C) in sec.
		Contrast Grade							
		WL	0	1	2	3	4	5	
Polycontrast	Warm-black	250	-	160	160	100	64	-	90
Polycontrast Rapid	Warm-black	500	-	320	320	200	100	-	90
Kodabromide	Neutral black	-	-	650	500	320	200	160	90
Ektalure	Brown-black	-	-	-	-	125	-	-	120/ 60
Portalure	Brown-black	50	-	32	-	20	-	-	120/ 60
Medalist	Warm-black	-	-	250	250	250	250	-	60/ 120
Mural	Warm-black	-	-	-	250	250	-	-	120

3.1.2.2 Papers' features

The various paper classes can be further categorized based on their characteristics, including weight, base tint, and surface properties (texture and glossiness).

- **Ilford sets**

The Ilford papers come in two base tint options (white and cream) and two weights – *Single* (SW) and *Double Weight* (DW). IM also includes the print *Bromide B.2.23 P Light Weight Lustre*, which might have a different weight category (*Light Weight*).

The surface features described in the sets refer either to the glossiness (e.g. *Matt, Glossy*) or to the texture (e.g. *Rayon*). The common surfaces for both IS and IM are *Glossy, Matt, Semi*

Matt, Velvet Stipple, Rough Lustre, Rayon, Grained Half Matt and *Satin*. IM also includes *Smooth Lustre,* and *Light Weight Lustre* papers.

- **Kodak set**

The Kodak papers have three weights: *Single* (SW), *Double* (DW), and *Light* (LW) and three base tints: white, warm-white and cream. Each of the 11 samples has a unique surface, designated by a capital letter, with texture and glossiness presented in *Table A.1, Appendix A.1*. The description provided also offers insights into printing uses and potential finishes like re-touching and hand-colouring.

Alphanumeric codes

- **Ilford sets**

Each sample is identified by an alphanumeric code found in either the index table or on the samples (*Figure 3.6 a and b*). Each letter or number corresponds to a characteristic of the paper.

The paper class is indicated by a capital letter: *B* for *Bromide*, *C* for *Contact*, and one of several letters (A, B, F, G, R, T, V) for Plastika. The number *2* in all codes signifies a *Normal Gradation*. A 1 or 2-digit number describes the surface type for *Bromide* and *Contact* papers. This numbering system matches the descriptions in *The Ilford Manual of Photography* (*Figure A.3, Appendix A.1*) [68].

All codes end with either the letter *P* or *K* indicating paper weight: P (*Papier*) for single-weight papers and K (*Karton*) for double-weight papers [46]. The code is followed by a surface description related to the gloss or texture. As most of the papers are white, the colour is only referenced when a different one – cream – is used.

- **Kodak set**

Kodak samples only display the paper class name and a capital letter for the surface type. (*Figure 3.6 c*).

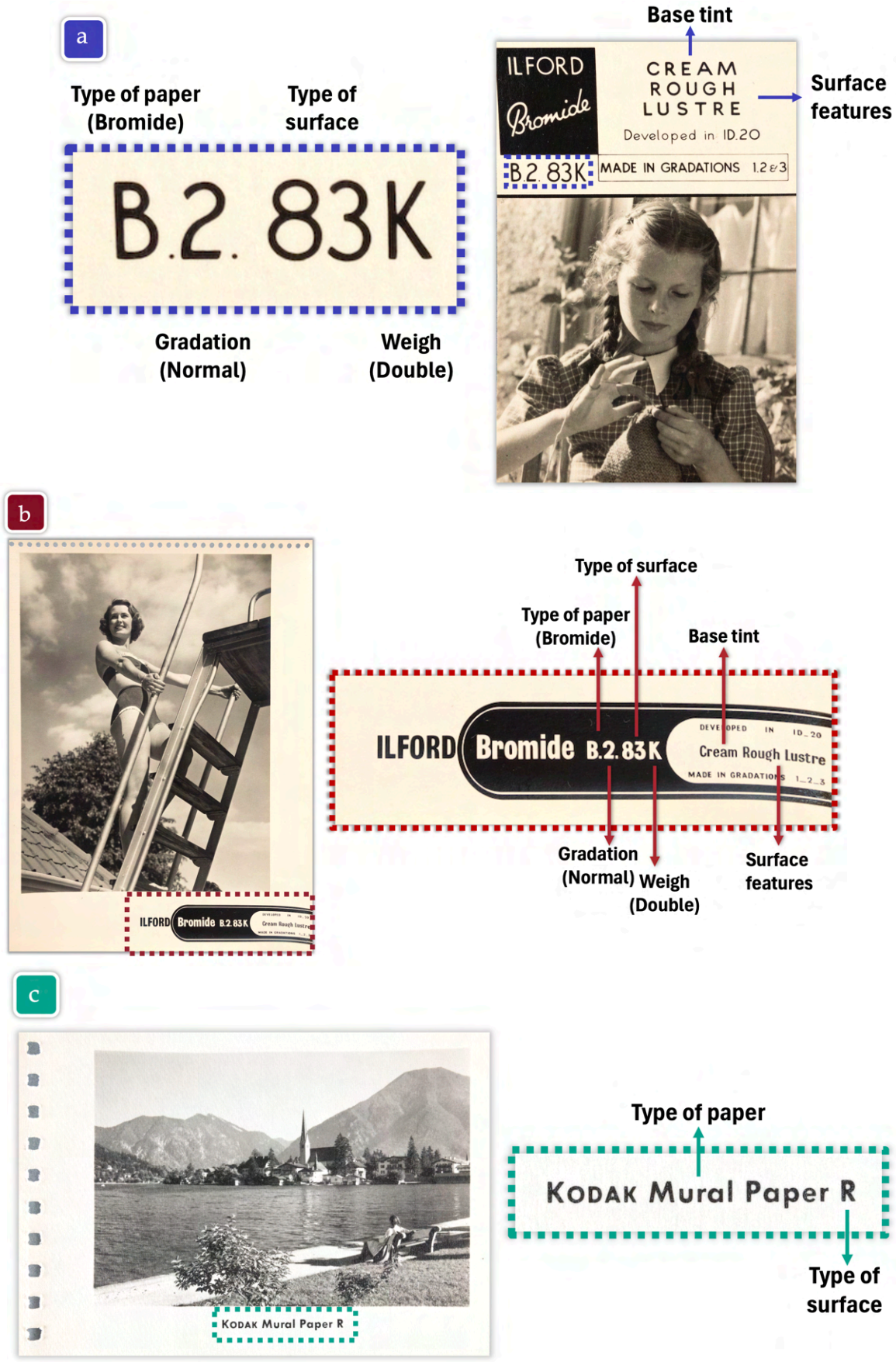

Figure 3.6 Alphanumeric code of the sample sets: (a) IS; (b) IM; (c) Kodak

3.1.2.3 Dating

- **Small-format Ilford set (IS)**

The textbook presents two alphanumeric codes on the last page – *PE/PLH/D.48* and *LUND HUMPHRIES 24524•3•48* – which could indicate that the production year is 1948 [14]. The set also does not include the *Multigrade* paper, which appears in the *Printing and Enlarging* second edition (1955) and was possibly discontinued between 1945 and 1953 [69].

- **Medium-format Ilford set (IM)**

Dating this sample book was not easy, as not much information is offered by the Ilford company that would allow us to relate the case study to the production timeline.

The types of paper included in the set are an indicator of the production date. *Plastika* paper was only introduced in 1939 [10], suggesting the set could not have been made earlier. The absence of *Multigrade* paper, likely discontinued between 1945 and 1953 [69], suggests the book might date from this interval, supported by a note in the book dated 1952 (*Figure 3.4*). The negatives used for the samples provide valuable dating information. Two negatives attributed to Karl Pollak (*IM_Bromide B.2.76 K* and *IM_Plastika D.2 K*) correspond to original photographs dated around 1948 in the National Portrait Gallery collection in London. This indicates that the sample book could not have been printed earlier than 1948, suggesting its production likely falls within the 1948-1953 timeframe.

- **Kodak set**

The publication was printed 1972, but the exact printing date of the samples remains unknown.

3.1.3 The values of the sets

While this research focuses primarily on photographic papers' materiality, it is essential to recognize the significance of their immaterial aspects. Conservation treatments address not only physical decay but also the object's values in the social, technical, scientific, and historical context, along with local resources and priorities [70].

The sample sets and reference papers are often described as unique and valuable research resources [3]. This study highlights the research value by using analytical techniques to gain insights into papers' composition, stratigraphy, and surface features. The rarity of these sets is another value [71], as finding photographic paper sample sets is challenging. While Kodak sets from after the 1960s are available on online marketplaces, Ilford sets, especially those for photographic studios, are much harder to locate.

The historical value [71] of these sets is also notable, illustrating how manufacturers shared available papers throughout the 20th century, including the surfaces offered and printing preferences. While the aesthetic value [71] of the printed images is complex to assess, the

IM set includes several photographs printed from negatives by professional photographers. Thus, future research could benefit from placing more emphasis on these other values.

3.1.4 Multi-analytical characterisation

By assessing the main steps in fibre-based DOP production and the typical analytical techniques used for characterisation, a methodology for multi-analytical characterisation has been established. This approach considers the advantages and disadvantages of various analyses, and the available equipment at the university.

The sequence starts by identifying the similarities and differences in visual characteristics, using techniques that do not require collecting samples. These techniques include photo-documentation using a digital camera and optical microscopy with different illumination setups, colourimetry, and measurement of thickness and weight.

Identifying clusters of papers with similar features allowed us to narrow down the samples analysed in the second round, which focused on material and stratigraphy characterization. This round included paper pulp identification through microchemical tests, μ-EDXRF spectrometry, ER-FTIR, SEM-EDS, and Raman spectroscopy. XRF, ER-FTIR, and Raman analyses did not require sampling, while fibre identification tests and SEM did necessitate sample collection. While sample collection cannot be performed on photographs in collections, the information obtained in this study can afterwards be correlated with the type of photographic paper identified by non-invasive methods.

Table 3.3 summarizes the sequence, goal, and samples analysed, while *Appendix A.2* presents a complete description of the setups, settings, and equipment used.

Table 3.3 Multi-analytical characterisation: sequence, goals and samples analysed

Order	Technique	Goals	Number of prints analysed	Sampling
1	**Photo-documentation**			
	Normal	Document the base tint and damages.	54	No sampling
	Raking	Document the texture		
	Specular	Document the glossiness		
	UV	Identification of OBAs and condition assessment.		
2	**Microscopy**			
	Optical microscope	Observing the paper support.	54	No sampling
	Stereo microscope	Documenting the texture in raking light.		
3	**Colourimetry**	Document the base tint and glossiness	54	No sampling
4	**Thickness and weight measurements**	Documenting and identifying differences between *Single* and *Double Weight papers.*	54	No sampling
5	**Fibre identification microchemical tests**	Identification of fibres and pulp types	IS:6 IM: 8 Kodak: 11	A few fibres were pulled from the margins
6	**μ-EDXRF**	Identification of image material, baryta layer, fillers, and impurities in the paper support, matting agents, pigments.	54	No sampling
7	**SEM-EDS**	Understanding the prints' stratigraphy; elemental attribution for each layer	IS: 5 IM: 7 Kodak: 5	ca. 1x0.5 mm
8	**Raman**	Colourant identification for the base tint (Ilford).	IS: 2 IM: 3	No sampling
9	**ER-FTIR**	Exploring the differences in ER-FTIR spectra of DOPs with various surface features, compositions and stratigraphy.	IS: 8 IM: 12 Kodak: 6	No sampling

4

Results and Discussions

All the analysis results are summarised in *Appendix B.2 – Tables B.1, B.2,* and *B.3.*

4.1 Visual characteristics: base tint, surface features, thickness and weight

4.1.1 Base tint characterisation

The distinction between the two Ilford base tints (white and cream) is visually perceivable. The distinction is stronger on the recto, but still visible for the prints' verso. This was documented during photo-documentation in normal light. While most white prints appeared similar, one IM print (*Bromide B.2.23P Light Weight Lustre*) stood out with a brighter white base tint. These differences are shown in *Figure 4.1*.

Under the microscope, it was noted that all Ilford prints contain particles embedded in the paper support. However, the cream prints exhibited more ochre particles, potentially indicating the presence of a pigment in the paper composition. An example is shown in *Figure 4.1* for the print *IM_Bromide B.2.85K Cream Rayon*. The particles in the white papers were more similar to impurities.

The difference among the white, warm-white and cream Kodak base tints was more subtle, barely visible to the naked eye. No particles in the paper support were spotted under the microscope.

To better understand the differences, *Figure 4.1* groups representative papers from the IM and Kodak sets with different base tints, displaying photo-documentation of the recto and verso in normal light, a microphotograph of the paper support, and the L*a*b* colourimetry values.

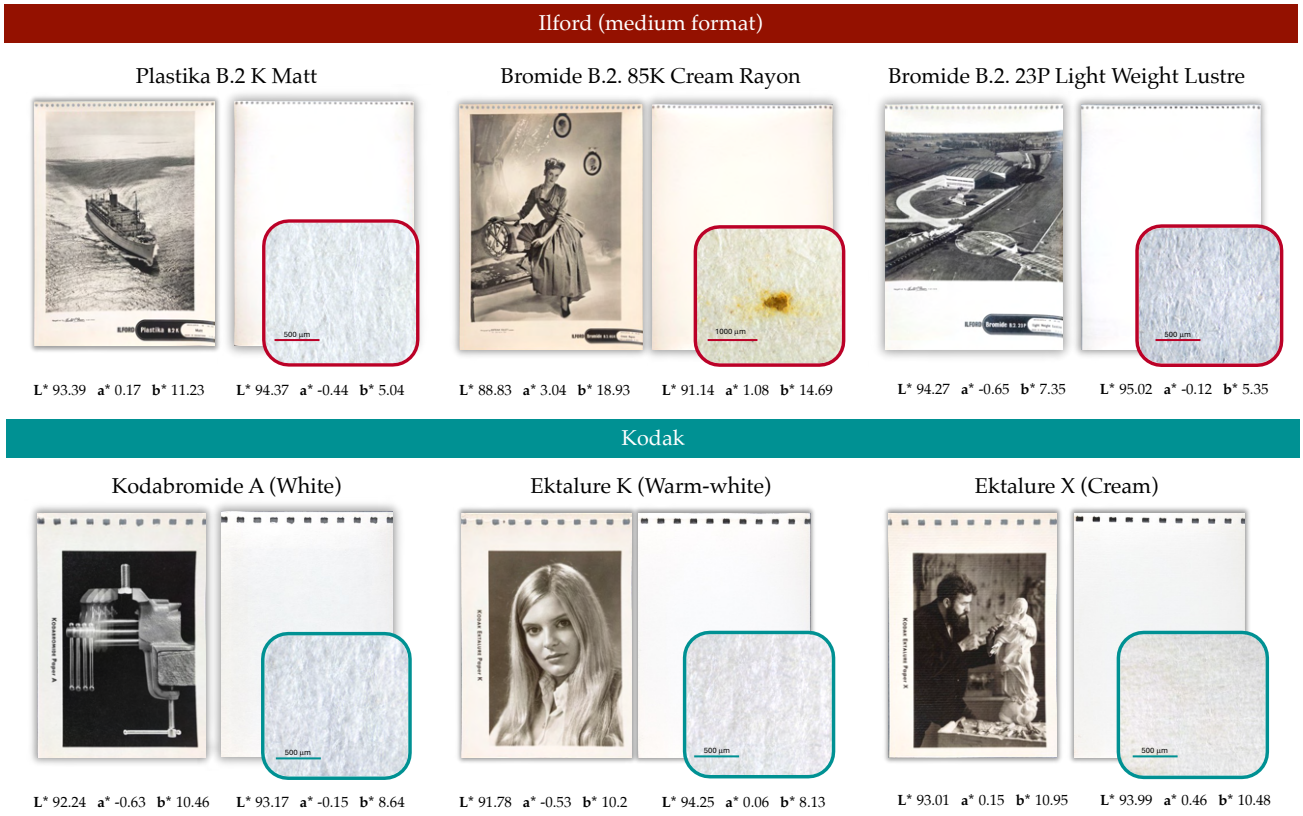

Figure 4.1 Differences in base tints between the Ilford and Kodak papers

Colourimetry helped to differentiate papers' colours more accurately. The three-dimensional representation of the L*a*b* values obtained from recto and verso measurements (*Figure 4.2*) shows that the Ilford cream papers cluster together, appearing more red and yellow than the others. The figure also highlights the subtle colour variations in the Kodak papers.

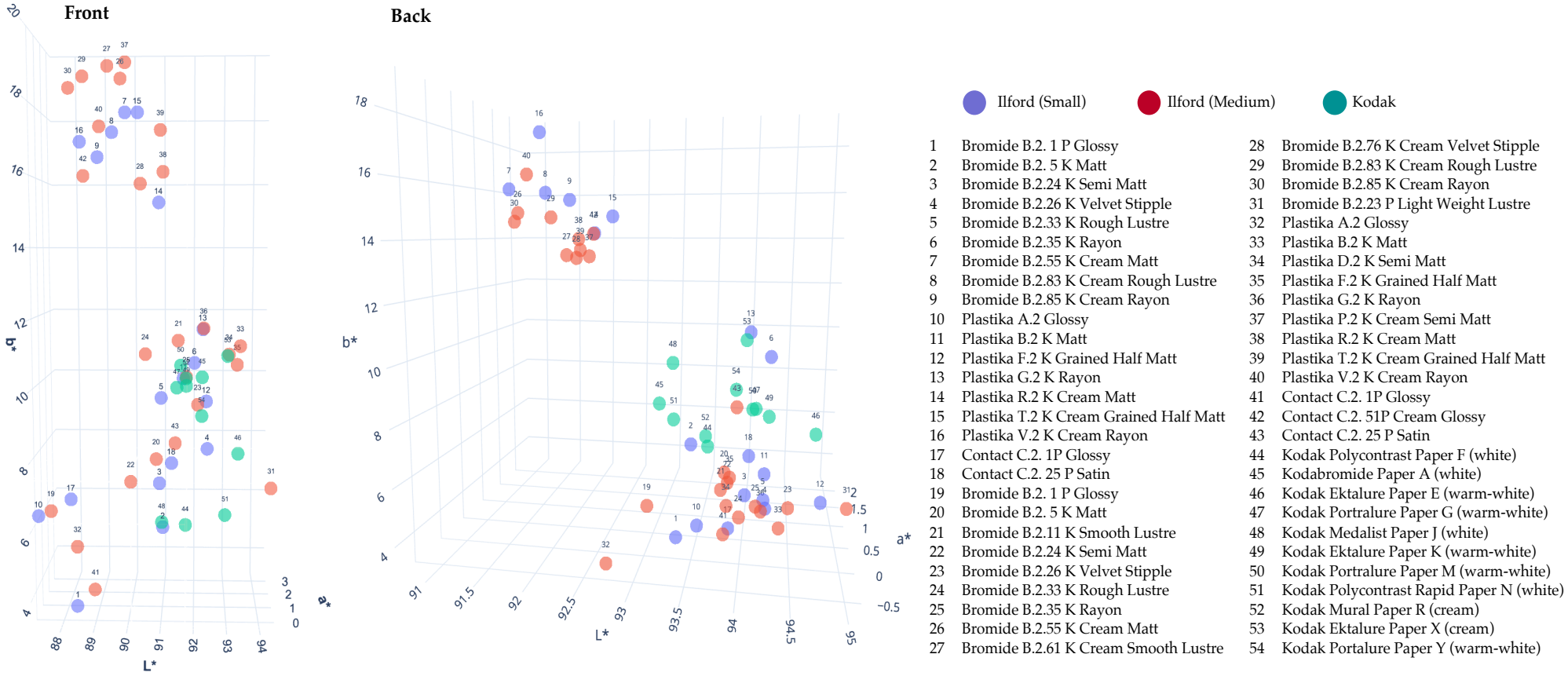

Figure 4.2 Three-dimensional representation of the papers L*a*b* values front and back

The difference in L*a*b* values between the recto and verso was assessed by determining the ΔE value, presented in *Figure 4.3*. The graph shows greater variations between the emulsion side and the paper support in the case of the two Ilford sets, compared with the Kodak one. This difference may be attributed to the production differences, such as the composition and opacity of the baryta layer and the number of baryta coats. Higher ΔE values were noted for the glossy Ilford prints, while other surfaces showed inconsistent values. For Kodak, the print with the highest ΔE value, *Medalist J*, features a smooth surface with a high lustre gloss. This is likely due to the manufacturing process requiring multiple rounds of baryta coatings, explaining the higher ΔE values for glossier prints [38].

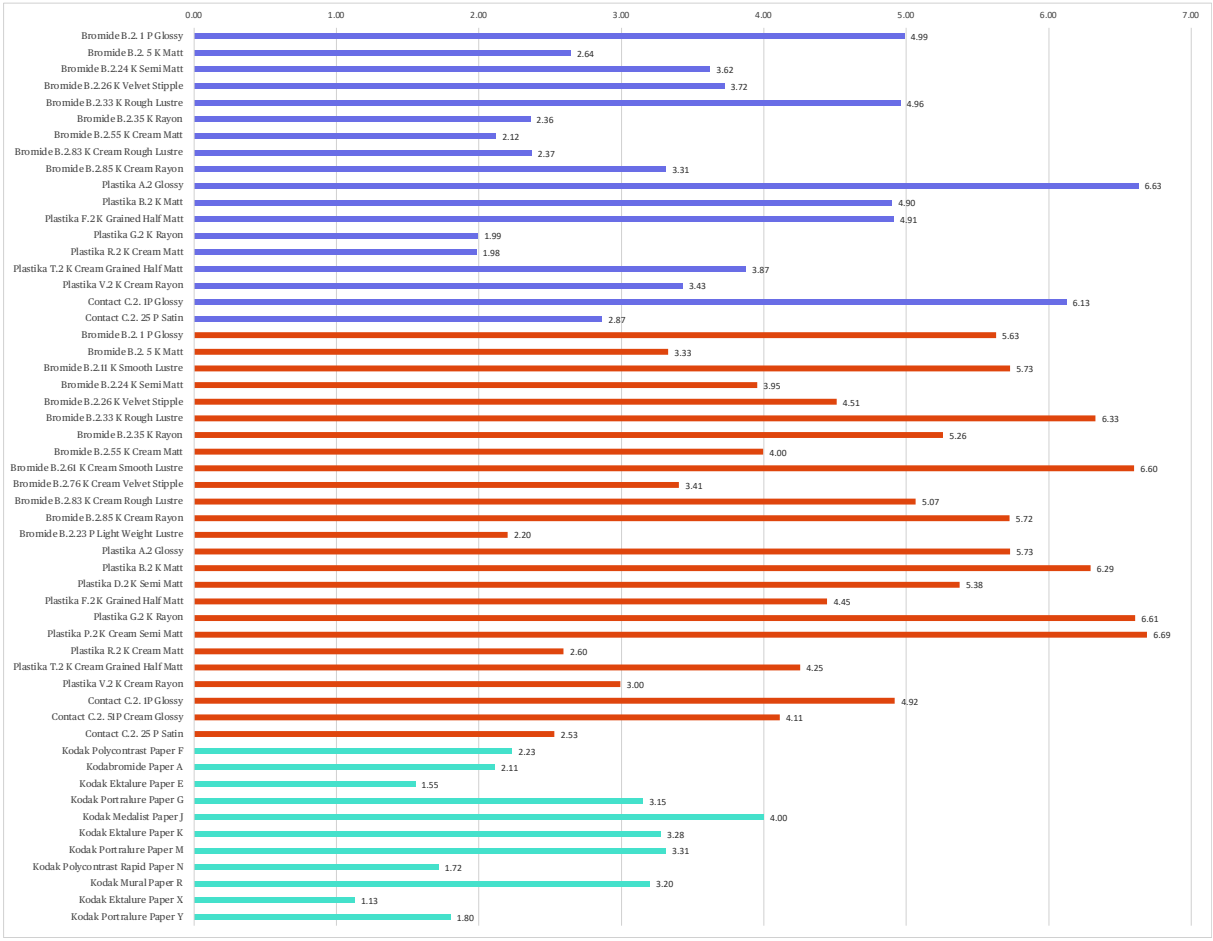

Figure 4.3 Difference between the front and back colour (ΔE value)

4.1.2 Surface features

Photo-documentation was crucial for surface characterization. The setup used for the *TextureScope* [42], facilitated the observation of texture differences. By visually examining the microphotographs in raking light, the available textures in the sets were categorized based on their smoothness or roughness. These findings are illustrated in *Figure 4.4.*

Figure 4.4 Microphotographs of the papers texture in raking light

Raking light observation helped to identify similar textures among the papers. For Kodak, *Ektalure K, Portalure G,* and *Ektalure E* are all marketed as having a *Fine Grained* texture. *Figure 4.5* compares microphotographs of these papers (top) with those from the *Paperbase* database (bottom), revealing that their textures are indeed similar.

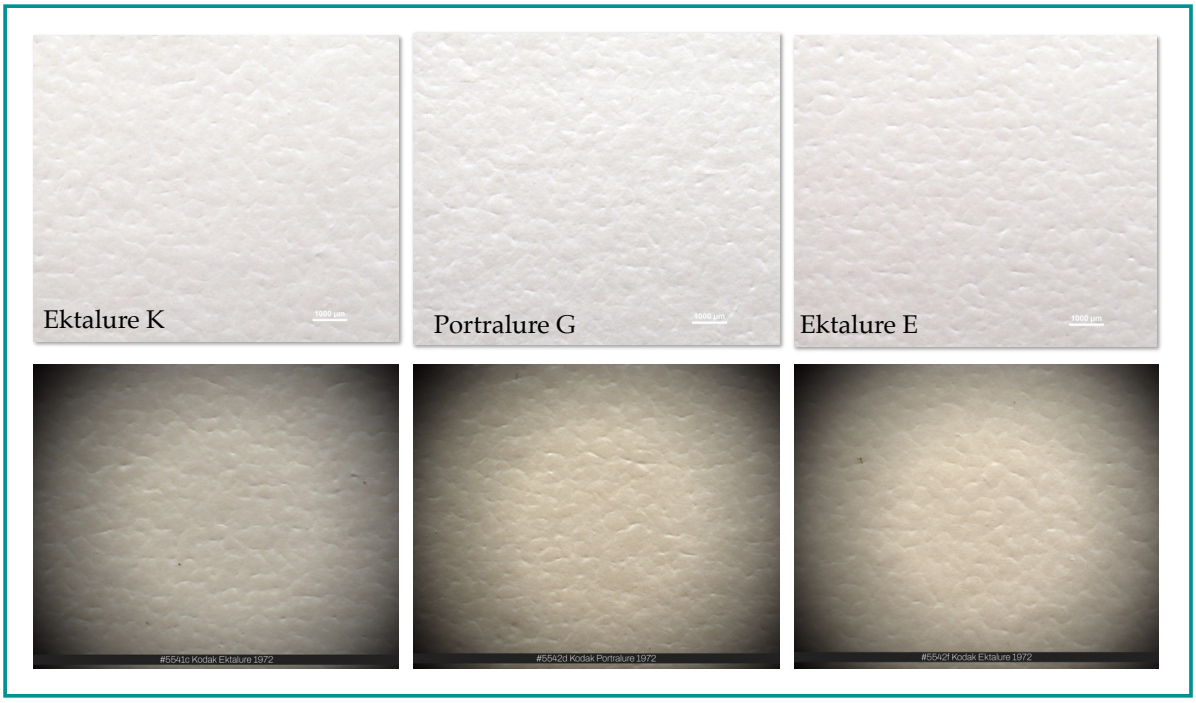

Figure 4.5 Microphotographs with the texture of *Ektalure K, Portalure G, and Ektalure E* papers – from the current study (top), and *Paperbase* (bottom)

The repetitive textures in the Ilford papers show a consistent appearance in raking light across all base tints and emulsion types. However, the *Matt* surface is smoother for *Bromide* papers and slightly rougher for *Plastika* samples, as demonstrated in both Ilford sets (*Figure 4.6).*

Figure 4.6 Microphotographs with the texture of Ilford *Matt* papers

Paper's gloss is significantly influenced by texture. Photo-documentation was used for glossines assessment using a specular axial light, with all images grouped in *Appendix B.2*. This setup effectively distinguished glossy prints from semi-reflective and matte ones in the Ilford sets (*Figure 4.7*), and glossy, high lustre, lustre, and matte finishes in the Kodak set (*Figure 4.8*).

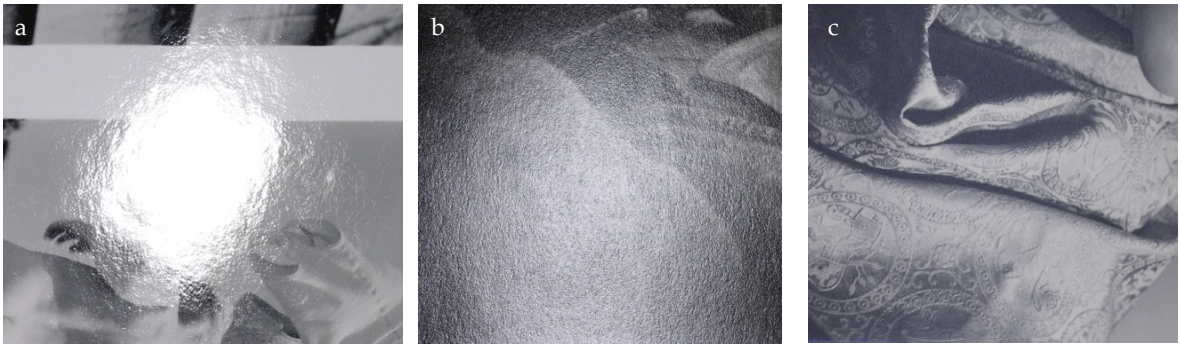

Figure 4.7 Close-up details in axial specular light from IM: (a) a glossy print (*Contact C.2. 1P Glossy*); (b) a semi reflective print (*Plastika P.2.K Cream Semi Matt*); and (c) a matte print (*Bromide B.2.25 K Cream Matt*)

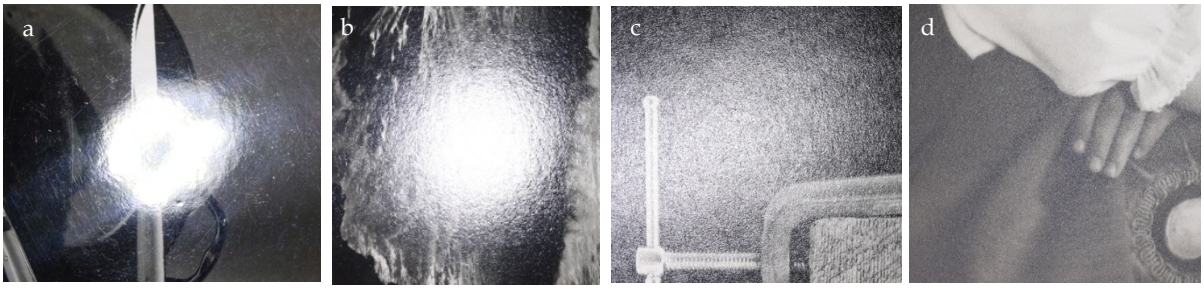

Figure 4.8 Close-up details in axial specular light from the Kodak samples with smooth texture and different glossiness: (a) glossy (*Polycontrast F*), two semi reflective prints – (b) high lustre (*Medalist J*); (c) lustre (*Kodabromide A*), and (d) a matte print (*Portalure M*)

The papers' glossiness characterization was also evaluated using colourimetry measurements (L* SCI-SCE), with results shown in *Figure 4.9*. *Glossy* prints exceeded values of 2 for the Ilford sets, while *Matt* prints were below 0.3. The other surfaces displayed more variability in their results. Kodak's values were slightly different, with *Glossy* and *High Lustre* prints closely aligned, but variations were noted among the *Lustre* samples. However, the Kodak matte print (0.21) was like that of Ilford.

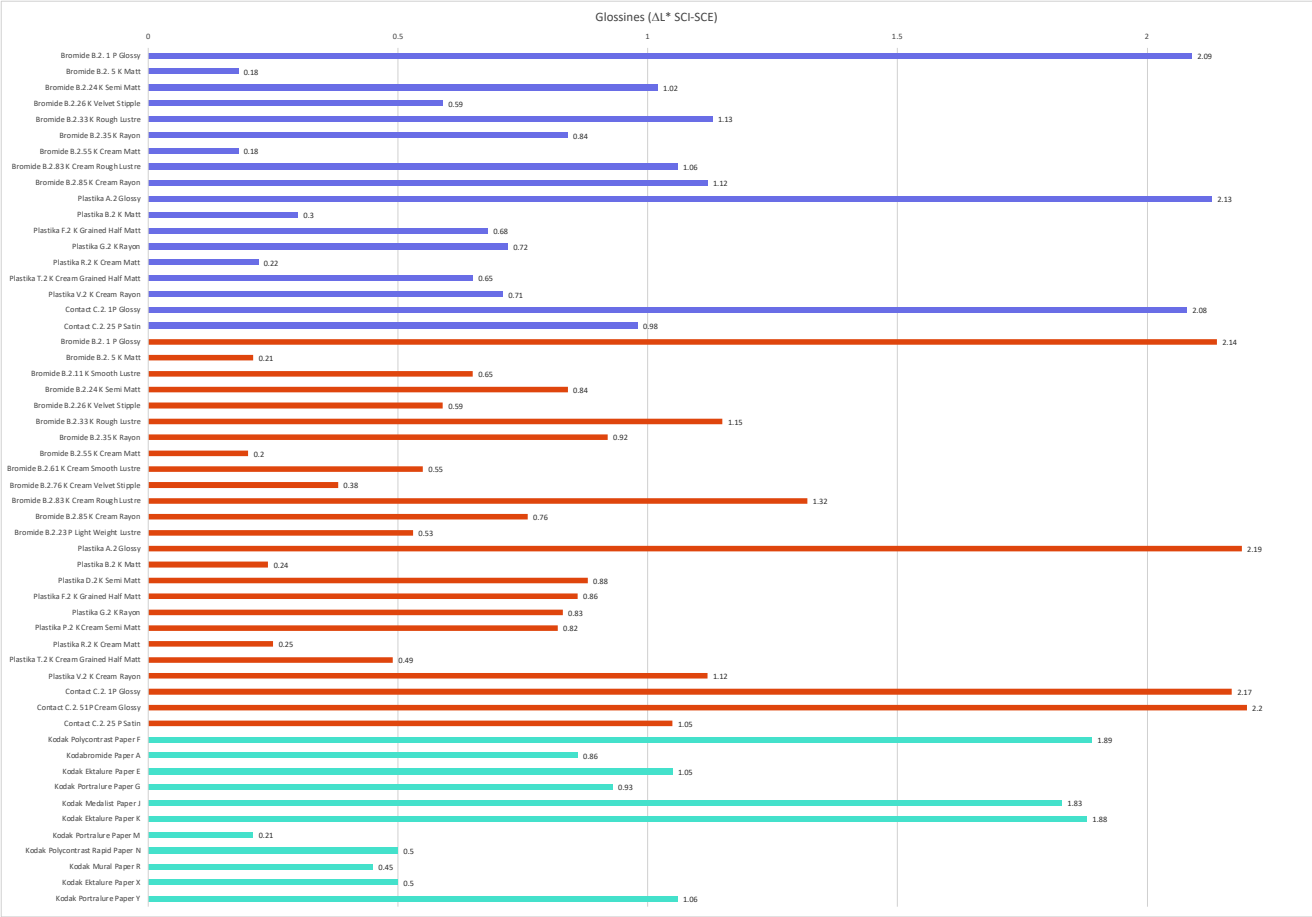

Figure 4.9 Glossiness characterisation through colourimetric measurements (ΔL*SCI-SCE)

The ΔL*SCI-SCE values for IS and Kodak were compared with the gloss units of corresponding samples from the *Paperbase* database (*Figure 4.10*). The resulting curves were generally similar, with some differences expected due to variations in prints' condition. These preliminary results suggest that ΔL*SCI-SCE values could potentially be used for the gloss characterization of photographic papers.

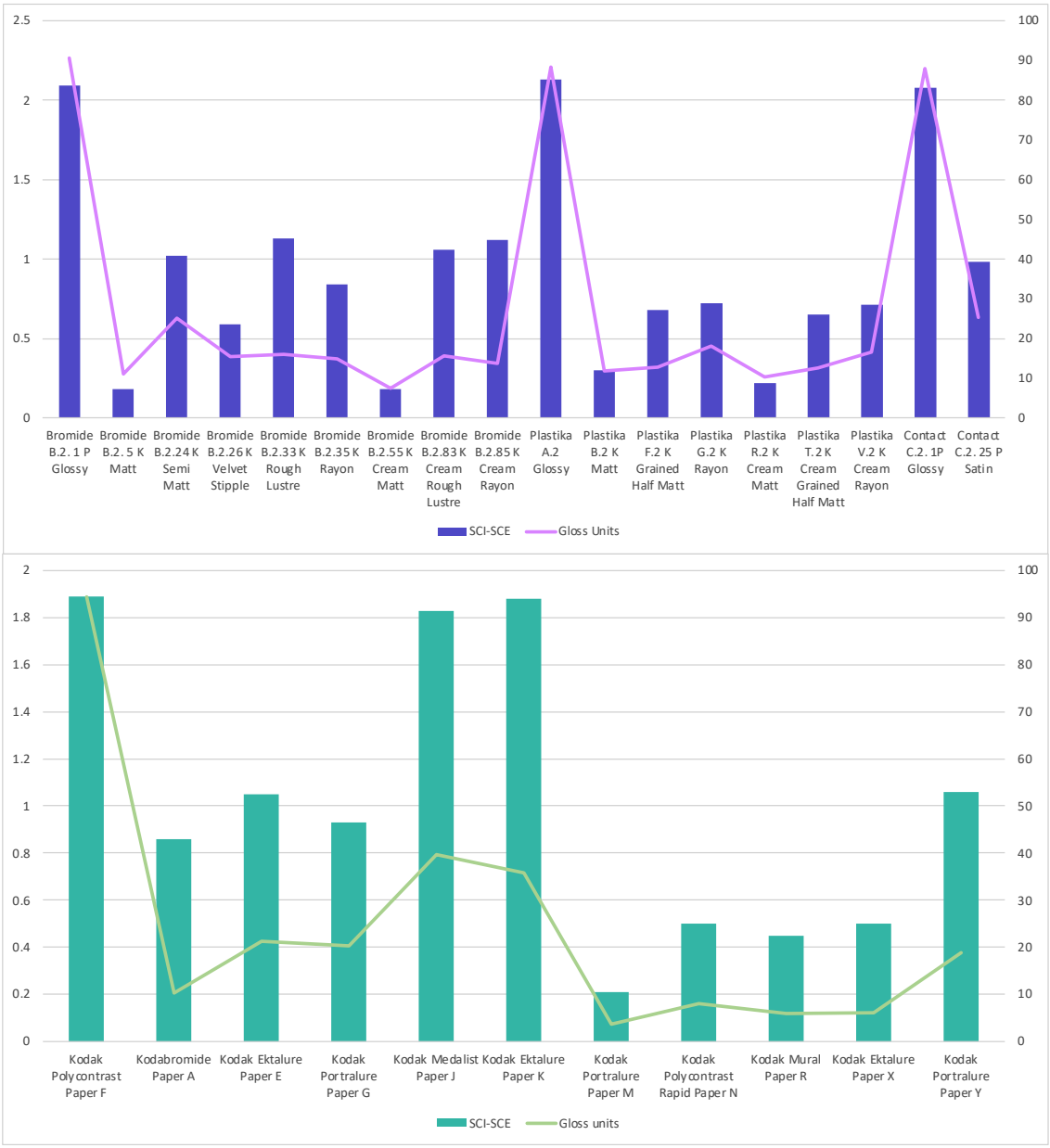

Figure 4.10 Difference between ΔL*SCI-SCE values and gloss units from *Paperbase* for IS and Kodak sets

4.1.3 Thickness and weight measurements

The average thickness and weight of the prints are shown in *Figure 4.11*.

• • Ilford sets

For both Ilford sets, the thickness of the *Single Weight* prints ranges from 0.16 to 0.20 mm, with available surfaces being *Glossy* and *Satin*. *Glossy* prints measure between 0.16 and 0.18 mm, while *Satin* prints are 0.20 mm thick. This difference can be attributed to production processes, as *Glossy* prints were heavily calendered [10]. An exception is *IM_Bromide B.2.23 P Light Weight Lustre*, which has a 0.9 mm thickness. The *Double Weight* papers exhibit more surface variety, reflected in their 0.26 to 0.31 mm thickness range.

There is a clear distinction in weight between the *Single* and *Double Weight* prints. However, the expectation that thicker samples would be heavier does not always hold true. In both sets, the *Glossy* prints are thinner than the *Satin* ones but also heavier. This can be attributed to production processes, suggesting that multiple baryta coats were likely applied to the *Glossy* prints, but the thickness was reduced through heavier calendering.

• Kodak set

The *Single Weight* samples have a similar thickness to the Ilford ones (0.18 - 0.20 mm). The *Light Weight* print, *Kodabromide A,* is thicker than *IM_Bromide B.2.23 P Light Weight Lustre*, having 0.12 mm. *Double Weight* papers are also slightly thicker, ranging from 0.31 to 0.35 mm. For Kodak samples, the thickness and weight appear more correlated, except for *Polycontrast Rapid N* and *Mural R*. *Polycontrast Rapid N* is thinner yet heavier than *Mural R*, indicating variations in the manufacturing process, possibly linked to the baryta layer.

The thicknesses of IS and Kodak samples were compared with corresponding *Paperbase* measurements and were found to be very similar, differing by a maximum of 0.03 mm in some cases. This discrepancy could be attributed to the measuring equipment, as *Paperbase* measurements have three digits, or to inconsistencies in thickness during production.

While thinner than the other *Double Weight* papers, *Portalure Y,* with a *silk* texture, is heavier. Literature indicates that silk texture was achieved by embossing the baryta-coated paper (see *Table 2.1*), which may have compressed the paper more, resulting in a thinner profile than others obtained through wet-pressing. The Ilford *Rayon* texture resembles the silk Kodak texture, with *Rayon* papers also generally being thinner yet heavier.

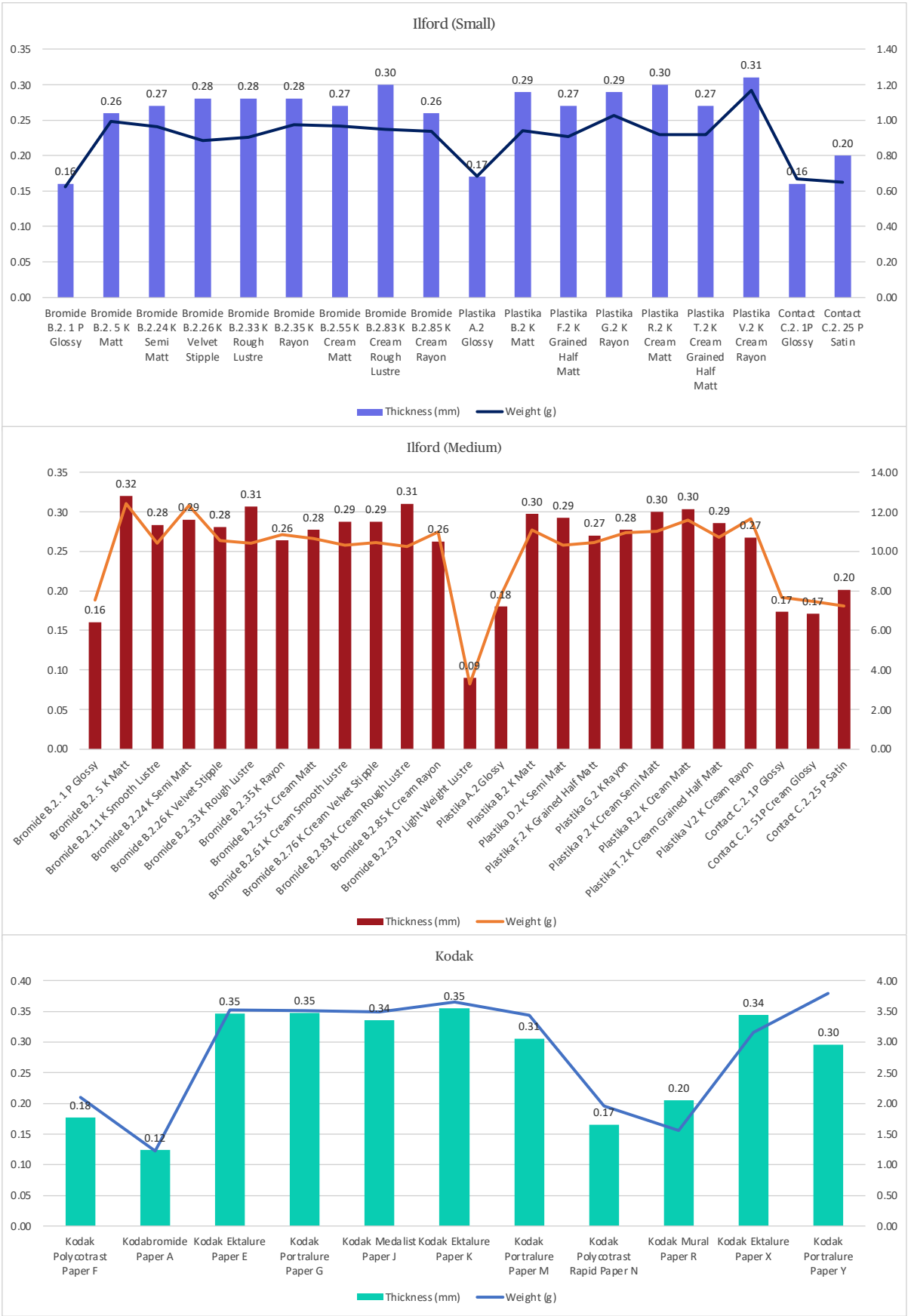

Figure 4.11 Thickness and weight measurements results

4.2 UV-induced visible fluorescence: photo-documentation and microscopy

One of the first aspects noted in UV-induced visible fluorescence was the varying degrees of fluorescence among the samples. Images capturing the emulsion side are presented in *Appendix B.2*, while those from the paper support are grouped in *Appendix B.3*.

Ilford sets

The IS prints do not present a considerable difference in fluorescence intensity. *Figure 4.12* illustrates how neither *Bromide* white and cream papers, nor *Plastika* and *Contact* samples present the characteristic OBA fluorescence. The weak fluorescence observed could be emitted by the baryta layer and not the OBAs [24]. Similar results were observed in *Paperbase* for an Ilford set from 1948. Besides the two Kodak London papers with OBAs from 1947, no other OBA papers were found before 1950.

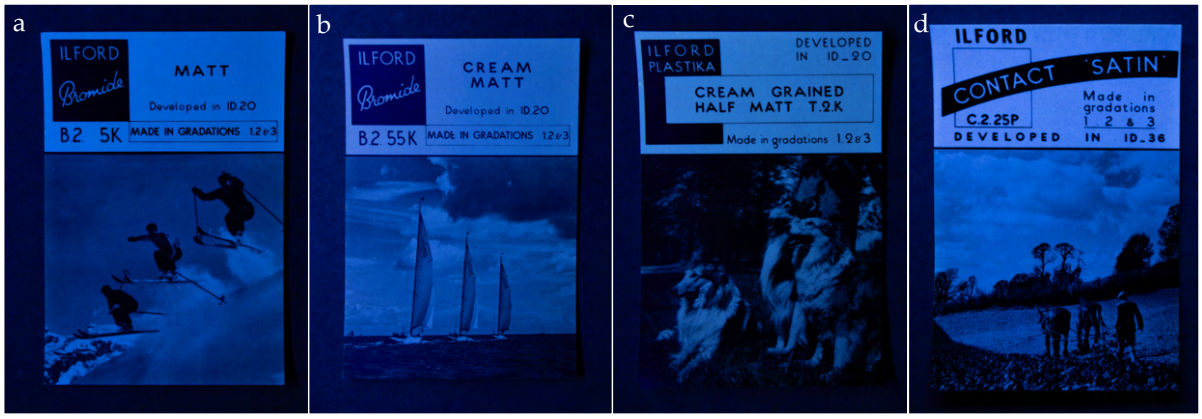

Figure 4.12 UV-induced visible fluorescence: (a) *IS_Bromide B.2. 5K Matt*; (b) *IS_Bromide B.2. 55K Cream Matt*; (c) *IS_Plastika T.2.K Cream Grained Half Matt*; (d) *IS_Contact C.2.25P Satin*

For IM, multiple variations in fluorescence intensity were observed. *Bromide* and *Contact* white papers have a strong fluorescence, compared to the IS samples and IM cream prints. *Plastika* white prints also fluoresced more than IS prints but less than the *Bromide* and *Contact* white IM prints, as shown in *Figure 4.13*. The observation of the prints under UV radiation

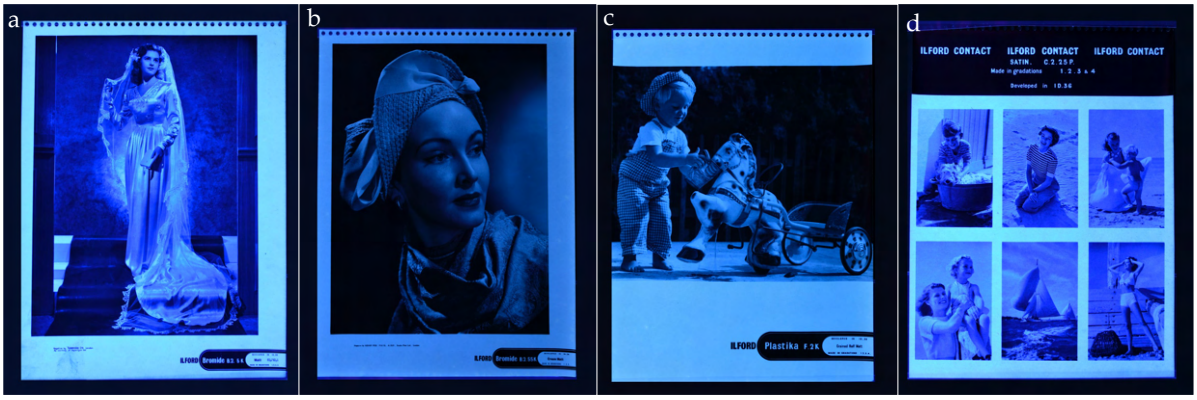

Figure 4.13 UV-induced visible fluorescence: (a) *IM_Bromide B.2. 5K Matt*; (b) *IM_Bromide B.2. 55K Cream Matt*; (c) *IM_Plastika F.2.K Grained Half Matt*; (d) *IM_Contact C.2.25P Satin*

could suggest that OBAs were used for all white papers by the time the IM set was produced, in a higher percentage for *Bromide and Contact* papers, and in a lower percentage for the *Plastika* paper. This may be linked to the *warm-black* image tone of the *Plastika* papers.

The presence of OBAs was also observed on the back of the white IM prints, possibly in a similar percentage to the prints' recto (*Figure 4.14*). Additionally, foxing was noted on the verso of the IM prints.

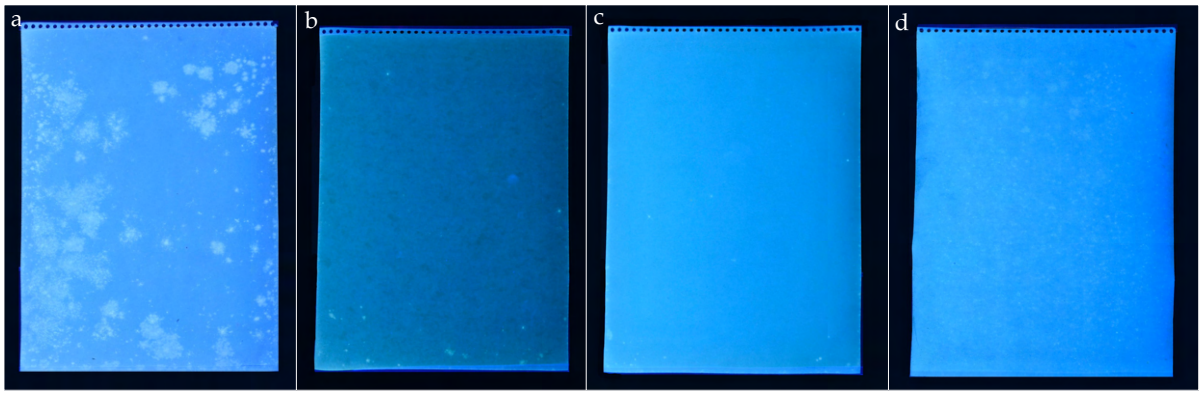

Figure 4.14 UV-induced visible fluorescence: verso of (a) *IM_Bromide B.2. 5K Matt*; (b) *IM_Bromide B.2. 55K Cream Matt*; (c) *IM_Plastika F.2.K Grained Half Matt*; (d) *IM_Contact C.2.25P Satin*

The print *IM_Bromide B.2.23 P Light Weight Lustre* represents a special case. While the emulsion side fluoresces as much as the white Bromide and Contact white prints, the back side has a more uneven violet fluorescence (*Figure 4.15*).

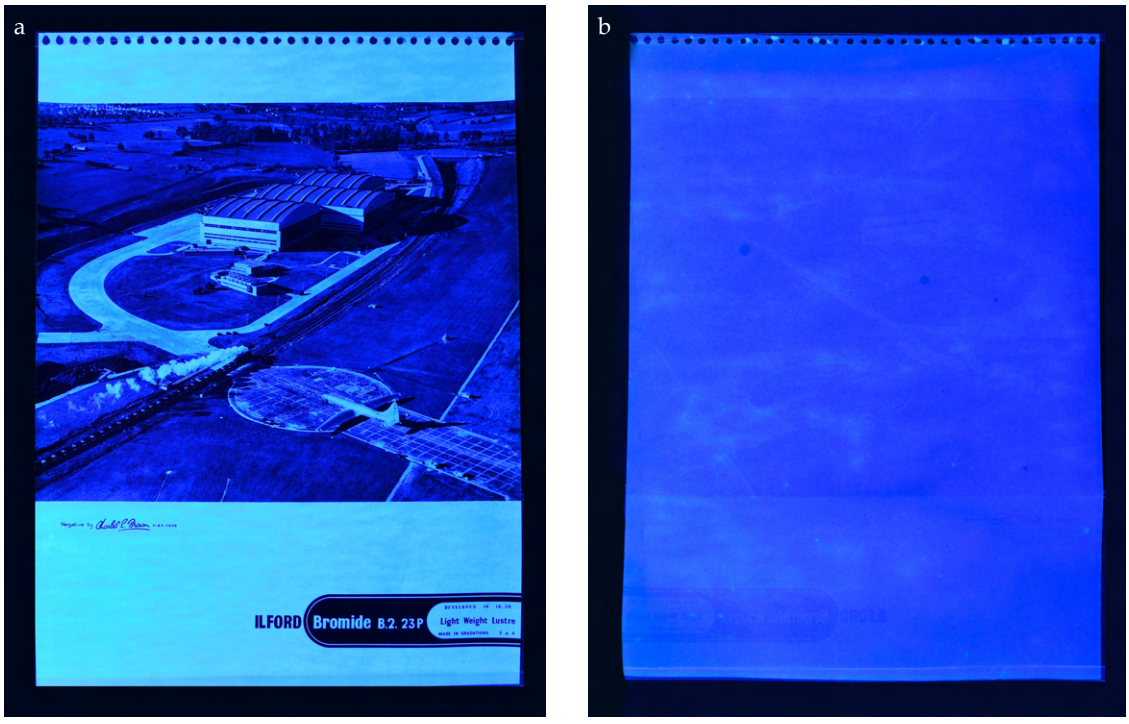

Figure 4.15 UV-induced visible fluorescence: *IM_Bromide B.2. 23 P Light Weigh Lustre*, recto (a), and verso (b)

Despite having a close production date, the UV-induced visible fluorescence allowed to determine that the two Ilford sets were not manufactured in the same year. Therefore, the production time frame for IM is reduced from 1948-1953 to 1949-1953. This also indicates that OBAs were introduced in Ilford photographic paper production between the same time 1949 and 1953, hypostasis also sustained by the information obtained from the interview with a former Ilford employee, who states that in 1949 Ilford was already producing papers with OBAs [12]. In the *Paperbase* results, the first OBAs occurring in Ilford papers start from 1951.

- **Kodak set**

All Kodak prints reflected the UV radiation, both on front and back, but with different intensities (*Figure 4.16.a*). Considering this and their production year (1972), it is possible that they all contain OBAs, but in different concentrations. By observing the verso of the prints, in the case of three prints (*Polycontrast F, Portalure G, and Ektalure X*) it was noted that part of the paper fibres fluoresces differently (*Figure 4.16.c and d*). This could indicate the use of different pulps in the paper support, as different pulps have variable degrees of dye absorption [24]. The UV examination of the back also revealed some degradations, such as brown spots (*Figure 4.17.a*) or various stains (*Figure 4.17.b*).

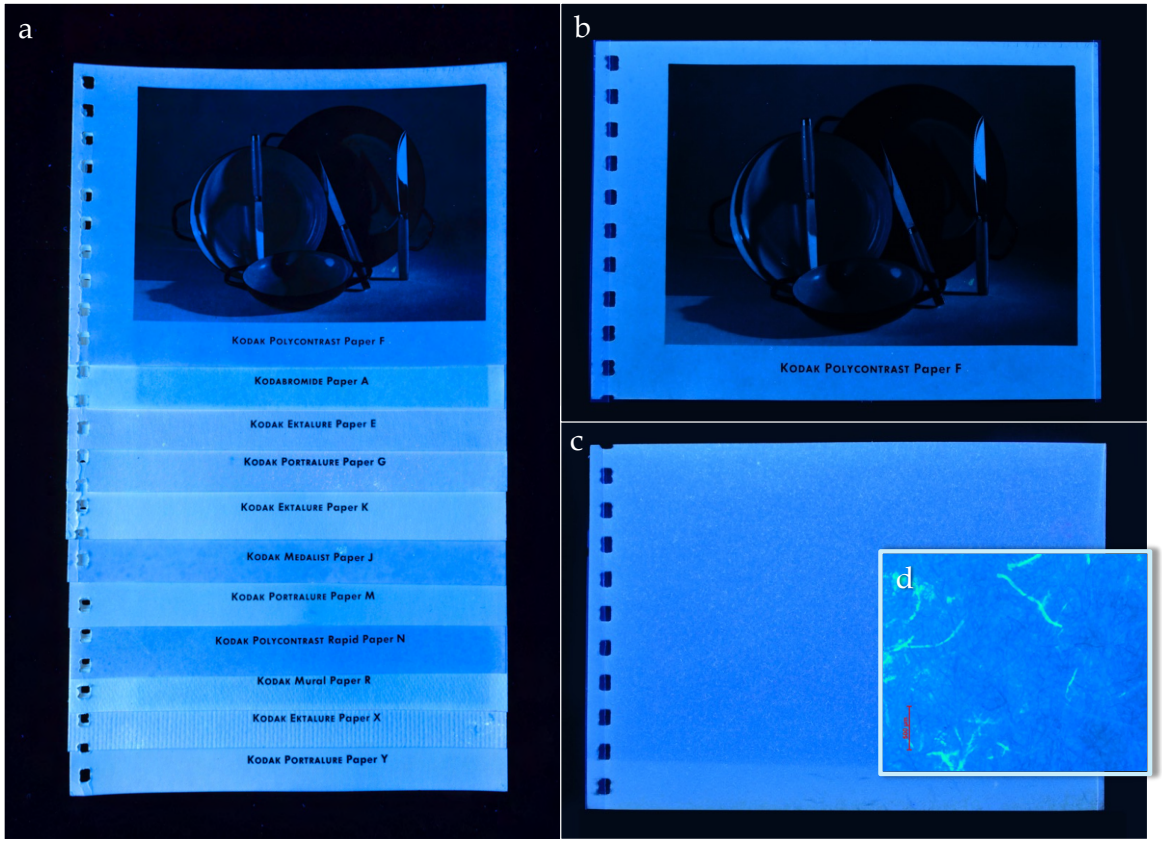

Figure 4.16 UV-induced visible fluorescence: Kodak samples (a); *Polycontrast F:* recto (b), verso (c), and microphotograph of the paper support (d)

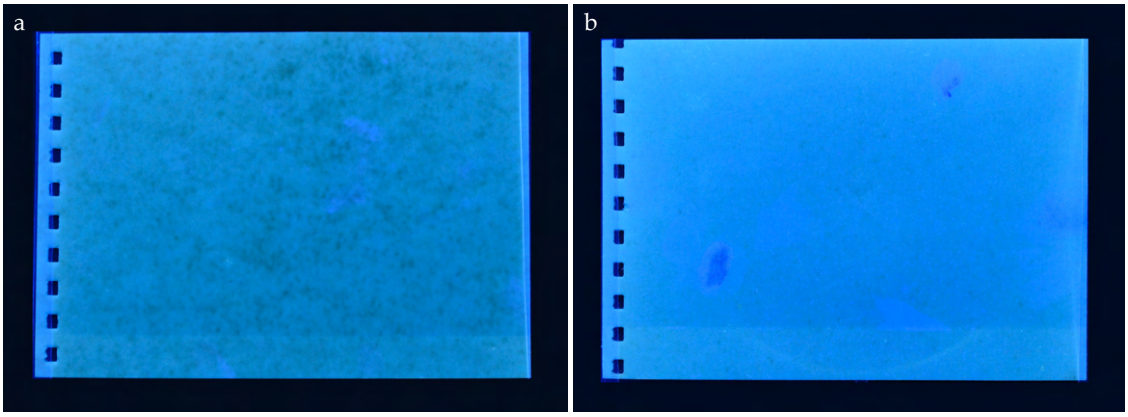

Figure 4.17 UV-induced visible fluorescence: verso of *Medalist J* sample (a) and of *Ektalure X* (b)

4.3 Stratigraphy and material composition: elemental and molecular approaches

4.3.1 Fibre and pulp identification

The test results for pulp identification are summarized in *Table 4.1*, with detailed microphotographs available in *Appendix B.2*. All Ilford prints analyzed, and six Kodak prints (*Kodabromide A, Ektalure E, Ektalure J, Portalure M, Portalure Y*) were determined to have a paper support made of softwood bleached sulphite pulp. The results for Ilford sets, dating from the mid-20th century, align with Messier's findings [1], as it was shown that by that time, softwood bleached sulphite pulp was used in photographic paper manufacturing. While in the 1970s other pulps started to be used, softwood bleached sulphite pulp continued to be used [1]. Therefore, the Kodak results are also expected.

The paper support of four Kodak prints (*Polycontrast F, Portalure G, Polycontrast Rapid N, Mural R*) appears to be made of a combination of two pulp types, also indicated by the UV examination. With the Graff "C" staining test, some fibres turned light brownish, indicating the softwood bleached sulphite pulp, and other turned bluish grey, suggesting the use hardwood bleached sulphite pulp. The use of hardwood pulp is also indicated by the vessel or vascular tracheid with profuse bordered pits identified in *Mural R* (*Figure 4.18*) and the different shapes and sizes of the fibres [72]. The ratio between softwood and hardwood seems to differ

Figure 4.18 Herzberg Stain on *Mural R* (200x); a possible vessel or vascular tracheid identified

among the prints, as observed in both the UV examination and Graff "C" staining.

The Graff "C" staining of *Ektalure X* showed a possible different result. Most fibres turned light brownish, indicating the use of softwood bleached sulphite pulp. However, one fibre appeared light bluish-grey, resembling the shape and form of other softwood fibres, suggesting the possible use of softwood bleached kraft pulp. This mixture is not mentioned in the trend identified in Messier's collection [1]. Nonetheless, the 1970s marked a period of advancements in paper production when sulphite pulp had already started to lose ground to the kraft process [73].

Table 4.1 Results for fibre identification microchemical tests

Samples	**Tests**			
All Ilford papers *Kodabromide A, Ektalure E, Ektalure J, Portalure M, Portalure Y*		**Herzberg**	**Lofton Merritt**	**Graff "C"**
	Micro-photographs (*Plastika V.2.K Cream Rayon*)	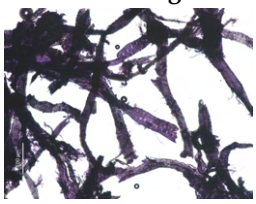	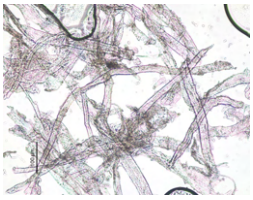	
	Colour	Dark purplish grey	Colourless	Light brownish
	Result[1]	Chemical pulp	Bleached chemical pulp	Softwood bleached sulphite pulp
Polycontrast F Portalure G Polycontrast Rapid N Mural R		**Herzberg**	**Lofton Merritt**	**Graff "C"**
	Micro-photographs (*Polycontrast Rapid N*)	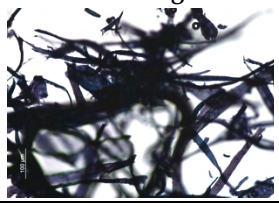	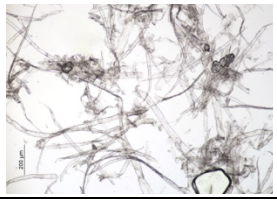	
	Colour	Dark purplish grey & blue	Colourless	Light brownish & bluish grey
	Result[1]	Chemical pulp	Bleached chemical pulp	Softwood bleached sulphite pulp & hardwood bleached sulphite pulp
Ektalure X		**Herzberg**	**Lofton Merritt**	**Graff "C"**
	Micro-photographs (*Ektalure X*)	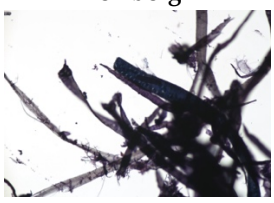		
	Colour	Dark purplish grey & bluish grey	Colourless	Light brownish & light bluish grey
	Result[1]	Chemical pulp	Bleached chemical pulp	Softwood bleached sulphite pulp & softwood bleached kraft pulp

[1] Results were interpreted using the ISO 9184-3, ISO 9184-4, and ISO 9184-5 from 1990.

4.3.2 μ–EDXRF

The results of μ–EDXRF analysis are presented for each sample in *Appendix B.2* and are summarized in *Table 4.2*.

All Ilford white papers, excepting *IM_Bromide B.2.23 P Light Weight Lustre*, showed a similar composition. The elements identified on the emulsion side are sulfur (S), calcium (Ca), strontium (Sr), silver (Ag), barium (Ba) and iron (Fe) (*Figure 4.19*). Additionally, in the paper support spectrum, potassium (K) was detected.

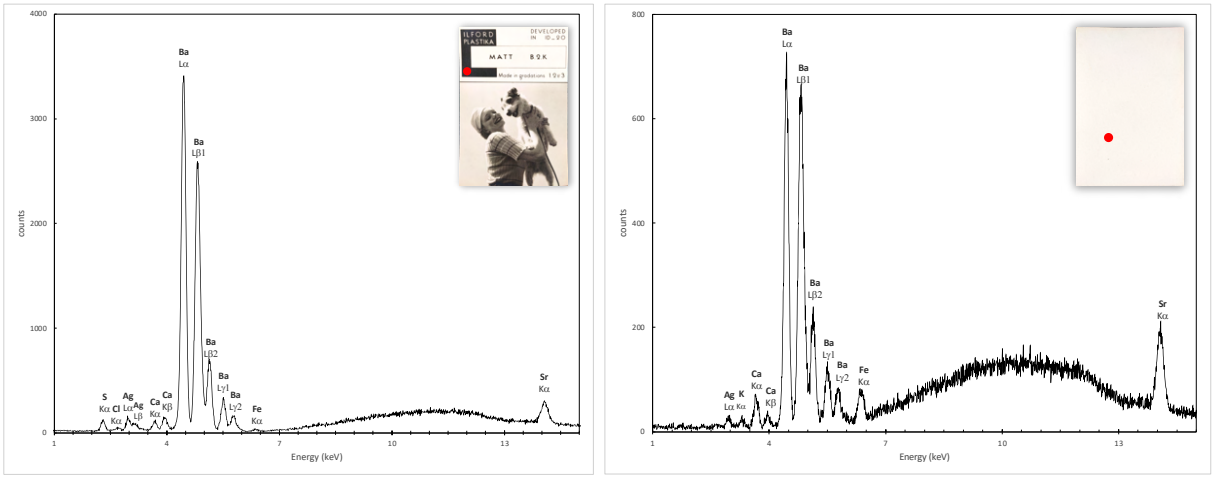

Figure 4.19 μ–EDXRF Spectra of *IS_Plastika B.2.K Matt*: recto (D_{max}) and verso

The same elements were identified in the cream Ilford prints, but the Fe signal was more intense on the back, showing both the Kα and Kβ lines (*Figure 4.20*). Print *IM_Bromide B.2.23 P Light Weight Lustre* exhibited a different elemental composition with only S, Ca, Ag, chromium (Cr) and titanium (Ti) (*Figure 4.21*). The print might not have a baryta coating to separate the paper support from the photographic emulsion.

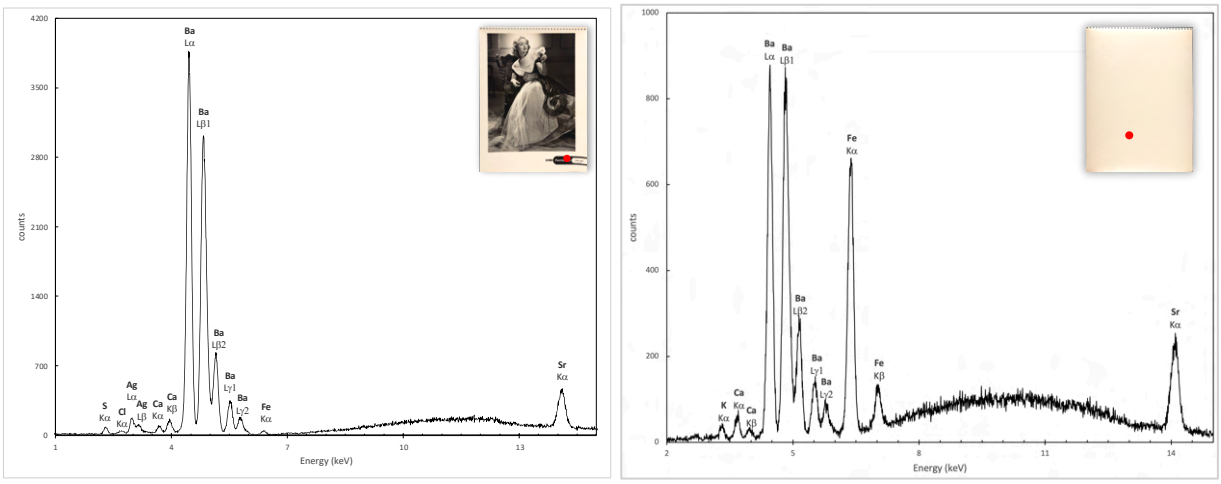

Figure 4.20 μ–EDXRF Spectra of *IM_Plastika V.2.K Cream Rayon*: recto (D_{max}) and verso

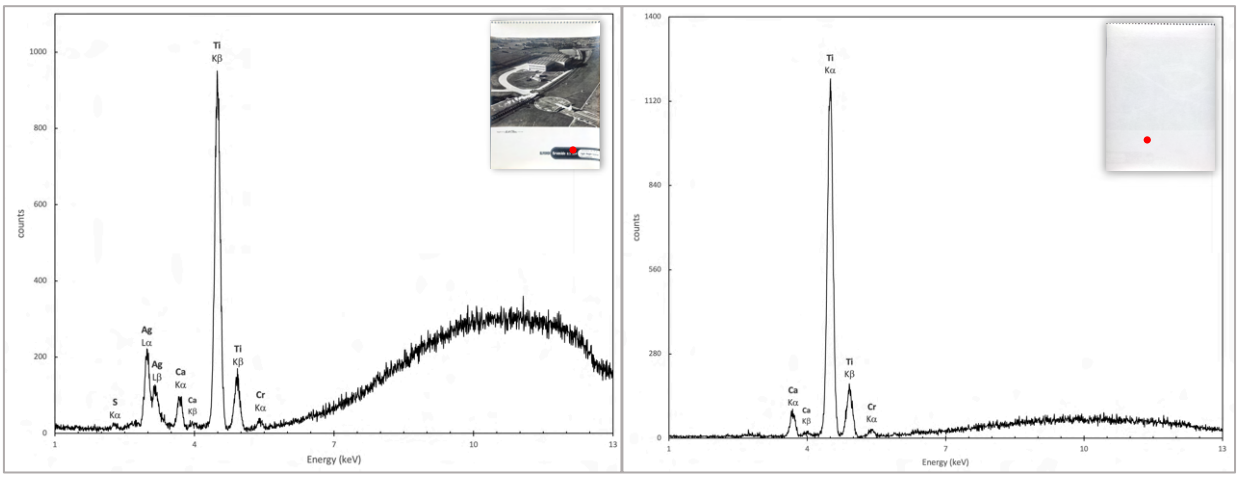

Figure 4.21 μ–EDXRF Spectra of *IM_Bromide B.2.23 P Light Weight Lustre:* recto (D_{max}) and verso

Some particles observed on the back of IM prints were analyzed, revealing the presence of metals such as zinc (Zn), copper (Cu), lead (Pb), and Fe (*Figure 4.22*). These metals may indicate possible contamination of the paper support during manufacturing. However, the ochre particle with a strong Fe signal, found on cream papers, might also suggest the use of an iron-based yellow pigment.

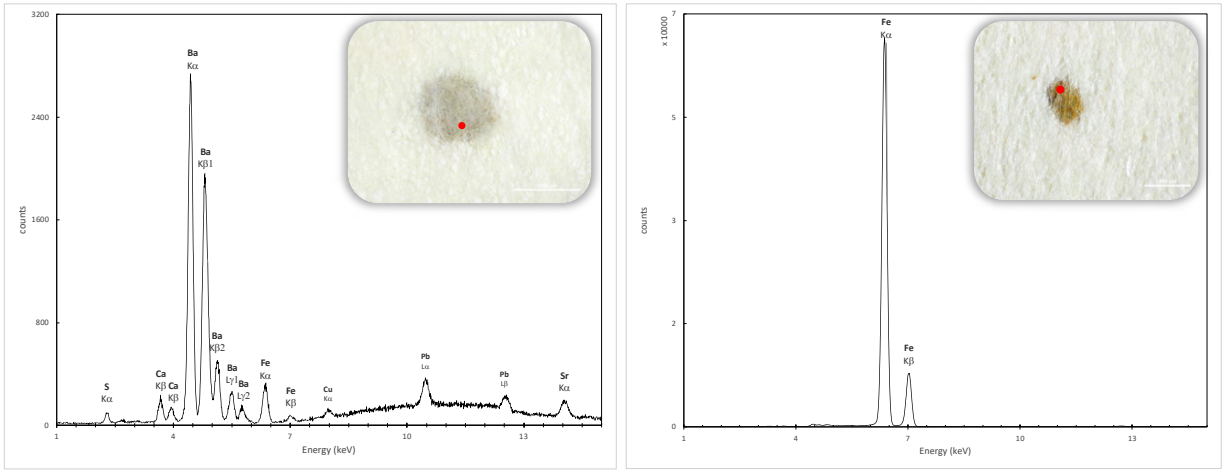

Figure 4.22 μ–EDXRF Spectra of particles identified on the back of *IM_Plastika D.2 K Semi Matt* and *IM_Plastika T.2 K Cream Grained Half Matt*

Excepting *Kodabromide A* and *Mural R*, Kodak prints are similar in composition to white Ilford papers, but they contain chlorine (Cl) on the emulsion side and do not contain Fe. *Portalure M*, which has a matte sheen, also contains silicon (Si) (*Figure 4.23*) on the emulsion side, which can be related to the use of silica (SiO_2) as the matting agent. *Kodabromide A* and *Mural R* prints could also be barytaless paper as *IM_Bromide B.2.23 P Light Weight Lustre*, containing S, Cl, Ag, and Ca but no Ti (*Figure 4.24)*.

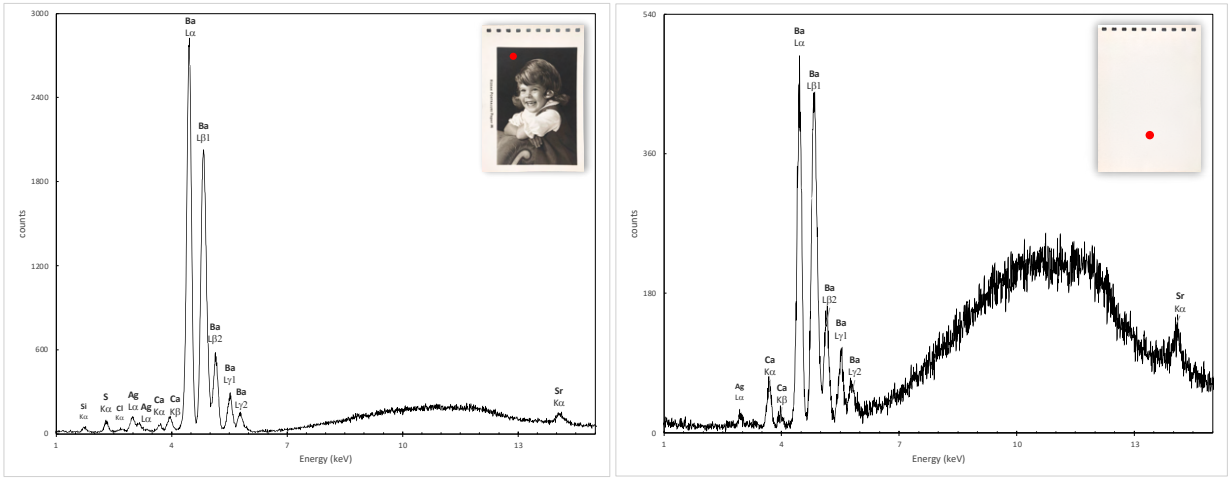

Figure 4.23 μ–EDXRF Spectra of *Portalure M*: recto (D_{max}) and verso

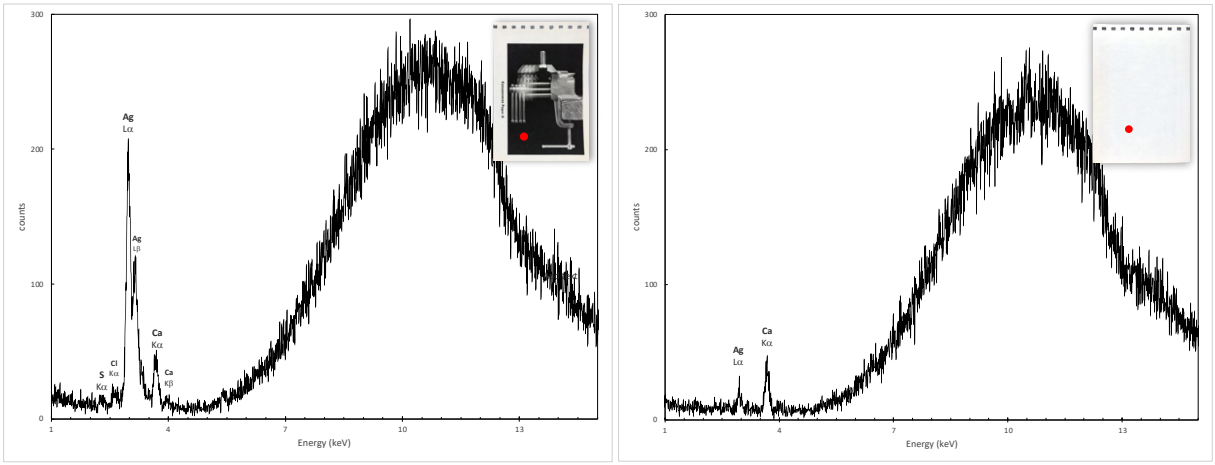

Figure 4.24 μ–EDXRF Spectra of *Kodabromide A*: recto (D_{max}) and verso

Table 4.2 Elements identified by μ–EDXRF (**major** and minor chemical elements)

Samples		**Elements Identified**
Ilford	White prints	**Ba**, Ca, Ag, Sr, S, Fe, K
	Cream prints	**Ba**, **Fe**, Ca, Ag, Sr, S, K
	IM_Bromide B.32.2K Light Weight Lustre	**Ti,** Ca, Ag, Cr, S
Kodak	White: *Polycontrast F, Medalist J, Polycontrast Rapid N* Warm-white: *Ektalure E, Portalure G, Ektalure K* Cream: *Ektalure X, Portalure Y*	**Ba**, Ca, Ag, Sr, S, Cl
	Portalure M	**Ba**, Ca, Ag, Sr, S, Si, Cl
	Kodabromide A & Mural R	**Ag**, Ca, Cl, S

4.3.3 SEM-EDS

Barytaless papers

SEM analysis of the cross-sections revealed that the prints where Ba was not detected did not have an additional isolation layer between the paper support and photographic emulsion, as shown in *Figure 4.25.*

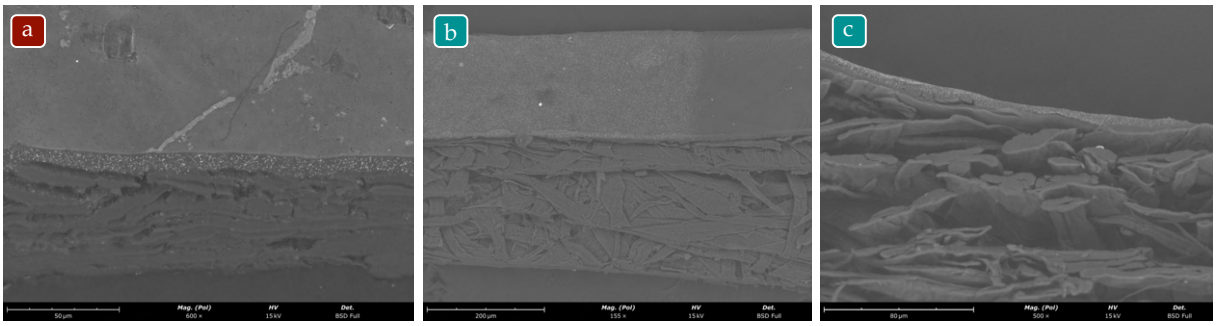

Figure 4.25 SEM-EDS cross-section of print *IM_Bromide B.2.23 P Light Weight Lustre* (a), *Kodabromide A* (b), and *Mural R* (c)

In the Ilford barytaless print, filler particles containing Al and Ti, along with carbon (C) and oxygen (O), were observed at the paper support level (*Appendix B.1, Figure B.1*). While Al cannot be detected with XRF, Ti was observed during μ-EDXRF investigation. The presence of Ti can be explained by a patent from Ilford's paper supplier, which mentions using TiO_2 as a filler to enhance the opacity of very thin papers [18]. No particles were observed for the barytaless Kodak papers, and only C and O were detected (*Appendix B.1*).

In all three barytaless papers, the emulsion layer contains Ag, S, Al, Ca, C, O, and N (*Appendix B.1*). Ag and S are likely related to the image-forming material, while Ca might originate from gelatin derived from bones and cartilages [60]. Al's presence can be attributed to its common use as a gelatine hardener [74].

The protective coating is observable only for the Ilford print, being thick enough that the Ag particles are not visible on the top. This layer contains Ag, S, and Ca (*Appendix B.1, Figure B.2*), with an element attribution similar to the emulsion layer.

Baryta papers

All the other analysed samples present a baryta coating. The cross-sections revealed differences between Ilford's and Kodak's manufacturing practices, and among different paper types. One is related to the paper support of Ilford and Kodak papers (*Figure 4.26*). Ilford samples present filler or sizing particles between the paper fibres, and contain Al, Si, S, C and O in the paper support (*Appendix B.1, Figure B.3*). This might indicate the use of kaolinite $[Al_2Si_2O_5(OH)_4]$ as a filler, as suggested by one patent from the Ilford's paper support supplier [17], or aluminium sulphate $[Al_2(SO_4)_3]$ as an additive to the sizing material (rosin) [60]. In contrast, Kodak samples did not show observable particles in the paper support, and only C and O were detected (*Appendix B.1, Figure B.4*).

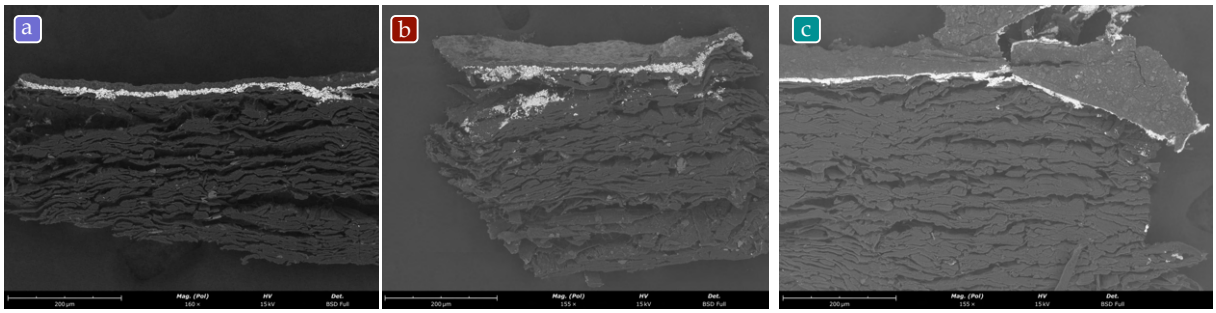

Figure 4.26 SEM-EDS cross-sections: variations of the baryta layer SEM-EDS cross-section of print *IS_Bromide B.2. 5K Matt* (a); *IM_Bromide B.2. 55K Cream Matt* (b); *Portalure M* (c)

The baryta layer differs notably between Ilford and Kodak papers. In Ilford papers, $BaSO_4$ particles vary in size, while Kodak papers have consistently fine and compact $BaSO_4$ particles (*Figure 4.27*). Ilford's glossy prints feature the thickest baryta layer with a flat top surface, containing fine, compact $BaSO_4$ particles. The *Bromide Matt* papers also have a thick baryta layer, but with very coarse particles. *Plastika Matt* and semi-reflective papers have baryta layers of varying thickness, with $BaSO_4$ particles coarser than those in glossy prints but finer than those in *Bromide Matt* papers.

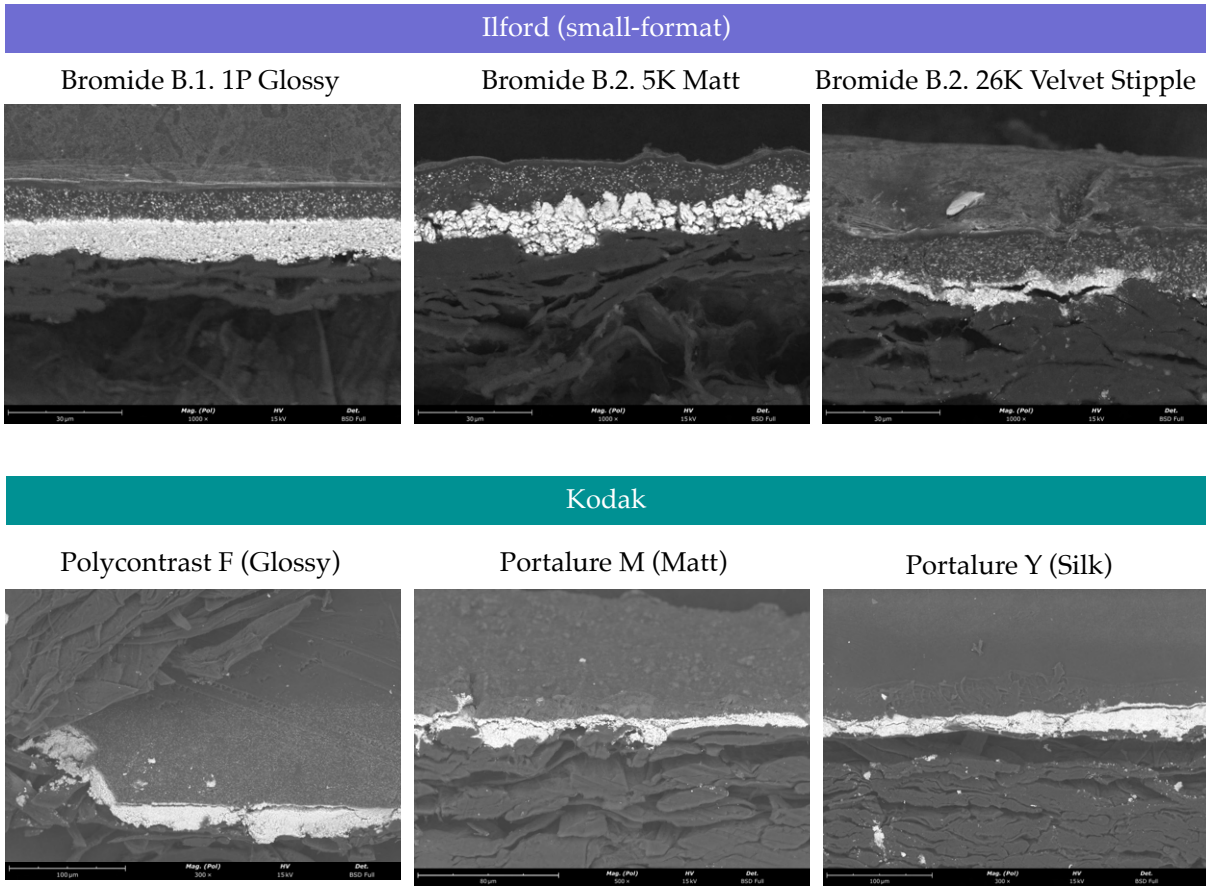

Figure 4.27 SEM-EDS cross-sections: variations of the baryta layer

The elements detected in the baryta layer also differ. Ba, S, Sr, Ca, C, and O were identified for the Ilford papers. Additionally, Al is present in the baryta coating of the Kodak papers. Al can again be related to the hardening agent for gelatine.

The analysis showed the presence of Ag, S, Ca, C, O, and N in the emulsion layer of Ilford samples, and Ag, S, Al, C, O, and N for Kodak. This can indicate that Al was used as a gelatine hardener at Kodak.

The topcoat of Ilford papers had a consistent thickness for all prints, presenting the same elements as the photographic emulsion coating. For Kodak, the topcoat was too thin to be clearly distinguished from the emulsion layer.

The matte prints presented different results for all three sets. In Ilford papers, the baryta layer of *Bromide Matt* differs from *Plastika Matt* papers (*Figure 4.28*). All analyzed matte prints contained Al and Si in the emulsion layer and topcoat. Al is likely linked to the gelatin hardener [74], while Si suggests using SiO_2 as a matting agent [6]. However, the μ-EDXRF analysis did not detect the Si, as with the matte Kodak print. The matte effect may also be due to coarse, large $BaSO_4$ particles. For *Portalure M*, SEM-EDS confirmed the presence of Si in both the baryta and emulsion layers (*Appendix B, Figure B.4*). μ–EDXRF also detected Si, indicating the probable use of SiO_2 as a matting agent.

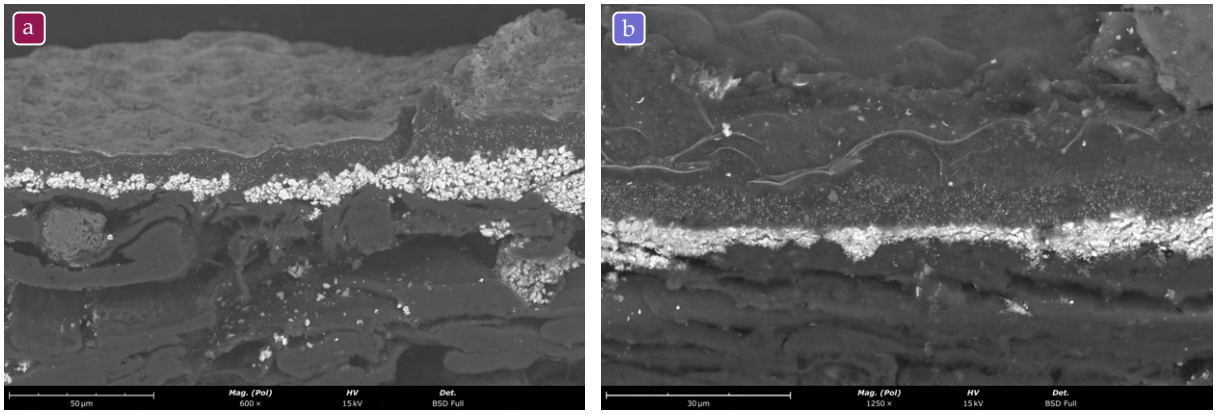

Figure 4.28 SEM-EDS cross-section of print *IM_Bromide B.2. 5K Matt* and *IS_Plastika R.2.K Cream Matt*

It was further remarked that no Fe was detected for any Ilford cream prints. This may be due to the small analysis area in SEM-EDS, which could miss Fe-containing particles or molecules.

4.3.4 Raman

The Raman spectrum from the paper support of the analysed white Ilford print only revealed the signals from the cellulose. However, when the cream papers were analysed on the ochre particles (*Figure 4.29*), the spectrum indicated the presence of an iron oxide yellow pigment. The characteristic bands centred around 243, 298, 394, and 549 cm^{-1} correspond to iron (III) oxide-hydroxide [FeO(OH)], suggesting the presence of either goethite [65] or a synthetic pigment known as Yellow 42. The band attributions are detailed in *Table 4.3*.

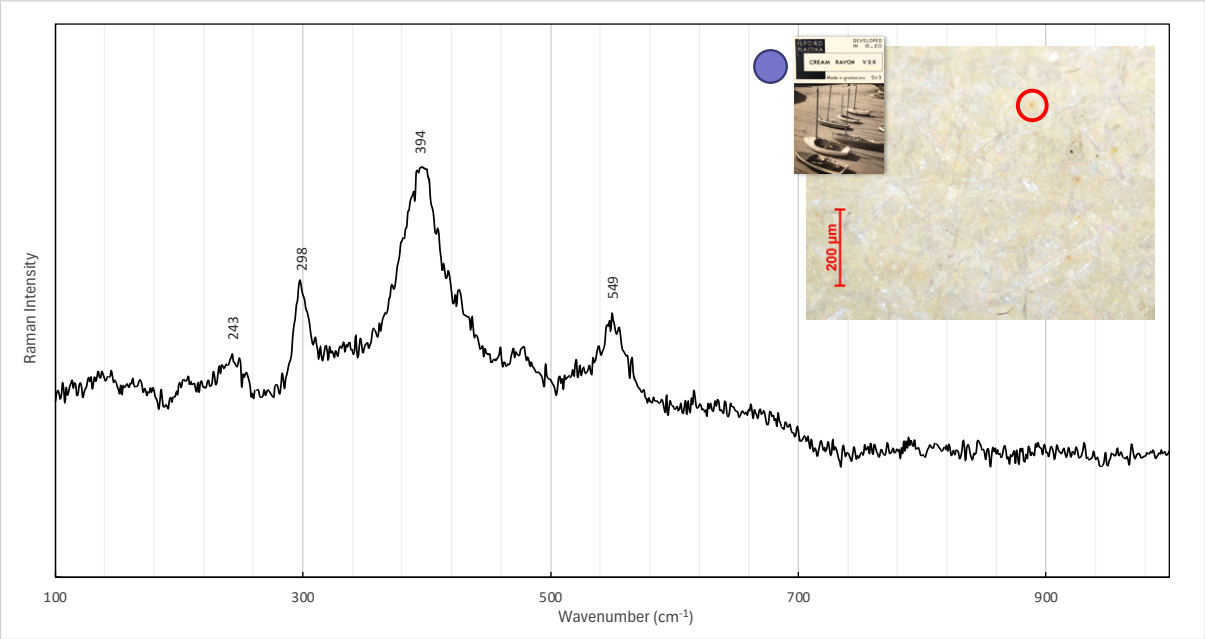

Figure 4.29 Raman spectrum of the yellow particle - *IS_Plastika V.2.K Cream Rayon* (paper support)

Table 4.3 Bands attribution for the yellow particle Raman spectrum - *IS_Plastika V.2.K Cream Rayon* (paper support)

Compound	Bands (cm^{-1})	Assignment [63]
FeO(OH)	243, 298	δ(FeO)
	394, 549	ν(FeO)

The spectrum of the *IM_Bromide B.2.23.P Light Weight Lustre* paper support (*Figure 4.30*) suggests the presence of titanium dioxide (TiO_2) in anatase form as showed by the bands around 142, 396, 521 and 640 cm^{-1} [75]. The bands attribution is presented in *Table 4.4.*

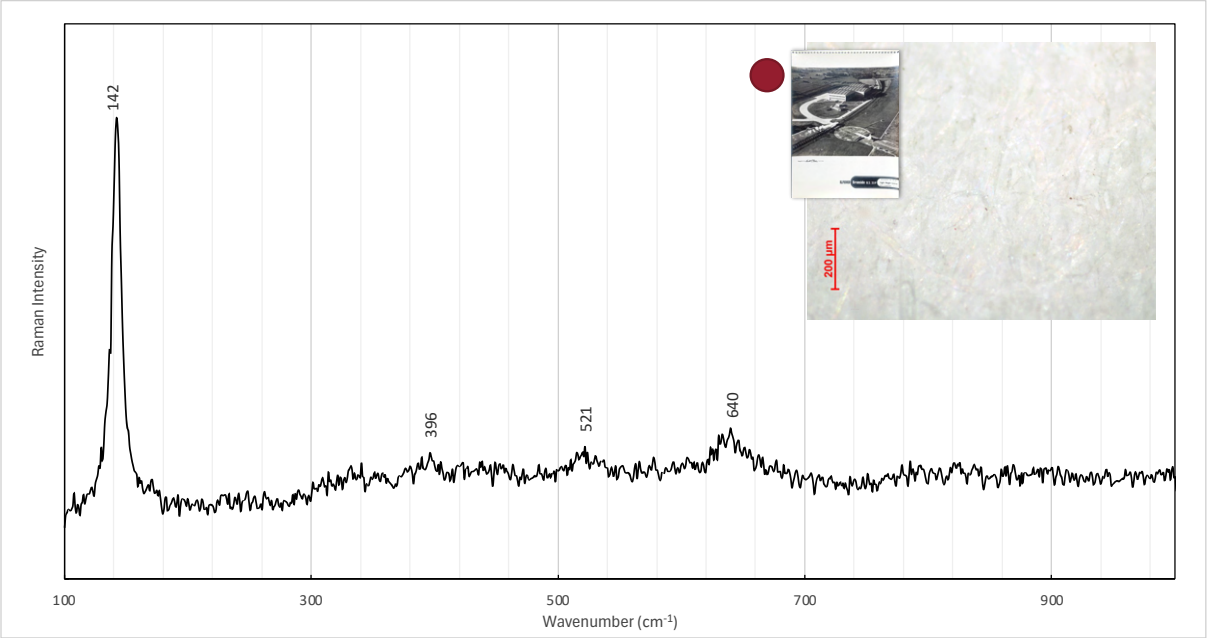

Figure 4.30 Raman spectrum of the *IM_Bromide B.2.23.K Light Weight Lustre* (paper support)

Table 4.4 Bands attribution in the Raman spectrum of *IM_Bromide B.2.23.K Light Weight Lustre* (paper support)

Compound	**Bands (cm^{-1})**	**Assignment** [80]
Anatase form of TiO_2	142, 640	ν_s (O-Ti-O)
	396	δ_s (O-Ti-O)
	521	δ_{as} (O-Ti-O)

4.3.5 ER-FTIR

As expected, the ER-FTIR spectra of the analysed samples show differences based on the analysis spot, surface features, and stratigraphy. In prints with a baryta layer, the spectra exhibit bands corresponding to the protein nature of the gelatin emulsion and the presence of $BaSO_4$. This is illustrated in *Figure 4.31*, where the spectrum of *IS_Bromide B.2.1.P Glossy* is compared with a reference ER-FTIR spectrum of gelatin. The band attributions are detailed in *Table 4.5*.

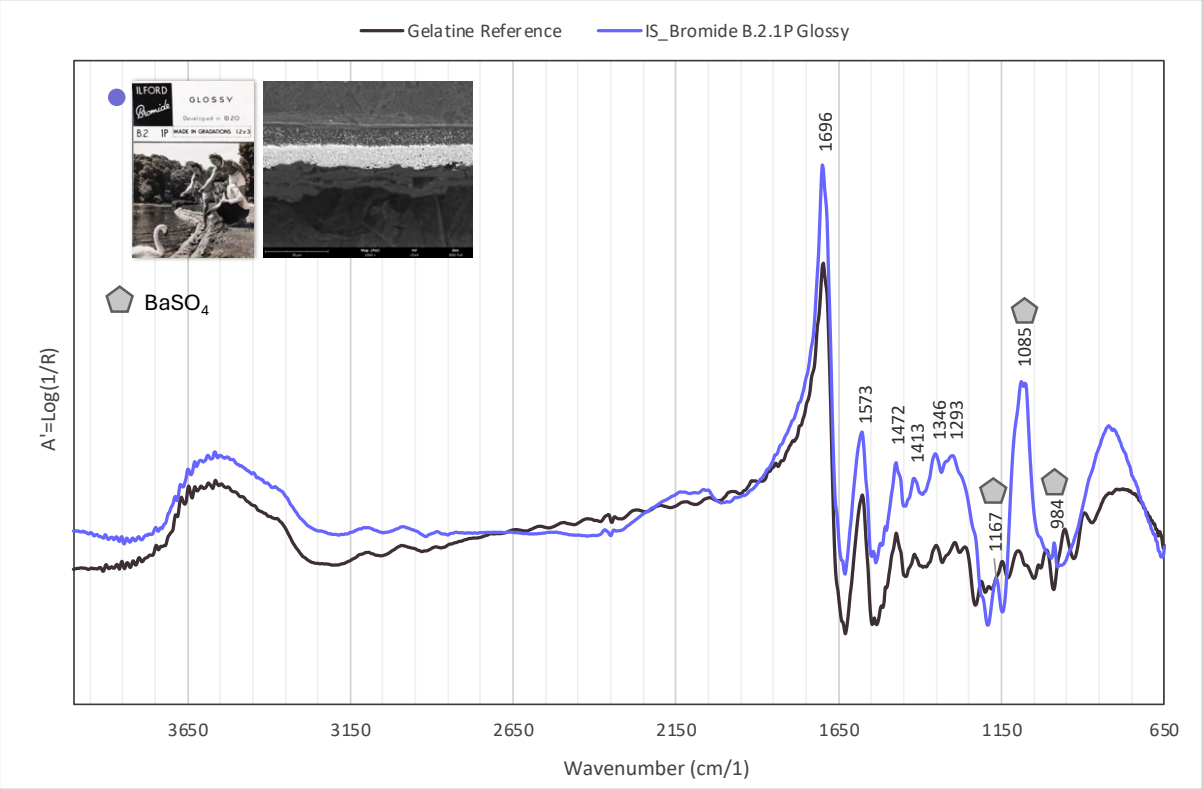

Figure 4.31 ER-FTIR spectrum of *IS_Bromide B.2.1.P Glossy* and gelatine ER-FTIR reference spectrum

Table 4.5 Bands attribution in the ER-FTIR spectrum of *IS_Bromide B.2.1 P Glossy*

Compound	Bands (cm^{-1})	Assignment
Protein binder (possible gelatine)	1696	Amide I
	1573	Amide II
	1472, 1413, 1346	δN–H ν(FeO)
Barium Sulphate	1167, 1085, 984	νSO_4^{-2}

Some differences were observed when measuring D_{max} areas, compared with D_{mid} and D_{min} (*Figure 4.32*). While the signal from the $BaSO_4$ is slightly less intense for D_{max} measurement, the bands are still visible. In the literature it was suggested $BaSO_4$ signal would be blocked in D_{max} regions [52]. This might be due to the variations in the baryta coating or the thickness of the image layer and protective topcoats.

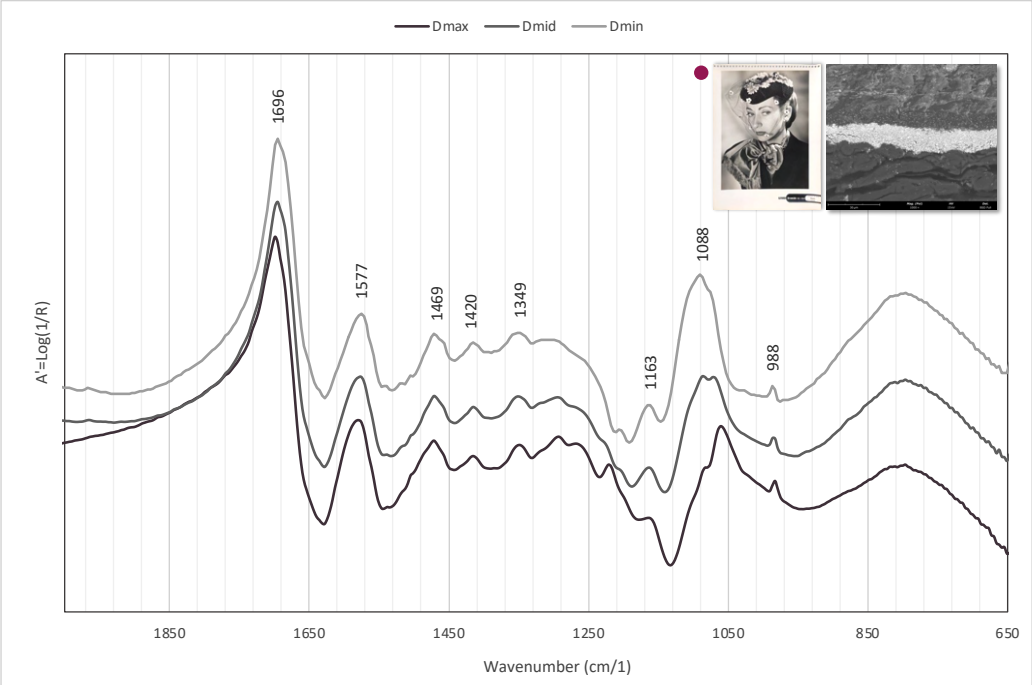

Figure 4.32 ER-FTIR spectra of *IM_Bromide B.2.35 K Rayon* for D_{max}, D_{mid}, and D_{min} analysis

In the spectra of glossy and semi-reflective papers, the contribution of the baryta layer is still visible even in areas with higher image densities. However, for matte papers, it becomes harder to identify, with the only distinguishable $BaSO_4$ band centered around 980 cm^{-1} (*Figure 4.33* and *4.34*). Identifying matting agents was not possible; although SEM-EDS analysis indicated the presence of Si in the emulsion layer of the Kodak matte print (*Portalure M*), no SiO_2 signals were detected in the ER-FTIR spectra.

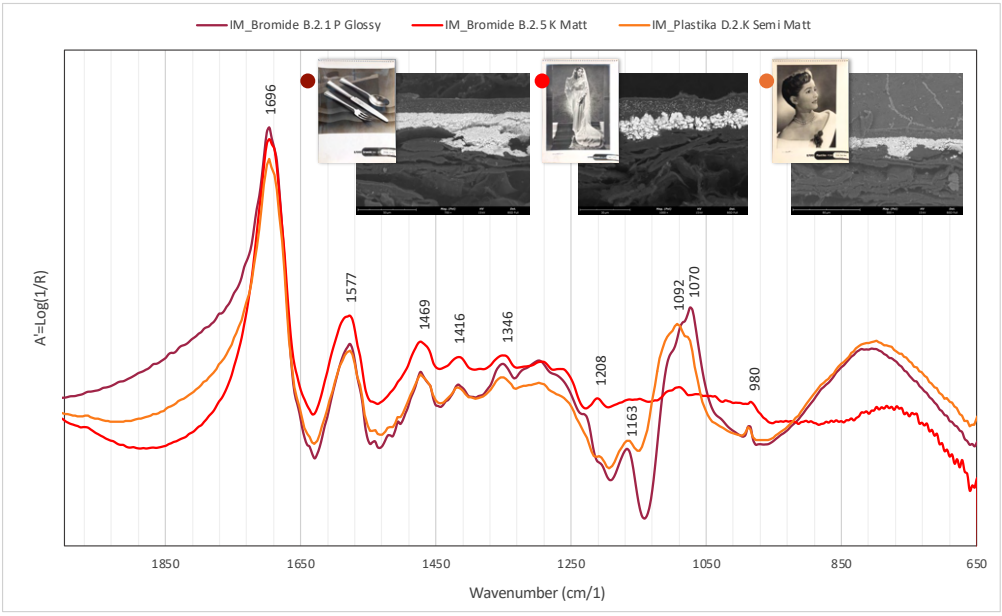

Figure 4.33 ER-FTIR spectra (D_{mid}) of IM papers with different surface features

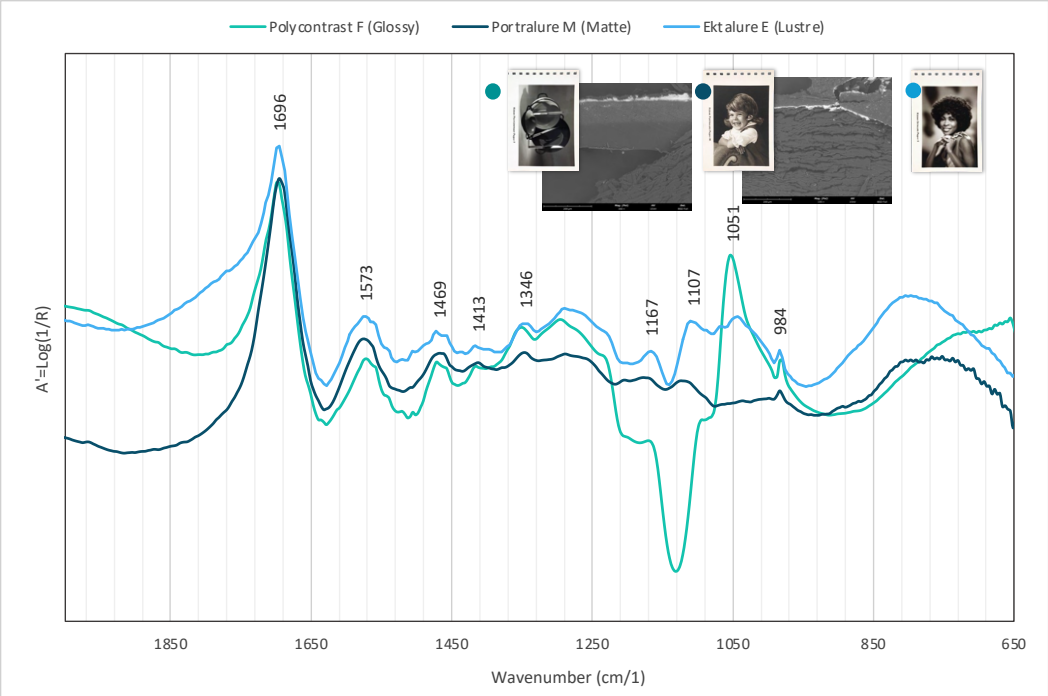

Figure 4.34 ER-FTIR spectra (D_{mid}) of Kodak papers with different surface features

The only case where the 980 cm^{-1} band for $BaSO_4$ is not detectable is in the spectra for the barytaless papers, where only the representative bands for gelatine are shown (*Figure 4.35*). This highlights the potential of the 980 cm^{-1} band as a more reliable marker for the baryta layer. While the previous study on ER-FTIR [52] focuses more on the band centred around 1080 cm^{-1}, the 980 cm^{-1} can also be seen in the spectra of those case studies.

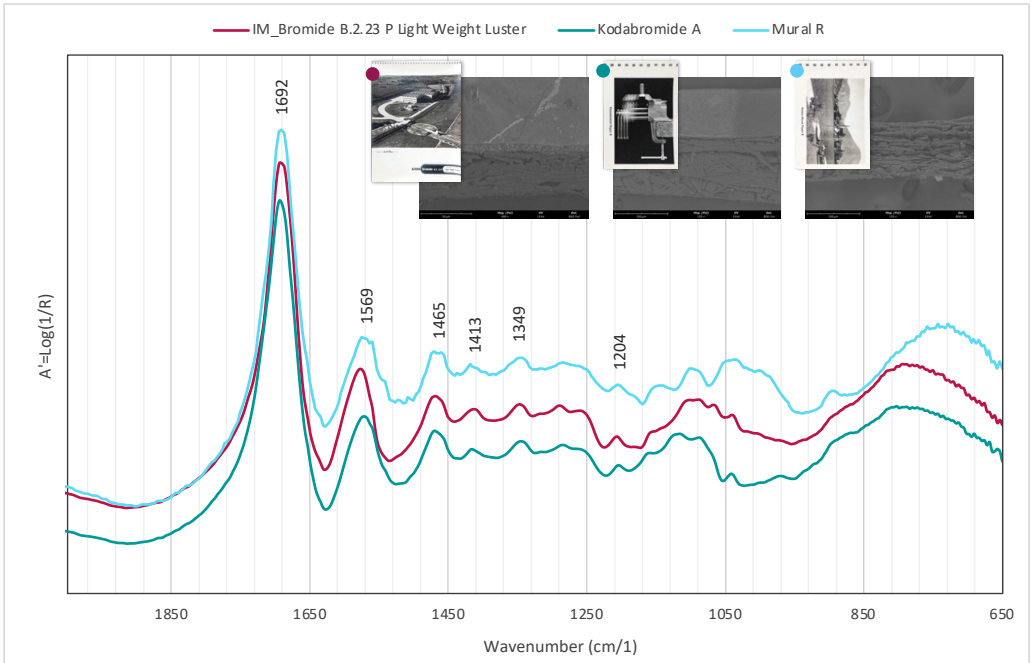

Figure 4.35 ER-FTIR spectra of samples without the baryta coating

The main observations gathered throughout the multi-analytical characterisation of the samples are summarised in *Table 4.6*.

Table 4.6 Summary of the multi-analytical characterisation of the sample sets

		Ilford small-format (IS)	Ilford medium-format (IM)	Kodak
General aspects	**Image of the sets**		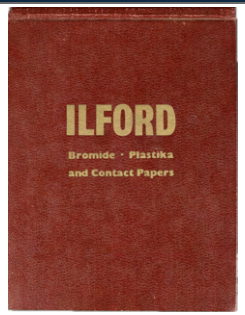	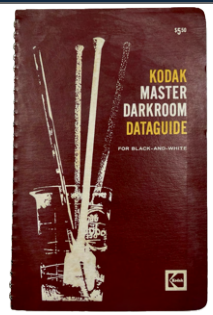
	Provenance	UK	UK	U.S.
	Production Date	Ca. 1948	Ca. 1948-1953	1972
	Target audience	amateur	professional	amateur
	Number of samples	18	25	11
	Samples' format (cm)	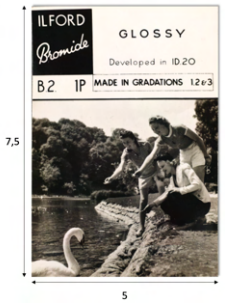		
	Paper classes (and the number of samples in the set)	Bromide (9) Plastika (7) Contact (2)	Bromide (13) Plastika (9) Contact (3)	Polycontrast (1) Polycontrast Rapid (1) Kodabromide (1) Ektalure (3) Portalure (3) Medalist (1) Mural (1)

Visual characteristics	**Base tint** Photo-documentation	The set contains two base tints: white and cream (easy to differentiated with the naked eye)	The set contains two base tints: white and cream, but *IM_Bromide B.2.23.P Light Weight Lustre* seems brighter than the white papers (easy to differentiated with the naked eye)	The set contains three base tints: white, warm-white, and cream (hard to differentiated with the naked eye).
	Colourimetry – range of L*a*b* values for recto	**White**: **L***: 88.27 - 92.4 **a***: (-0.41) - 0.93 **b***: 3.62 -11.65 **Cream**: **L***: 88.11 - 90.84 **a***: 1.72- 3.55 **b***: 15.38 -17.98	**White**: **L***: 87.71 - 93.39 **a***: (-0.38) - 0.22 **b***: 4.01 -11.73 **Cream**: **L***: 88.27 - 90.91 **a***: 1.07- 3.2 **b***: 16.26 -19.51 *IM_Bromide B.2.23.P Light Weight Lustre:* **L***: 94.27 **a***: - 0.65 **b***: 7.34	**White**: **L***: 91.03 - 92.93 **a***: (-0.63) - (-0.19) **b***: 6.19 -10.46 **Warm-white**: **L***: 91.5 - 93.3 **a***: (-0.64) - (-0.4) **b***: 8.29 -10.75 **Cream**: **L***: 91.77 - 93.01 **a***:(-0.52) – 0.15 **b***: 10.41 -10.95
	Surface features Texture (microphotographs in raking light)	The available surfaces are: *Glossy* *Matt* *Semi Matt* *Velvet Stipple* *Rough Lustre* *Rayon* *Grained Half Matt* *Satin*	The available surfaces are: *Glossy* *Matt* *Smooth Lustre* *Semi Matt* *Velvet Stipple* *Rough Lustre* *Rayon* *Light Weight Lustre* *Grained Half Matt* *Satin*	The available surfaces are: *F: Smooth, Glossy* *A: Smooth, Lustre* *E: Fine grained, Lustre* *G: Fine grained, Lustre* *J: Smooth, High Lustre* *K: Fine grained, High Lustre* *M: Smooth, Matte* *N: Smooth, Lustre* *R: Tweed, Lustre* *X: Tapestry, Lustre* *Y: Silk, High Lustre*
	Glossiness (range of ΔL*SCI-SCE values)	Glossy: 2.08 – 2.13 Semi reflective: 0.59 – 1.13 Matt: 0.18-0.3 The trend observed is similar to the one of the gloss units (*Paperbase*)	Glossy: 2.14 – 2.2 Semi reflective: 0.39 – 1.32 Matt: 0.2-0.25	Glossy: 1.89 Lustre: 1.06 – 1.88 Heigh lustre: 0.82 – 1.05 Matt: 0.21 The trend observed is similar to the one of the gloss units (*Paperbase*)
	Thickness (mm) and weight (g)	The set contains prints in two weights: *Single Weight* Thickness: 0.16 – 0.2 Weight: 0.62 – 0.68	The set contains prints in two weights: *Single Weight* Thickness: 0.16 – 0.2 Weight: 7.22 – 7.78	The set contains prints in three weights: *Single Weight* Thickness: 0.17 – 0.2 Weight: 1.56 - 2.09

		Double Weight Thickness: 0.26 – 0.31 Weight: 0.91 – 1.17	*Double Weight* Thickness: 0.26 – 0.32 Weight: 10.32 – 12.41 *IM_Bromide B.2.23.P Light Weight Lustre* Thickness: 0.09 Weight: 3.28	*Double Weight* Thickness: 0.3 – 0.35 Weight: 3.16 – 3.8 *Light Weight* Thickness: 0.12 Weight: 1.22
	UV- induced visible flourescence photo-documentation	• No OBAs were detected. • Only a few flourescent spot were observed on the back.	• OBAs were detected in all white papers, in higher concentration for *Bromide* and *Contact*, and lower concentrations in *Plastika*. • *IM_Bromide B.2.23.P Light Weight Lustre* has an uneven, more violet flourescence on the back. • Numerous foxing spots were observed.	• OBAs were detected in all papers, but in different concentrations. • For *Polycontrast F, Portalure G, and Ektalure X* it was noted that part of the paper fibres fluorescence differently. • Only a few spots and stains were observed on the back.
Stratigraphy and composition	**Stratigraphy** SEM-EDS	All prints contain four main layers: ▪ paper support ▪ baryta layer ▪ photographic emulsion layer ▪ topcoat 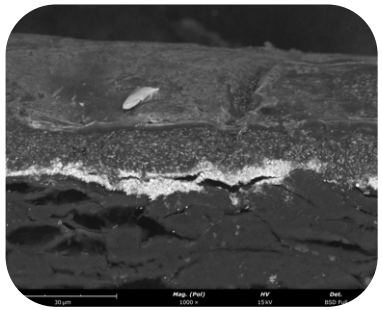	Same as IS. 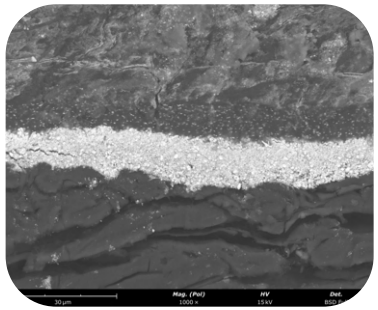 Except for *IM_Bromide B.2.23.P Light Weight Lustre* which does not have a baryta layer:	Same as IS. 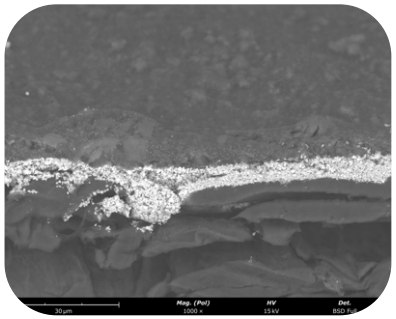 Except for *Kodabromide A* and *Mural R* which do not have a baryta layer:

	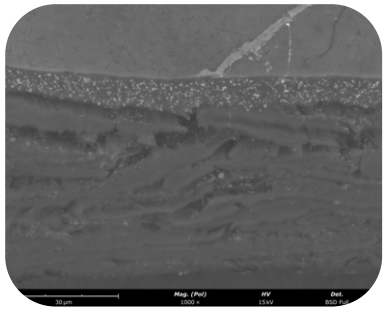		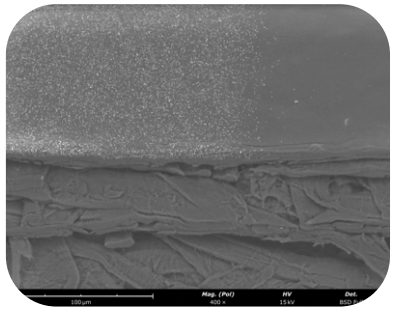
Composition (by layer**):**			
Paper support			
Pulp identification	• Softwood bleached sulphite pulp.	• Same as IS.	• Softwood bleached sulphite pulp - *Kodabromide A, Ektalure E, Ektalure J, Portalure M, Portalure Y.* • Softwood bleached sulphite pulp & hardwood bleached sulphite pulp – *Polycontrast F, Portalure G, Polycontrast Rapid N, Mural R.* • Softwood bleached sulphite pulp & softwood bleached kraft pulp - *Ektalure X*
Elements identified SEM-EDS & µEDXRF	• SEM showed that filler or sizing particles present in the paper support. • Elements identified: Al, Si, K, Ca, Fe. • Fe signal is significantly stronger for the cream papers.	• Same as IS. • The *IM_Bromide B.2.23.P Light Weight Lustre* has a different composition, containing: Al, Ca, and Ti.	• With SEM, no particles were observed in the paper support. • SEM only detected C and O in the paper support, and from the µ-EDXRF results, Ca could possibly be linked to the paper support.
Raman	• Iron (III) oxide-hydroxide [FeO(OH)] was detected, suggesting the presence of goethite or Yellow 42.	• TiO_2 in the form of anatase was identifed	

	Baryta layer			
	SEM-EDS & µEDXRF	• SEM showed that the thickness of the layer and the size of $BaSO_4$ particles varies significantly with the prints' type. • Elements identified: Ba, S, Sr, and Ca.	• Same as IS	• SEM showed that while the thickness of the layer can vary, the size of $BaSO_4$ particles is consistent. • Elements identified: Ba, S, Sr, and Al.
	ER-FTIR	• The baryta layer could be identified in all papers with ER-FTIR	• Same as IS	• Same as IS
	Photograhic emulsion layer			
	SEM-EDS & µEDXRF	• Elements identified: Ag, S, and Ca. * Matte prints present **Al** and **Si (**only detected with SEM-EDS)	• Same as IS	• Elements identified: Ag, S, and Al (possibly a gelatine hardener). * Matte print contains **Si** (also detected with XRF)
	Protective topcoats			
	SEM-EDS & µEDXRF	• Same elements as the emulsion • The thickness of all prints' topcoats is similar.	• Same as IS	• It was very hard to observe the difference between emulsion layer and the topcoat.

4.4 Composition implications in the conservation of the case studies

Documenting paper features and analysing their composition help us understand conservation challenges that may arise during treatment or exhibition. Various surface features can pose challenges, particularly during surface cleaning and flattening treatments.

Identifying OBAs in white IM and Kodak prints through UV-induced visible fluorescence was also beneficial for their conservation. To prevent OBA degradation, aqueous treatments should be avoided, and they should be protected from UV radiation when displayed. UV examination also revealed foxing on the back of most IM prints and, to a lesser extent, on Kodak prints.

SEM-EDS cross-section analysis indicated that Ilford papers have a thicker protective topcoat, potentially making their surface more resistant to physical degradation than Kodak papers.

The anatase form of TiO_2 present in *IM_Bromide B.2.23P Light Weight Lustre* can be problematic, as anatase is considered the less stable form of TiO_2. Additionally, the literature suggests that the rutile form contributes to OBA degradation [22]. However, no specific references were found regarding anatase's effect on OBAs.

Additionally, no studies were found concerning the effects on photographic paper of the iron (III) oxide-hydroxide pigment, present in the cream Ilford papers.

4.5 Methodology proposal for material composition identification: advantages and disadvantages

In this initial attempt to characterize fibre-based DOPs regarding surface features, composition, and stratigraphy, various advantages and disadvantages of the analytical techniques were identified. These are grouped in *Table 4.7*.

Table 4.7 Advantages and disadvantages of the methodology used.

Analytical technique	Advantages	Disadvantages
Photo-documentation	• Helps to observe the main visual differences. • No sampling required or contact with the object.	• The observation can be subjective.
Thickness and weight measurements	• Easily available equipment. • No sampling required.	• Thickness measurements require contact with the print, but polyester sheets are used for protection.
Colourimetry	• Accurate colour documentation and comparison. • Can also be used for glossiness characterisation.	• Difficult to compare results obtained with different equipment.

	• No sampling required or direct contact.	
Fibre identification microchemical tests	• Simultaneous identification of pulp and fibre types. • Minimal sample required.	• Requires sampling. • Colour identification depends on illumination, reference samples available and operator's experience.
XRF	• Does not require contact with the prints or sampling. • It is useful for a qualitative elemental characterisation.	• Difficult elements attribution for each layer. • Limited to analysis from Al to U. • Limited to small areas, which restricts comprehensive material characterisation.
SEM-EDS	• Elemental information about each layer.	• Requires sampling. • Cannot be used on artworks.
Raman	• Molecular information about small particles (2μm). • No sampling necessary.	• Can burn the samples or cause crystallographic transformation [63].
ER-FTIR	• Does not require contact with the prints or sampling.	• Hard to interpret spectra. • Lack of reference libraries.

While the current methodology effectively uncovered numerous details about the prints, there are multiple ways to improved it. For texture characterization, using a profilometer for roughness measurements might provide more accurate data. To enhance glossiness characterization, incorporating gloss measurements could verify whether the glossiness classification determined through colourimetric measurements aligns with values from a gloss meter.

The identification of OBAs could be improved through photo-documentation consistency in UV-induced visible fluorescence. Using a UV calibration target could ensure consistent colour intensity. Additionally, fluorescence spectroscopy could be used to confirm the presence of OBAs in case of uncertainties.

For composition analysis, using ATR-FTIR or micro-FTIR on the white Ilford prints could help identify whether the Al and Si signals detected with SEM-EDS in the paper support are due to kaolinite or aluminium sulphate sizing.

Additionally, applying statistical methods like PCA could significantly advance the identification of papers using non-contact techniques that do not require sampling. ER-FTIR, in particular, might benefit from this approach, given the variation in spectra with changes in surface features and stratigraphy.

5
CONCLUSIONS

This research aimed to deepen the understanding of 20th-century fibre-based DOPs by examining their manufacturing processes and characterizing their surface features, stratigraphy, and composition. Through a multi-analytical characterization of three sample sets – two from Ilford (mid-20th century) and one from Kodak (1972) – the study aimed to address a significant gap in understanding European photographic papers.

The work started by researching the photographic paper manufacturing process, detailing the main production steps, methods to achieve various surface features, and important aspects of paper composition. By consulting patents and interviews with former employees in the photographic paper industry, it was discovered that by 1949, Ilford was producing the *Bromide* paper with OBAs. They also introduced ascorbic acid to counteract the Fe contamination. The supplier for paper support was also using kaolinite and TiO_2 as fillers.

To establish the methodology for the samples' multi-analytical characterization, current and prior studies on reference papers were reviewed, and common approaches for characterizing fibre-based DOPs were researched.

The methodology followed brought many insights into samples' composition, stratigraphy and surface characteristics. The analysis of visible characteristics represented the first step into observing the main differences between the papers. While photo-documentation, colourimetry, and thickness and weight measurements helped accurately document the papers' physical properties, they also gave some clues about print manufacturing. By comparing the thickness and weight measurements, and the colourimetric difference between prints' recto and verso, it was possible to gain a better understanding of potential variations in the thickness and opacity of the baryta layer. While not currently used for characterising prints' glossiness, the colourimetry measurements (L* SCI-SCE) could become a valuable option if tested alongside a glossmeter in the future.

The UV-induced visible fluorescence allowed us to observe the presence of OBAs in the white papers from the IM set and in Kodak papers. For the IM set, this discovery helped narrowing the potential production timeframe to 1949-1953. For the Kodak papers, it indicated that some papers were made from pulp mixtures, a conclusion further supported by the microchemical tests for fibre and pulp identification.

With the analytical techniques used for understanding papers stratigraphy and composition, the differences between the sets and types of papers were further enhanced. One of

the first observation was the presence of papers without baryta coating from both manufacturers, one sample being included in the IM set and two in the Kodak one. *IM_Bromide B.2.23 K Light Weight Lustre*, presented multiple distinguishing features, being thinner, lighter, and brighter than the rest and having an uneven violet fluorescence on the back. The presence of the anatase form of TiO2 was also detected in the paper support.

Differences in composition further consisted of the fact that all Ilford papers presented Al and Si in the paper support, which might indicate use of kaolinite as a filler, or aluminium sulphate as an additive to the sizing material. Fe was also detected with XRF in the Ilford papers, having a weak signal for the white papers and a stronger one for the cream ones. The possible use of an iron-based pigment for obtaining the cream base tint was sustained by the Raman spectroscopy, which detected the iron (III) oxide-hydroxide in the composition.

With SEM-EDS analysis, the stratigraphy differences were observed. The baryta layer of Ilford papers varied considerably with surface type, while for Kodak, was more consistent. Ilford papers also presented a thicker protective topcoat on all samples. In the Kodak papers, Al was detected in the baryta coating and emulsion layer, which could be related to the hardening agent used.

The methodology used also helped identify the matting agent in the Kodak paper, possibly SiO_2. For the Ilford matte paper, only weak signals of Si were obtained with SEM-EDS. However, considering the baryta coating, the matte surface could be produced by the coarse and large $BaSO_4$ particles.

The ER-FTIR analysis reflected the changes in surface characteristics and stratigraphy. It helped distinguish the papers with and without the baryta coating, based on the $BaSO_4$ characteristic band centred at 980 cm^{-1}. The differences observed in the spectra of papers with various surface features could be a promising clue that this method could help with photographic paper identification if combined with statistical methods.

The results were also helpful in understanding the conservation implications of the prints characteristics, composition and stratigraphy in their treatment, display, and storage. Although the data obtained contain valuable information, the research could further benefit from the use of statistical methods to facilitate the identification of papers. Testing the effects of different conservation treatments could be a future step in this study, together with researching the effect of iron (III) oxide-hydroxide and anatase form of TiO_2 on photographic papers.

BIBLIOGRAPHY

[1] P. Messier, 'Notes on Dating Photographic Paper', *Topics in Photographic Preservation*, vol. 11, pp. 123–130, 2005.

[2] B. E. Savedoff, *Transforming images: how photography complicates the picture*. Ithaca, NY: Cornell University Press, 2000.

[3] D. Stulik, A. Kaplan, *The atlas of analytical signatures of photographic processes. Silver gelatin*. Los Angeles, The Getty Conservation Institute, 2013.

[4] W. Wei, S. Stigter, 'Surface Roughness, Appearance, and Identification of AGFA-Gevaert', *Topics in Photographic Preservation*, vol. 17, pp. 11–24, 2017.

[5] B. Lavédrine, *Photographs of the past: process and preservation*. Los Angeles: Getty Conservation Institute, 2009.

[6] G. Weaver, *A Guide to Fiber-Base Gelatin Silver Print Condition and deterioration*. Rochester, NY, 2008.

[7] P. Messier, 'Les Émulsions Industrielles au XXe Siècle/20th Century Black and White Papers', *Le Vocabulaire de la Photographie*, 2008.

[8] J. M. Reilly, *Care and identification of 19th-century photographic prints*. G-2S. Rochester, NY: Eastman Kodak Co, 1986.

[9] K. Funderburk, G. Weaver, *A Guide to Surface Characteristics: Kodak Fibre Base Black-and-White Papers*, 2009.

[10] R. J. Hercock, G. Jones, *Silver by the ton: the history of Ilford Limited, 1879-1979*. London; New York: McGraw-Hill Book Co, 1979.

[11] A. Catford, 'Report on the export trade of Ilford Limited'. Sep. 04, 1947.

[12] A. Farnley, 'My Life in the Photographic Industry: Part 1', *The Quarterly. The Journal of the British Association of Paper Historians*, no. 99, pp. 8–13, Jul. 2016.

[13] A. Farnley, 'My Life in the Photographic Industry: Part 2', *The Quarterly. The Journal of the British Association of Paper Historians*, no. 101, pp. 15–20, Jan. 2017.

[14] M. Fisher, 'Ilford History and Chronology'. Accessed: Oct. 09, 2022. [Online]. Available: https://www.photomemorabilia.co.uk/Ilford/Chronology%20-%20Intro.html

[15] Glory Mill, *Glory Mill*. Wiggins Teape Limited, 1977.

[16] H. Holik, Ed., *Handbook of paper and board*. Weinheim: Wiley-VCH, 2006.

[17] F. Herbert, 'Improvements in the production of photographic printing paper', GB908075A, 1960

[18] The Wiggins Teape Group Limited, 'Improvements in and relating to the manufacture of paper and other cellulosic sheet materials', GB627759A, 1947

[19] G. Harrison, 'The laboratories of Ilford Limited', *Proc. R. Soc. Lond. B*, vol. 142, no. 906, pp. 9–20, Feb. 1954, doi: 10.1098/rspb.1954.0002.
[20] M. Fisher, 'Ilford Roden Street 1944'. Accessed: Oct. 16, 2022. [Online]. Available: https://www.photomemorabilia.co.uk/Ilford/RodenSt_1944.html
[21] J. Jarché, *Daily Herald Photograph: Ilford factory, applying photographic emulsion*. 1934. Accessed: Aug. 10, 2024. [Black-and-white photography]. Available: https://collection.sciencemuseumgroup.org.uk/objects/co8825562/daily-herald-photograph-ilford-factory-applying-photographic-emulsion
[22] R. Mustalish, 'Optical brighteners: history and technology', *Studies in Conservation*, vol. 45, pp. 133–136, Jan. 2000, doi: 10.1179/sic.2000.45.Supplement-1.133.
[23] R. Wetzel, 'Optical Brighteners - A Study of Water Solubility', *Topics in Photographic Preservation*, vol. 11, pp. 73–78, 2005.
[24] P. Messier *et al.*, 'Optical Brightening Agents in Photographic Paper', *Journal of the American Institute for Conservation*, vol. 44, no. 1, pp. 1–12, 2005.
[25] Lens Media Lab, 'Paperbase'. Accessed: Aug. 23, 2024. [Online]. Available: https://paperbase.xyz
[26] D. H. Norris, J. Gutierrez, Eds., *Issues in the conservation of photographs*. in Readings in conservation. Los Angeles: Getty Conservation Institute, 2010.
[27] S. Connors-Rowe *et al.*, 'Optical Brighteners in Black-and-White Photographic Paper: Appearance and Degradation', *Journal of the American Institute for Conservation*, vol. 46, no. 3, pp. 199–213, Jan. 2007, doi: 10.1179/019713607806112251.
[28] S. Stigter, 'To replace or not to replace? Photographic material in site-specific conceptual art', *ICOM-CC 14th Triennial meeting preprints*, vol. I, 2005, Accessed: May 12, 2024. [Online]. Available: https://www.academia.edu/1073615/To_replace_or_not_to_replace_Photographic_material_in_site_specific_conceptual_art
[29] C. R. Johnson *et al.*, 'Pursuing automated classification of historic photographic papers from raking light images', *Journal of the American Institute for Conservation*, vol. 53, no. 3, pp. 159–170, Aug. 2014, doi: 10.1179/1945233014Y.0000000024.
[30] Lens Media Lab, 'Lens Media Lab', Yale University. [Online]. Available: https://lml.yale.edu
[31] C. Dune *et al.*, 'Characterization of black-and-white silver gelatin fiber-based photographic prints', *Topics in Photographic Preservation*, vol. 11, Jan. 2005.
[32] Fotomuseum Antwerp, 'The Gevaert paper project, unlocking a historical collection', Fotomuseum Antwerp Collection. Accessed: Dec. 07, 2023. [Online]. Available: https://fomu.be/en/watch-read/the-gevaert-paper-project-unlocking-a-historical-collection
[33] J. Warda, Ed., *The AIC guide to digital photography and conservation documentation*, Third edition. Washington, DC: American Institute for Conservation of Historic and Artistic Works, 2017.
[34] R. Boatright, 'The Graphics Atlas: Applied', *Topics in Photographic Preservation*, vol. 14, 2011.

[35] K. Vessot *et al.*, 'Correlation between gloss reflectance and surface texture in photographic paper', *Scanning*, vol. 37, no. 3, pp. 204–217, May 2015, doi: 10.1002/sca.21201.
[36] S. Wagner *et al.*, 'Linnaeus Tripe and Lightly Albumenized Prints in the 1850s: Characterization, Analysis and Process Identification', *Journal of the American Institute for Conservation*, vol. 59, no. 3–4, pp. 218–234, Oct. 2020, doi: 10.1080/01971360.2019.1609824.
[37] P. Carnazza *et al.*, 'Retouching matt contemporary paint layers: a new approach using natural polymers', *5th Edition of the International Meeting on Retouching of Cultural Heritage*, pp. 384–393, 2019.
[38] E. Fisher, 'Decoding: A Guide to Kodak Paper Surface Characteristics', *Collections*, vol. 14, no. 2, pp. 207–225, Jun. 2018, doi: 10.1177/155019061801400207.
[39] P. Abry *et al.*, 'Multiscale Anisotropic Texture Analysis and Classification of Photographic Prints: Art scholarship meets image processing algorithms', *IEEE Signal Process. Mag.*, vol. 32, no. 4, pp. 18–27, Jul. 2015, doi: 10.1109/MSP.2015.2402056.
[40] A. G. Klein *et al.*, 'Deep learning classification of photographic paper based on clustering by domain experts', in *2016 50th Asilomar Conference on Signals, Systems and Computers*, Pacific Grove, CA, USA: IEEE, Nov. 2016, pp. 139–143. doi: 10.1109/ACSSC.2016.7869011.
[41] C. Parker, P. Messier, 'Automating art print authentication using metric learning', presented at Proceedings of the Twenty-First Innovative Applications of Artificial Intelligence Conference, 2009.
[42] P. Messier, E. Frank, 'Art into data | engineering WImBo', in *2018 52nd Annual Conference on Information Sciences and Systems*, Princeton, Mar. 2018, pp. 1–4. doi: 10.1109/CISS.2018.8362311.
[43] Abbaspour, M. *et al.*, 'Object:Photo. Modern Photographs: The Thomas Walther Collection 1909–1949 at The Museum of Modern Art.', Object:Photo. Accessed: Jun. 28, 2023. [Online]. Available: moma.org/objectphoto
[44] K. Pollmeier, J. Arney, 'Edge reflection analysis: a new technique for the documentation and characterization of photographic and other glossy surfaces', *Studies in Conservation*, vol. 47, no. sup3, pp. 160–164, Sep. 2002, doi: 10.1179/sic.2002.47.s3.033.
[45] W. Wei, *Innovative technology in art conservation: original appearance and viewer perception*. in Conservation in focus. Routledge, Taylor & Francis Group, 2024.
[46] J. M. Sexton, P. Messier, 'Photographic Paper XYZ: "De Facto" Standard Sizes for Silver Gelatin Paper', *Journal of the American Institute for Conservation*, vol. 53, no. 4, pp. 219–235, Nov. 2014, doi: 10.1179/1945233014Y.0000000030.
[47] TAPPI, *Fiber analysis of paper and paperboard*, T401, 2008.
[48] ISO, *Paper, board and pulps - Fibre furnish analysis - Part 5: Lofton-Merritt staining test*, ISO 9184-5, 1990.
[49] ISO, *Paper, board and pulps - Fibre furnish analysis - Part 4: Graff 'C' staining test*, ISO 9184-4, 1990.
[50] M. Camille, 'An analytical study of Eugène Atget's photographs at the Museum of Modern Art', *Topics in Photographic Preservation*, vol. 12, Jan. 2007.

[51] C. B. Zamboni *et al.*, 'Non-destructive analysis in the study of historical photographs by pXRF and ATR-FTIR spectroscopies', *Journal of Forensic Sciences*, vol. 66, no. 3, pp. 1048–1055, 2021, doi: 10.1111/1556-4029.14680.

[52] J. M. Walker, B. Berrie, 'Influence of image density and interfacial surfaces on ER-FTIR spectra of 19th century photographic print processes', *Journal of Cultural Heritage*, vol. 63, pp. 1–10, Sep. 2023, doi: 10.1016/j.culher.2023.07.007.

[53] A. McClelland *et al.* 'Specular Reflection FTIR: A Non-Contact Method for Analyzing Coatings on Photographs and Other Cultural Materials', *Journal of the American Institute for Conservation*, vol. 59, no. 2, pp. 123–136, Apr. 2020, doi: 10.1080/01971360.2019.1660546.

[54] J. M. Walker, 'ER-FTIR spectroscopy as a characterization tool for 20th century silver gelatin photographs', presented at the Materials of Photography: an interdisciplinary symposium organised by The National Archives and the Victoria and Albert (V&A) Museum, online, Sep. 2023.

[55] M. Oravec *et al.* 'Identification of the historic photographic print materials using portable NIR and PCA', *Microchemical Journal*, vol. 150, p. 104202, Nov. 2019, doi: 10.1016/j.microc.2019.104202.

[56] A. Martins, *et al.*, 'Non-destructive dating of fiber-based gelatin silver prints using near-infrared spectroscopy and multivariate analysis', *Analytical and Bioanalytical Chemistry*, vol. 402, no. 4, pp. 1459–1469, Feb. 2012, doi: 10.1007/s00216-011-5566-2.

[57] Dusan Stulik, A. Kaplan, 'The Atlas of Analytical Signatures of Photographic Processes: Its Past, Present, and the Future', vol. Topics in Photographic Preservation, no. 15, pp. 249–263, 2013.

[58] T. Čechák, *et al.*, 'Application of X-ray fluorescence in an investigation of photographic heritage', *Radiation Physics and Chemistry*, vol. 116, pp. 8–13, Nov. 2015, doi: 10.1016/j.radphyschem.2015.05.015.

[59] A. Modica *et al.*, 'XRF analysis to identify historical photographic processes: The case of some Interguglielmi Jr.'s images from the Palermo Municipal Archive', *Radiation Physics and Chemistry*, vol. 135, pp. 76–80, Jun. 2017, doi: 10.1016/j.radphyschem.2017.02.026.

[60] R. Herrera Garrido, *Conservación y restauración de fotografía*. Madrid: Editorial Síntesis, 2022.

[61] L. J. O. Fernandes, 'Characterization and Identification of Printed Objects', Master, Universidade de Nova de Lisboa, Lisbon, 2008.

[62] P. Messier, D. Stulik, *Understanding 20th-century photographs: the baryta layer symposium*. 2006.

[63] B. Stuart, *Analytical techniques in materials conservation*. Chichester, England ; Hoboken, NJ: John Wiley & Sons, 2007.

[64] Ilford, *Printing and Enlarging*, First Edition. London: Ilford Limited, 1948.

[65] Ilford, 'Albums for Societies', *Ilford News for Photographic Societies*, no. 4, Feb. 1939.

[66] Kodak, *Kodak Papers*. England: Kodak Limited, 1949.

[67] Kodak, *Kodak Master Darkroom Dataguide for Black-and-White*, 4th ed. U.S.: Kodak, 1972.

[68] J. Mitchell, *The Ilford Manual of Photography*. 1945. Accessed: Oct. 15, 2022. [Online]. Available: http://archive.org/details/aa086-IlfordManualOfPhotography
[69] M. Fisher, 'ILFORD Multigrade Printing Paper', Photographic Memorabilia. Accessed: Oct. 13, 2022. [Online]. Available: https://www.photomemorabilia.co.uk/Ilford/Multigrade.html
[70] E. Avrami *et al.*, 'Report on Research', in *Values and Heritage Conservation*, Los Angeles: Getty Conservation Institute, 2000.
[71] B. Appelbaum, *Conservation treatment methodology*. USA, 2010.
[72] M. Ilvessalo-Pfäffli, Ed., *Fiber Atlas: identification of papermaking fibers*, Berlin Heidelberg: Springer, 2011.
[73] H. Sixta, Ed., *Handbook of pulp*. Weinheim : [Chichester: Wiley-VCH ; John Wiley, distributor], 2006.
[74] T. H. James, Ed., *The theory of the photographic process*, 4. ed. New York: Macmillan, 1977.
[75] A. Sacco *et al.*, 'Quantification of titanium dioxide (TiO_2) anatase and rutile polymorphs in binary mixtures by Raman spectroscopy: an interlaboratory comparison', *Metrologia*, vol. 60, no. 5, p. 055011, Oct. 2023, doi: 10.1088/1681-7575/acf76d.
[76] B. Stuart, D. Ando, *Biological applications of infrared spectroscopy*. in Analytical Chemistry by Open Learning. Chichester ; New York: Published on behalf of ACOL by John Wiley, 1997.

A

METHODOLOGY

A.1 Details about the case studies

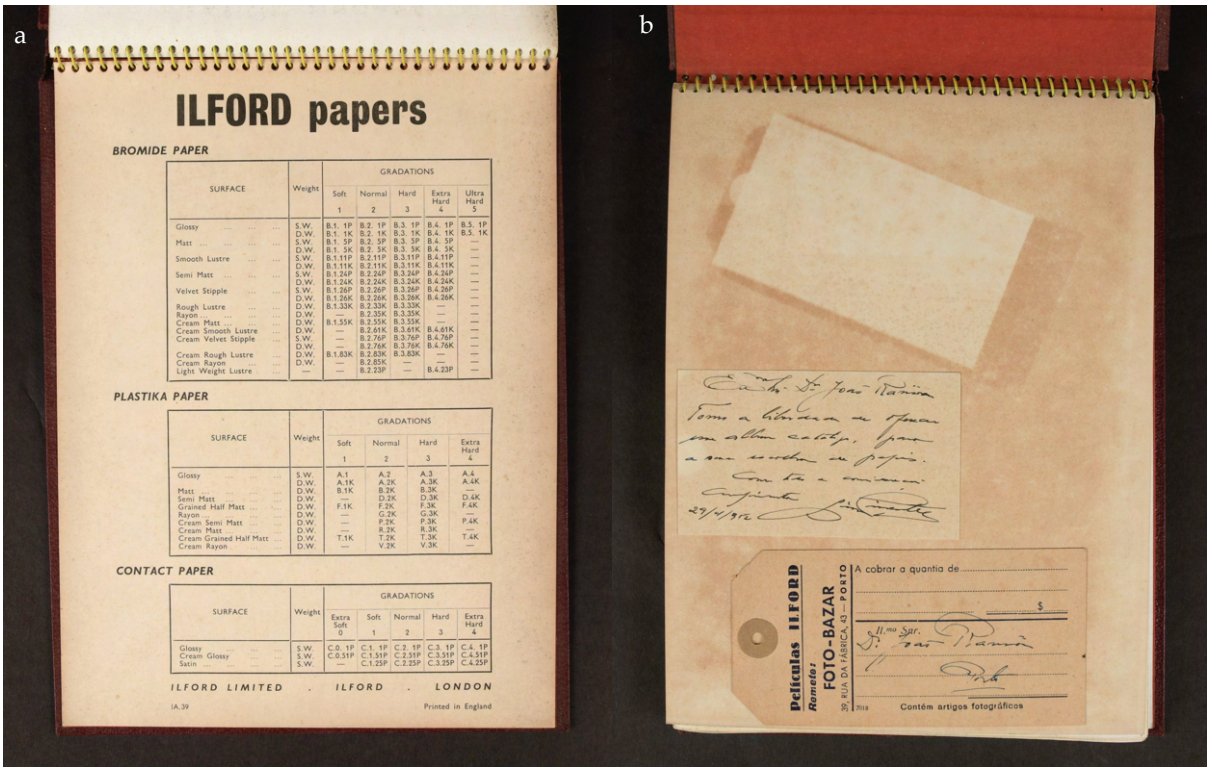

Figure A. 1 IM set: (a) Index page, and (b) the notes found in the back.

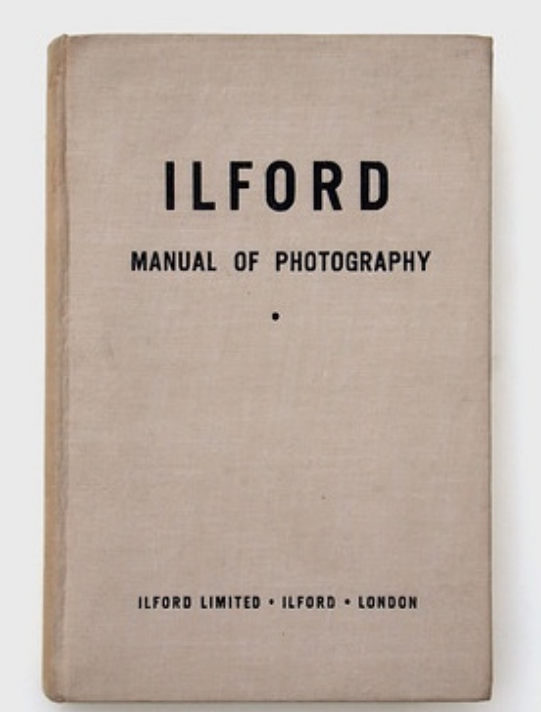

264 MANUAL OF PHOTOGRAPHY

A DESCRIPTION OF THE SURFACES OF ILFORD PAPERS

Ilford papers are available in a wide variety of surfaces which may be briefly classified and described as follows:—

No.

1 **Glossy**
A highly glossy smooth surface with a fine mauve-white base.

5 **Special Smooth Matt**
A perfectly smooth matt surface with a fine mauve-white base.

22 **Natural Grain Smooth**
A perfectly smooth dead matt surface with a pure white tint base. Suitable for colouring.

72 **Cream Smooth Natural Grain**
A similar surface to Natural Grain Smooth but with a cream tint base.

26 **Velvet**
A semi-matt surface but possessing an even grain, producing a velvety appearance.

32 **Rough Natural Grain**
A rough dead matt natural surface with a white-tint base.

6 **Eggshell**
A smooth surface with a trace of sheen with a mauve-white tint base.

56 **Cream Eggshell**
A similar surface to Eggshell but with a warm cream-tint base.

11 **Smooth Lustre**
A smooth natural surface with sheen, giving a lustre effect, with a pure white-tint base.

71 **Cream Fine Grain Lustre**
A similar surface to Fine Grain Lustre with a cream-tint base.

31 **Grained Lustre**
A heavy grained surface with lustre effect on a white-tint base.

33 **Rough Lustre**
A natural rough grain surface with lustre effect on a toned white-tint base, suitable for broad effects.

83 **Cream Rough Lustre**
A similar surface to Rough Lustre but with a cream-tint base.

91 **Cream Extra Rough Lustre**
An extra rough grain surface with lustre effect on a cream-tint base, for very broad effects.

27 **Silika**
A fine texture and delicate sheen resembling the frosty sparkle of fused silica ware.

77 **Cream Silika**
With similar characteristics to Silika, but on a cream base of the palest shade.

Figure A. 2 *Ilford Manual of Photography* (1945) – Details about papers' features

Table A. 1 Surfaces available in the Kodak set with their description from the *Dataguide* [67]

Surface	Texture	Gloss	Description
A	Smooth	Lustre	*This paper is thin enough for the illustrative pages in a report or manual. Folds without cracking.*
E	Fine Grained	Lustre	*This surface preserves fine detail and is suitable for illustrative work where a white base is desirable*
F	Smooth	Glossy	*The general favourite for pictures to be reproduced photomechanically. Widely used for exhibition prints. Can be ferrotyped.*
G	Fine Grained	Lustre	*Fine-grain, lustre on a cream-white base. This is a popular surface for small and medium size portraits and for oil colouring*
J	Smooth	High Lustre	*Designed for the illustrator; preserves detail and produces highest-quality photomechanical reproductions.*
K	Fine Grained	High Lustre	*High lustre counterpart of G although it imparts a feeling of greater brilliance and life of the picture. Not recommended for oils.*
M	Smooth	Matte	*Smooth Matte is a surface with practically no sheen. It is particularly suitable for portraiture and pictorial subjects when a subdued effect is desirable or when surface reflections must be eliminated*
N	Smooth	Lustre	*Smooth – between lustre and matte. Especially designed for retouching on the print. Accepts strong pencilling and preserves fine detail.*
R	Tweed	Lustre	*Popular tweed surface. Minimizing need for fine retouching. Especially good for breaking up large areas. Popular in photomural work.*
X	Tapestry	Lustre	*Extremely coarse-textured and designed for heavy subjects. Effective for very large heads of men. Frequently coloured with opaque oils, which gives effect of an oil painting on canvas.*
Y	Silk	High Lustre	*Simulates silk, is popular for wedding photography. Also, a very attractive medium for expressing brightness in snow scenes, seascapes.*

A.2 Methodology

Photo-documentation

Digital camera

All 54 prints were photographed under visible light (30°) and UV-induced visible fluorescence on both front and back sides. For raking and specular light, only the front side was photographed as the goal was to document the surface characteristics.

To maintain the white balance consistent in the case of normal light images and to capture the accurate colours, a X-Rite ColorChecker NANO Target was used. All the photographs were afterwards edited in Adobe Photoshop in RGB levels, by adjusting the white balance to the Colour checker.

Table A. 2 Illumination setup and camera settings

	Normal light	**Ranking light**	**Specular axial**	**UVA/visible fluorescence**
Lighting source	2x tungsten lamps Photoflex Starlite QL (FV-BSL3200) with Soft box shell SilverDome® Nxt	1x Walimex Daylight 600 AC220-240v 50Hz	1x LED lamp	1x UVA Lamp
(approximate angle)	30°	10°	90°	90°
Image capturing settings				
White-balance settings	Custom	Auto	Auto	Auto
ISO	100	100	100	100
f-stop	11	11	11	8
Shutter Speed (sec)	1/5	0.8	1/5	2
Camera and lenses	Canon EOS R5, using Canon RF 24-70mm F2.8L IS USM Lens			Nikon D500, with Nikon Lens AF-S DX Zoom-Nikon 18-70 mm f/3.5-4.5G IF ED

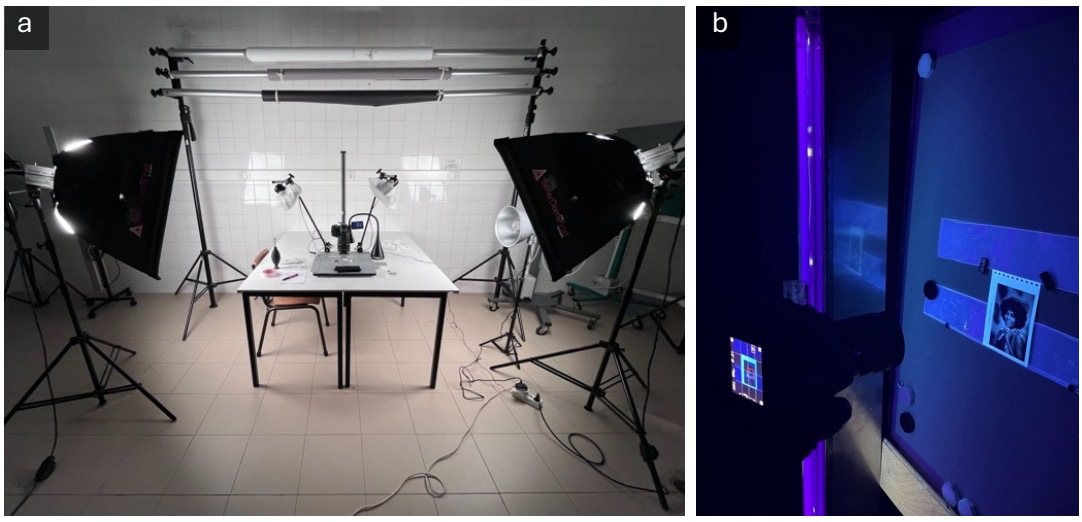

Figure A. 3 Illumination setup for (a) normal, ranking and axial specular; (b) UV-induced visible fluorescence

Microscopy

All 54 prints were examined and photographed under a Nikon SMZ745 stereomicroscope (67x - 200x zoom range), equipped with a Nikon DS-Fi3 digital camera, and a fibre-optic light Leica system (Leica KI 1500 LCD).

Both fibre-optic lights were used for the normal light mode, positioned at a 30° angle. For the raking light setup, used for texture documentation, a similar system has been used as in the case of *TextureScope*. The microspore was brought close to the paper to represent an area of 1.00x1.35 cm². An LED light was placed at 25°, 7 cm away from the photographed area and 3 cm up from the paper. To keep the prints flat, they were covered with cardboard which had a small cut window. The system is shown in *Figure A.4*

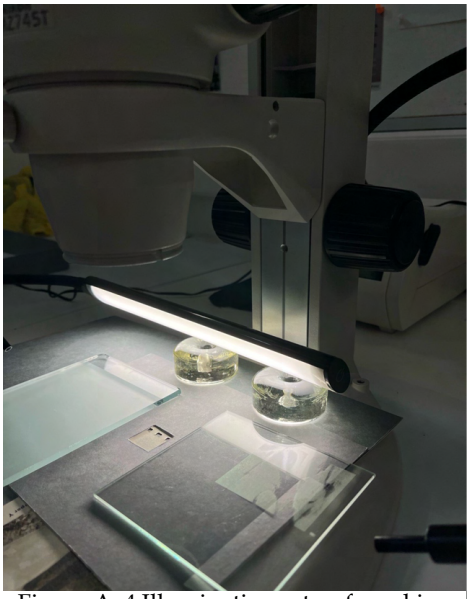

Figure A. 4 Illumination setup for raking light photo-documentation of the texture under the microscope

Optical Microscope

The paper support of all 54 prints was examined under a Zeiss Axioplan 2 microscope, equipped with a Nikon Digital Sight 10 digital camera, at 100x and 200x magnification, in UV radiation.

Thickness and weight measurements

The thickness of all 54 prints was measured using a digital thickness gauge. The setup, similar to the one followed in *Object:Photo* [45], is illustrated in *Figure A.5 (a).* To protect the prints during the measurements, they were placed between two sheets of polyester slightly larger than the prints, having a thickness of 0.8 mm each. As most of the papers were curled, glass weights were used to flatten them during the measurement. The thickness was measured in millimetres to two decimals points.

Three random spots were selected from each print and measured three times. The nine values were registered manually in an Excel spreadsheet subtracting the 0.16 mm thickness of the polyester sheets, and the average and standard deviation were calculated. The average was rounded to two decimal points.

The weight of the prints was measured with a Nahita blue scale, series 5172, 300g/0.01g (*Figure A.5 b*). Three measurements were done, values were manually registered in an Excel spreadsheet, and the average and standard deviation were calculated. The average was rounded to two decimal points.

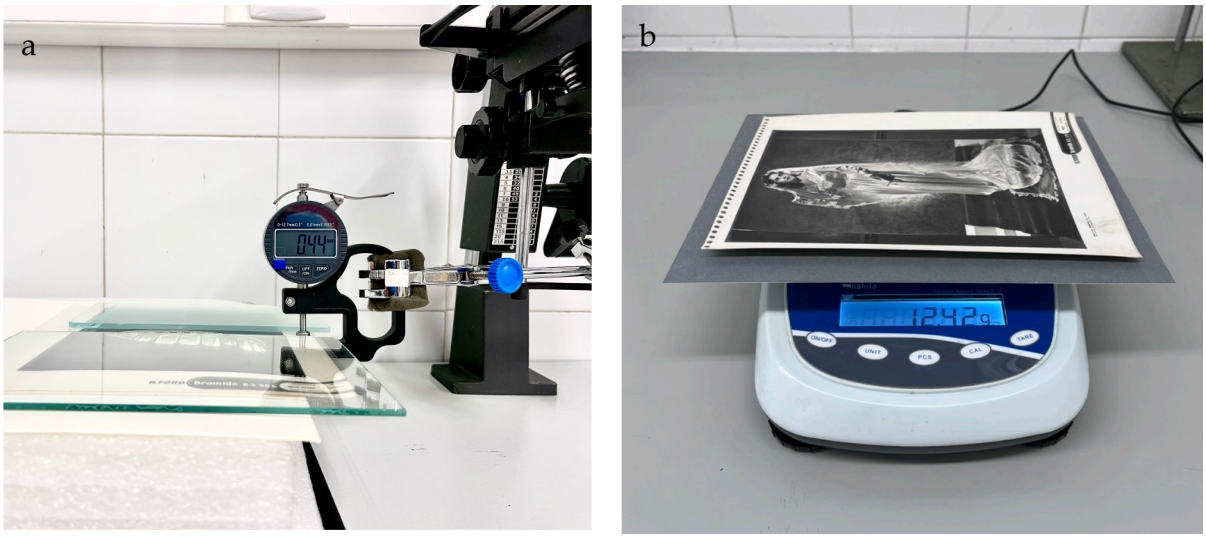

Figure A. 5 Thickness (a) and weight (b) measurements setups

Colourimetry

Colourimetry measurements were conducted using a Konica Minolta® Spectrophotometer CM-700d in the CIELab system. One point from the front and one from the back side of each print were measured three times. For the front side, the measurements were done in SCE (Specular Component Excluded) and in SCI (Specular Component Included) modes. For the back, only SCE mode was used. All values were manually registered in an Excel spreadsheet, and the average and standard deviation were calculated. The average was rounded to two decimal points.

To determine the colour difference between the recto and verso, the following formula was used:

$$\Delta E = \sqrt{(\Delta L^{*2} + \Delta a^{*2} + \Delta b^{*2}}$$

$$\Delta L^* = L^*_{recto} - L^*_{verso}$$

$$\Delta a^* = a^*_{recto} - a^*_{verso}$$

$$\Delta b^* = b^*_{recto} - b^*_{verso}$$

To determine the glossiness value, the following formula was used with the recto values.

$$L^*SCI - L^*SCE$$

For the 3D representation of the prints' SCE values (recto and verso), an online software was used – *Plotly. Chart Studio* (https://chart-studio.plotly.com/create/).

Fibre and pulp identification

The prints were selected based on their characteristics and the observations made using photo-documentation in UV-induced visible light. For the Ilford sets, the UV radiation showed, although in different intensities, a uniform fluorescence, enhancing only the foxing

on the paper support. Therefore, only six IS prints and eight IM prints were selected for the analysis, considering their emulsion type (*Bromide, Plastika* and *Contact*), weight, texture, sheen, and base tints. If the results had shown variations, samples from all papers would have been collected. The uneven UV radiation reflected by the fibres in some of the Kodak papers suggested the combination of different types of pulps. Because of that, all 11 prints were analysed.

The methodology consisted of the following steps:

1. With pointed tweezers, a few fibres were pulled from the paper at corners or edges where the paper support was already detaching from the baryta support.
2. The fibres were placed on labelled glass slides in a drop of distilled water.
3. Under magnification, the fibres were separated using needles.
4. The glass slide was put on a heating plate.
5. When dry, a drop of reagent was added (Herzberg, Lofton-Merritt Staining and Graff "C" solutions).
6. The samples were covered with a cover glass.
7. The prepared samples were analysed and photographed in bright field transmitted light under a Zeiss Axio-plan 2 microscope, equipped with a Nikon Digital Sight 10 digital camera, at 100x and 200x magnification.

μ–EDXRF

The analysis was carried out using the ArtTAX Micro-EDXRF spectrometer of Intax GmbH, having a molybdenum (Mo), an Xflash detector, and a mobile arm. The element range was from aluminium (Al) to uranium (U) with an analysis spot size of, approximately, 70 μm. The spectrometer was used at a current of 300 μA, a voltage of 40 kV, and a collection time of 120 seconds in Helium Atmosphere. Measurements were performed in helium atmosphere. The spectra were interpreted in the Bruker Spectra ArtTAX (version 7.4.0.0).

All 54 prints were analysed. Two spots have been measured on the emulsion side (D_{max} and D_{min}), and one spot on the paper support. Additional areas were analysed when impurities and stains embedded in the paper fibres were observed. Each measurement was carried out three times for each spot.

SEM-EDS

Seventeen prints (five from IS, seven from IM, and five from Kodak) were selected for this analysis. The papers were chosen to cover different types of emulsions, base tints, weight, and surface features. Papers with a similar texture were also analysed in different base tints or brands to see if differences appeared.

The samples were collected from the D_{max} areas with carbon steel single-edge industrial razor blades. The dimension of the samples was about 1x0.5 mm. The samples were placed on the sample holder and analysed.

The analysis was run at the *Electron Microscopy* Lab at Instituto Superior Técnico, from Universidade de Lisboa. The samples were analysed using Hitachi S2400 analytical SEM and Bruker light elements EDS detector.

Raman

A Labram 300 Jobin Yvon Raman Spectrometer by Horiba was used, equipped with a HeNe laser 17mW operating at 632.8 nm, and coupled with the Confocal Microscope Olympus BX 41. For focusing the laser beam, an Olympus LMPlanFL N 50x or 100x was used, with a 2 μm spot size. Collection time was 5 seconds and 5 scans; the laser power was varied with neutral density filters (optical densities: 0.3, 0.6 and 1.0 filters).

One white and three Ilford cream prints were analysed focusing the beam on the ochre particles (for the cream prints) and *IM_Bromide B.2.23. P Light Weight Lustre*. Three different spots were analysed for all the samples. The Raman data analysis was performed using Lab-Spec 5 software.

ER-FTIR

The ER-FTIR analysis was carried out directly on the emulsion side of the prints on three different spots (D_{max}, D_{mid}, and D_{min}), using a Handheld Agilent 4300 spectrophotometer, equipped with a ZnSe beam splitter, a Michelson interferometer, and a thermoelectrically cooled DTGS detector, with a specular spectral acquisition interface. All measurements were performed positioning the samples horizontally, on top of the external reflectance module with a measurement spot of 10 mm in diameter. The spectral range was 4000–650 cm^1, with 8 cm^1 resolution; 128 scans were acquired for the background using a gold flat mirror as reference, and 128 scans were recorded on the samples to optimize the signal-to-noise ratio (S/N). OMNIC software was used to analyze and interpret the spectra.

B
RESULTS

B.1 SEM-EDS – elemental composition by layer

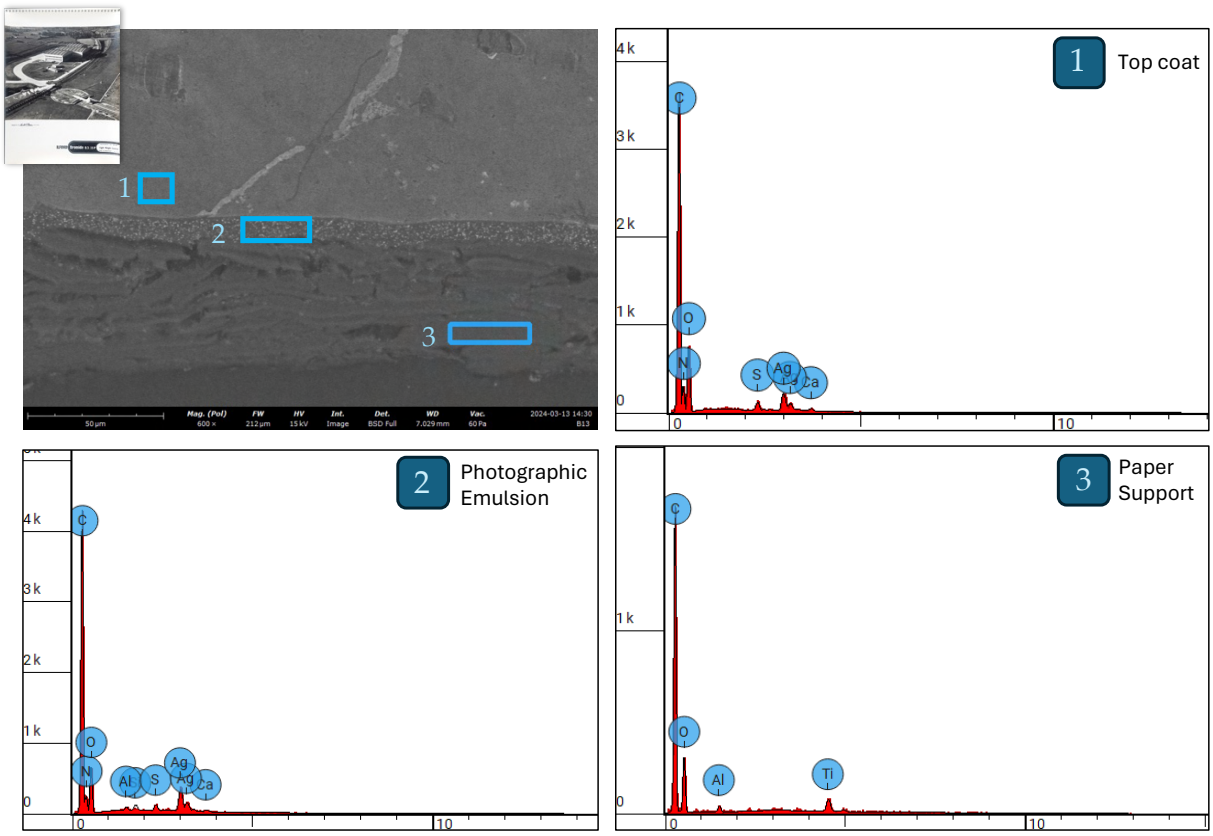

Figure B. 1 SEM-EDS elemental composition by layer for *IM_Bromide B.2.23 P Light Weight Lustre*

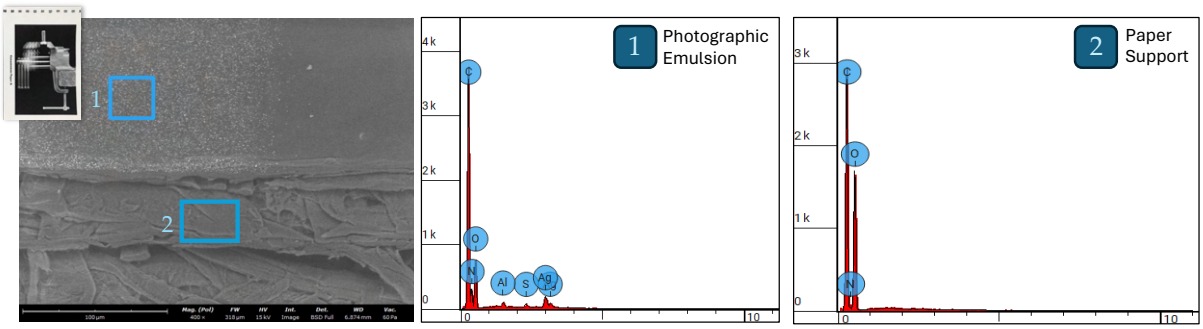

Figure B. 2 SEM-EDS elemental composition by layer for *Kodabromide A*

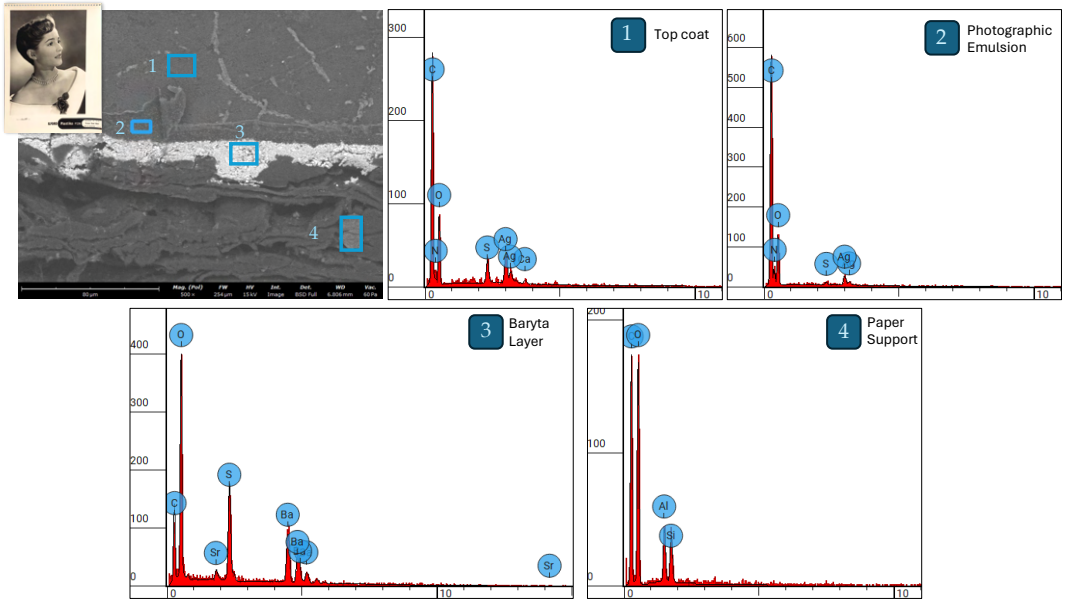

Figure B. 3 SEM-EDS elemental composition by layer for *IM_Plastika P.2.K Cream Semi Matt*

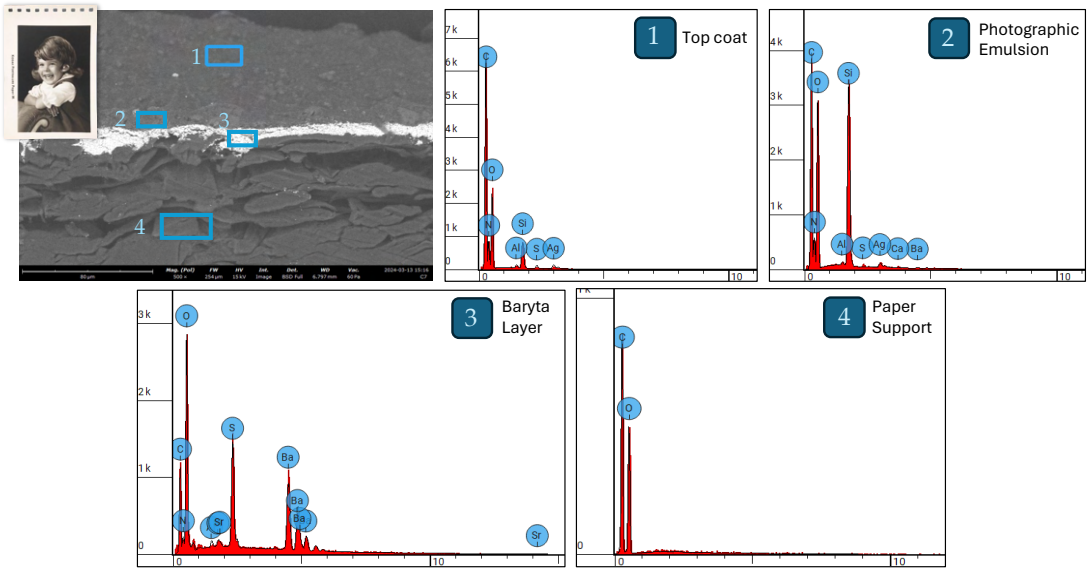

Figure B. 4 SEM-EDS elemental composition by layer for *Portralure M*

B.2 Analysis summary tables

The following tables are gathering the results obtained during the multi-analytical characterisation of all the prints. The tables do not contain the ER-FTIR spectra and the UV-induced visible fluorescence photo-documentation of the back (provided in *Appendix B.3*).

Table B. 1 Multi-analytical characterisation results of small-format Ilford set (IS)

Bromide B.2. 1P Glossy

Thickness: 0.16 mm
Weight: 0.62 g
Colourimetry:

Colour coordinates (SCE)	Recto	Verso
	L* 88.43 ± 0.04	**L*** 93.38 ± 0.02
	a* -0.12 ± 0.01	**a*** -0.3 ± 0.01
	b* 3.62 ± 0.05	**b*** 4.22 ± 0

ΔE (recto and verso) 4.99
ΔSCI-SCE (recto) 2.09

Photo-documentation

Normal light

UVA / visible fluorescence

Specular light

Raking light

Fibre identification

Herzberg

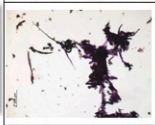

Lofton Merritt

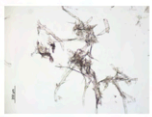

Graff C

SEM

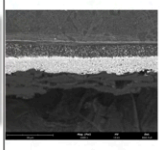

Composition

XRF:
Elements identified: S, Ca, Sr, Ag, Ba, Fe (Kα), K
SEM:
Top coat: Ag, S, Ca
Emulsion: Ag, S
Baryta layer: Ba, S, Sr
Paper: Al, Si, S

Bromide B.2. 5K Matt

Thickness: 0.26 mm
Weight: 0.99 g
Colourimetry:

Colour coordinates (SCE)	Recto	Verso
	L* 91.07 ± 0.05	**L*** 93.48 ± 0.043
	a* -0.41 ± 0.06	**a*** -0.05 ± 0.01
	b* 6.12 ± 0.01	**b*** 7.15

ΔE (recto and verso) 2.64
ΔSCI-SCE (recto) 0.18

Photo-documentation

Normal light

UVA / visible fluorescence

Specular light

Raking light

Fibre identification

Herzberg

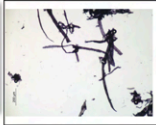

Lofton Merritt

Graff C

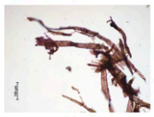

SEM

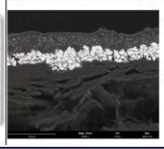

Composition

XRF:
Elements identified: S, Ca, Sr, Ag, Ba, Fe (Kα), K
SEM:
Emulsion: Ag, S, Ca, Al, Si
Baryta layer: Ba, S, Sr
Paper: Al, Si, S

Bromide B.2. 24K Semi Matt

Thickness: 0.27 mm
Weight: 0.96 g
Colourimetry:

Colour coordinates (SCE)	Recto	Verso
	L* 90.96 ± 0.01	**L*** 94.03 ± 0.02
	a* -0.08 ± 0	**a*** 0.02 ± 0.02
	b* 7.3 ± 0.01	**b*** 5.37 ± 0.02

ΔE (recto and verso) 3.62
ΔSCI-SCE (recto) 1.02

Photo-documentation

Normal light

UVA / visible fluorescence

Specular light

Raking light

Fibre identification

Herzberg | Lofton Merritt | Graff C

SEM

Composition

XRF:
Elements identified: S, Ca, Sr, Ag, Ba, Fe (Kα), K

Bromide B.2 26K Velvet Stipple

Thickness: 0.28 mm

Weight: 0.88 g

Colourimetry:

Colour coordinates (SCE)	Recto	Verso
	L* 92.40 ± 0.02	**L*** 94.24 ± 0.01
	a* -0.07 ± 0	**a*** -0.07 ± 0
	b* 8.31 ± 0.25	**b*** 5.08 ± 0.01
ΔE (recto and verso)	3.72	
ΔSCI-SCE (recto)	0.59	

Photo-documentation

Normal light

UVA/visible fluorescence

Specular light

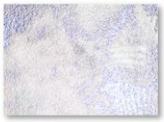

Raking light

Fibre identification

Herzberg | Lofton Merritt | Graff C

SEM

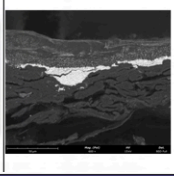

Composition

XRF:
Elements identified: S, Ca, Sr, Ag, Ba, Fe (Kα), K

SEM:
Topcoat: Al, Si, S, Ca, Ag
Emulsion: Ag, S, Ca
Baryta layer: Ba, S, Sr, Ca
Paper: Al, Si,
Particle: Al, Si, S, Ca, Ba

Bromide B.2. 33K Rough Lustre

Thickness: 0.28 mm

Weight: 0.90 g

Colourimetry:

Colour coordinates (SCE)	Recto	Verso
	L* 91.10 ± 0.07	**L*** 94.22 ± 0.01
	a* 0.08 ± 0.02	**a*** -0.43 ± 0.01
	b* 9.81 ± 0.01	**b*** 5.92 ± 0.02
ΔE (recto and verso)	4.96	
ΔSCI-SCE (recto)	1.13	

Photo-documentation

Normal light

UVA/visible fluorescence

Specular light

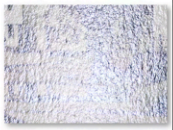

Raking light

Fibre identification

Herzberg | Lofton Merritt | Graff C

SEM

Composition

XRF:
Elements identified: S, Ca, Sr, Ag, Ba, Fe (Kα), K

Bromide B.2. 35K Rayon

Thickness: 0.28 mm

Weight: 0.97 g

Colourimetry:

Colour coordinates (SCE)	Recto	Verso
	L* 92.01 ± 0.02	**L*** 94.25 ± 0.04
	a* 0.65 ± 0.01	**a*** 0.30 ± 0.01
	b* 10.68 ± 0.02	**b*** 10.01 ± 0.07
ΔE (recto and verso)	2.36	
ΔSCI-SCE (recto)	0.84	

Photo-documentation

Normal light

UVA/visible fluorescence

Specular light

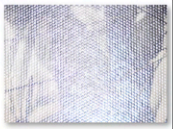

Raking light

Fibre identification

Herzberg | Lofton Merritt | Graff C

SEM

Composition

XRF:
Elements identified: S, Ca, Sr, Ag, Ba, Fe (Kα), K

Bromide B.2. 55K Cream Matt

Thickness: 0.27 mm

Weight: 0.97 g

Colourimetry:

Colour coordinates (SCE)	Recto	Verso
	L* 89.81 ± 0.01	**L*** 90.82 ± 0.01
	a* 1.78 ± 0.01	**a*** 1.65 ± 0.03
	b* 17.98 ± 0.02	**b*** 16.12 ± 0.02
ΔE (recto and verso)	2.12	
ΔSCI-SCE (recto)	0.18	

Photo-documentation

Normal light

UVA/visible fluorescence

Specular light

Raking light

Fibre identification

Herzberg | Lofton Merritt | Graff C

SEM

Composition

XRF:
Elements identified: S, Ca, Sr, Ag, Ba, Fe (Kα+ Kβ), K

Raman:
Yellow particles: FeO(OH)

Bromide B.2. 83K Cream Rough Lustre

Thickness: 0.30 mm

Weight: 0.95 g

Colourimetry:

Colour coordinates (SCE)	Recto	Verso
	L* 89.40 ± 0.05	**L*** 91.29 ± 0.03
	a* 1.72 ± 0.01	**a*** 1.71 ± 0.05
	b* 18.4 ± 0.05	**b*** 15.97 ± 0.09
ΔE (recto and verso)	2.37	
ΔSCI-SCE (recto)	1.06	

Photo-documentation

Normal light

UVA/visible fluorescence

Specular light

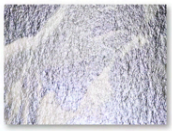

Raking light

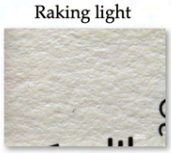

Fibre identification

Herzberg

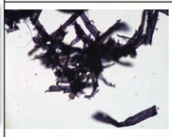

Lofton Merritt

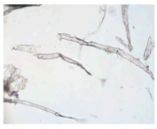

Graff C

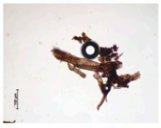

SEM

Composition

XRF:
Elements identified: S, Ca, Sr, Ag, Ba, Fe (Kα+ Kβ), K

Bromide B.2. 85K Cream Rayon

Thickness: 0.26 mm

Weight: 0.94 g

Colourimetry:

Colour coordinates (SCE)	Recto	Verso
	L* 88.77 ± 0.01	**L*** 91.60 ± 0.01
	a* 3.03 ± 0.01	**a*** 1.76 ± 0
	b* 16.82 ± 0.02	**b*** 15.67 ± 0.03
ΔE (recto and verso)	3.31	
ΔSCI-SCE (recto)	1.12	

Photo-documentation

Normal light

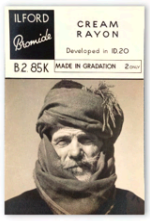

UVA/visible fluorescence

Specular light

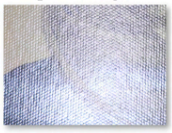

Raking light

Fibre identification

Herzberg

Lofton Merritt

Graff C

SEM

Composition

XRF:
Elements identified: S, Ca, Sr, Ag, Ba, Fe (Kα+ Kβ), K

Plastika A.2 Glossy

Thickness: 0.17 mm

Weight: 0.68 g

Colourimetry:

Colour coordinates (SCE)	Recto	Verso
	L* 87.36 ± 0.02	**L*** 93.55 ± 0.01
	a* -0.53 ± 0.01	**a*** 0.01 ± 0.01
	b* 6.45 ± 0.01	**b*** 4.16 ± 0.02
ΔE (recto and verso)	6.63	
ΔSCI-SCE (recto)	2.13	

Photo-documentation

Normal light

UVA/visible fluorescence

Specular light

Raking light

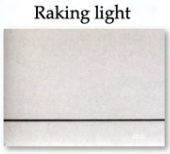

Fibre identification

Herzberg

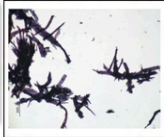

Lofton Merritt

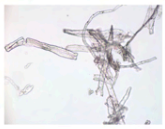

Graff C

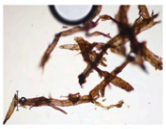

SEM

Composition

XRF:
Elements identified: S, Ca, Sr, Ag, Ba, Fe (Kα), K

Plastika B.2.K Matt

Thickness: 0.29 mm

Weight: 0.94 g

Colourimetry:

Colour coordinates (SCE)	Recto	Verso
	L* 91.66 ± 0.02	**L*** 94.22 ± 0.01
	a* 0.93 ± 0.01	**a*** 0.07 ± 0
	b* 10.18 ± 0.01	**b*** 6.09 ± 0.02
ΔE (recto and verso)	4.9	
ΔSCI-SCE (recto)	0.3	

Photo-documentation

Normal light

UVA/visible fluorescence

Specular light

Raking light

Fibre identification

Herzberg

Lofton Merritt

Graff C

SEM

Composition

XRF:
Elements identified: S, Ca, Sr, Ag, Ba, Fe (Kα), K

Plastika F.2.K Grained Half Matt

Thickness: 0.27 mm

Weight: 0.91 g

Colourimetry:

	Recto	Verso
Colour coordinates (SCE)	**L*** 92.37 ± 0.02	**L*** 94.78 ± 0.04
	a* 0.15 ± 0	**a*** -0.03 ± 0.02
	b* 9.64 ± 0.08	**b*** 5.36 ± 0.02
ΔE (recto and verso)	4.91	
ΔSCI-SCE (recto)	0.68	

Photo-documentation

Normal light

UVA / visible fluorescence

Specular light

Raking light

Fibre identification

Herzberg	Lofton Merritt	Graff C

SEM

Composition

XRF:
Elements identified: S, Ca, Sr, Ag, Ba, Fe (Kα), K

Plastika G.2.K Rayon

Thickness: 0.29 mm

Weight: 1.03 g

Colourimetry:

	Recto	Verso
Colour coordinates (SCE)	**L*** 92.27 ± 0.06	**L*** 94.03 ± 0.01
	a* 0.78 ± 0.01	**a*** 0.45 ± 0.01
	b* 11.65 ± 0.02	**b*** 10.77 ± 0.02
ΔE (recto and verso)	1.99	
ΔSCI-SCE (recto)	0.72	

Photo-documentation

Normal light

UVA / visible fluorescence

Specular light

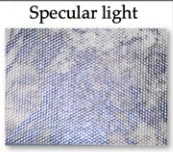

Raking light

Fibre identification

Herzberg	Lofton Merritt	Graff C

SEM

Composition

XRF:
Elements identified: S, Ca, Sr, Ag, Ba, Fe (Kα), K

Plastika R.2.K Cream Matt

Thickness: 0.30 mm

Weight: 0.92 g

Colourimetry:

	Recto	Verso
Colour coordinates (SCE)	**L*** 90.84 ± 0.02	**L*** 92.07 ± 0.02
	a* 2.35 ± 0.02	**a*** 1.32 ± 0.02
	b* 15.38 ± 0.01	**b*** 14.23 ± 0.03
ΔE (recto and verso)	1.98	
ΔSCI-SCE (recto)	0.22	

Photo-documentation

Normal light

UVA / visible fluorescence

Specular light

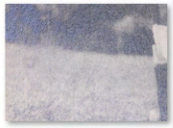

Raking light

Fibre identification

Herzberg	Lofton Merritt	Graff C
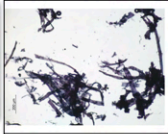	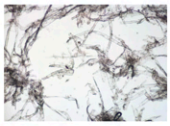	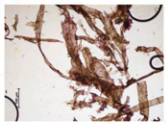

SEM

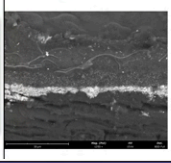

Composition

XRF:
Elements identified: S, Ca, Sr, Ag, Ba, Fe (Kα+ Kβ), K

SEM:
Topcoat: Al, Si, S, Cl, Ca, Ag
Emulsion: Ag, S, Ca, Al, Si
Baryta layer: Ba, S, Sr, Ca
Paper: Al, Si, S, Ca[?]

Plastika T.2.K Cream Grained Half Matt

Thickness: 0.27 mm

Weight: 0.92 g

Colourimetry:

	Recto	Verso
Colour coordinates (SCE)	**L*** 90.15 ± 0.02	**L*** 92.21 ± 0
	a* 2.52 ± 0.01	**a*** 1.62 ± 0.02
	b* 18.10 ± 0.01	**b*** 14.94 ± 0.05
ΔE (recto and verso)	3.87	
ΔSCI-SCE (recto)	0.65	

Photo-documentation

Normal light

UVA / visible fluorescence

Specular light

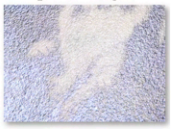

Raking light

Fibre identification

Herzberg	Lofton Merritt	Graff C

SEM

Composition

XRF:
Elements identified: S, Ca, Sr, Ag, Ba, Fe (Kα+ Kβ), K

Plastika V.2.K Cream Rayon

Thickness: 0.31 mm

Weight: 1.17 g

Colourimetry:

Colour coordinates (SCE)	Recto	Verso
	L* 88.11 ± 0.03	**L*** 90.95 ± 0.025
	a* 3.55 ± 0.02	**a*** 2.39 ± 0.01
	b* 17.36 ± 0.06	**b*** 18.91 ± 0.03
ΔE (recto and verso)	3.43	
ΔSCI-SCE (recto)	0.71	

Photo-documentation

Normal light

UVA / visible fluorescence

Specular light

Raking light

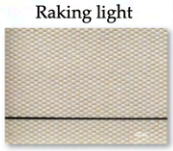

Fibre identification

Herzberg	Lofton Merritt	Graff C

SEM	Composition
	XRF: Elements identified: S, Ca, Sr, Ag, Ba, Fe (Kα+ Kβ), K **Raman:** Yellow particles: FeO(OH)

Contact C.2. 1P Glossy

Thickness: 0.16 mm

Weight: 0.67 g

Colourimetry:

Colour coordinates (SCE)	Recto	Verso
	L* 88.27 ± 0.01	**L*** 93.88 ± 0.02
	a* -0.1 ± 0.01	**a*** -0.11 ± 0.01
	b* 6.81 ± 0	**b*** 4.35 ± 0.01
ΔE (recto and verso)	6.13	
ΔSCI-SCE (recto)	2.08	

Photo-documentation

Normal light

UVA / visible fluorescence

Specular light

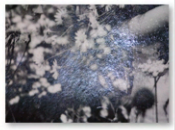

Raking light

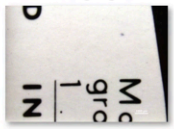

Fibre identification

Herzberg	Lofton Merritt	Graff C

SEM	Composition
	XRF: Elements identified: S, Ca, Sr, Ag, Ba, Fe (Kα), K

Contact C.2. 25P Satin

Thickness: 0.20 mm

Weight: 0.65 g

Colourimetry:

Colour coordinates (SCE)	Recto	Verso
	L* 91.32 ± 0.02	**L*** 94.07 ± 0.01
	a* 0.12 ± 0.01	**a*** -0.31 ± 0.01
	b* 7.84 ± 0.02	**b*** 7.18
ΔE (recto and verso)	2.87	
ΔSCI-SCE (recto)	0.98	

Photo-documentation

Normal light

UVA / visible fluorescence

Specular light

Raking light

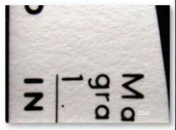

Fibre identification

Herzberg	Lofton Merritt	Graff C
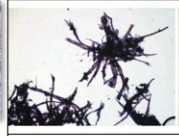	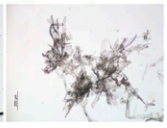	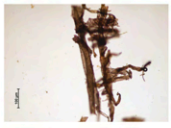

SEM	Composition
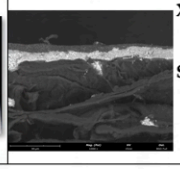	**XRF:** Elements identified: S, Ca, Sr, Ag, Ba, Fe (Kα), K **SEM:** Emulsion: Ag, S, Ca Baryta layer: Ba, S, Sr, Ca Paper: Al, Si, S

Table B. 2 Multi-analytical characterisation results of the medium-format Ilford set (IM)

Bromide B.2. 1P Glossy

Thickness: 0.16 ± 0 mm
Weight: 7.53 ± 0.01 g
Colourimetry:

Colour coordinates (SCE)	Recto	Verso
	L* 87.71 ± 0.0	**L*** 93.02 ± 0.03
	a* -0.38 ± 0.01	**a*** 0.02 ±
	b* 6.55 ± 0.01	**b*** 4.73 ± 0.06
ΔE (recto and verso)	5.63	
ΔSCI-SCE (recto)	2.14	

Photo-documentation

Normal light

UVA/visible fluorescence

Specular light

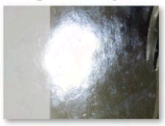

Raking light

Fibre identification: Softwood bleached sulfite pulp

Herzberg

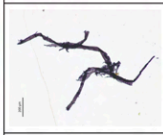

Lofton Merritt

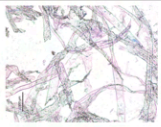

Graff C

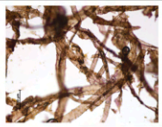

SEM

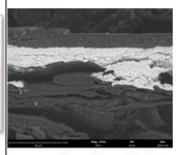

Composition

XRF:
Elements identified: S, Ca, Sr, Ag, Ba, Fe (Kα), K

SEM:
Top coat: not analysed
Emulsion: Al, Si, S, Cl, Ca, Ag, Ba
Baryta layer: Ba, S, Sr
Paper: Al, Si

Bromide B.2. 5K Matt

Thickness: 0.32 ± 0 mm
Weight: 12.41 ± 0.01 g
Colourimetry:

Colour coordinates (SCE)	Recto	Verso
	L* 90.85 ± 0.06	**L*** 93.84 ± 0.03
	a* 0.20 ± 0.01	**a*** -0.28 ± 0.01
	b* 7.83 ± 0.03	**b*** 6.54 ± 0.03
ΔE (recto and verso)	3.33	
ΔSCI-SCE (recto)	0.21	

Photo-documentation

Normal light

UVA/visible fluorescence

Specular light

Raking light

Fibre identification: Softwood bleached sulfite pulp

Herzberg

Lofton Merritt

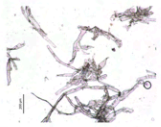

Graff C

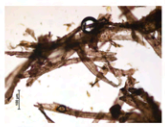

SEM

Composition

XRF:
Elements identified: S, Ca, Sr, Ag, Ba, Fe (Kα), K

Bromide B.2. 11K Smooth Lustre

Thickness: 0.28 ± 0.01 mm
Weight: 10.42 ± 0.01 g
Colourimetry:

Colour coordinates (SCE)	Recto	Verso
	L* 91.52 ± 0.03	**L*** 93.82 ± 0.01
	a* 0.02 ± 0.01	**a*** -0.44 ± 0.01
	b* 11.38 ± 0.01	**b*** 6.18 ± 0.01
ΔE (recto and verso)	5.73	
ΔSCI-SCE (recto)	0.65	

Photo-documentation

Normal light

UVA/visible fluorescence

Specular light

Raking light

Fibre identification

Herzberg

Lofton Merritt

Graff C

SEM

Composition

XRF:
Elements identified: S, Ca, Sr, Ag, Ba, Fe (Kα), K

Bromide B.2. 24K Semi Matt

Thickness: 0.29 ± 0 mm
Weight: 12.33 ± 0.01 g
Colourimetry:

Colour coordinates (SCE)	Recto	Verso
	L* 90.11 ± 0	**L*** 93.87 ± 0.01
	a* -0.31 ± 0.01	**a*** -0.26 ± 0.01
	b* 7.4 ± 0.01	**b*** 6.17 ± 0.02
ΔE (recto and verso)	3.95	
ΔSCI-SCE (recto)	0.84	

Photo-documentation

Normal light

UVA/visible fluorescence

Specular light

Raking light

Fibre identification

Herzberg

Lofton Merritt

Graff C

SEM

Composition

XRF:
Elements identified: S, Ca, Sr, Ag, Ba, Fe (Kα), K

Bromide B.2 26K Velvet Stipple

Thickness: 0.28 ± 0.01 mm

Weight: 10.55 ± 0.01 g

Colourimetry:

Colour coordinates (SCE)	Recto	Verso
	L* 92.11 ± 0.02	**L*** 94.45 ± 0.02
	a* 0.01 ± 0.01	**a*** -0.44 ± 0.01
	b* 9.57 ± 0.07	**b*** 5.73 ± 0.02
ΔE (recto and verso)	4.51	
ΔSCI-SCE (recto)	0.59	

Photo-documentation

Normal light

UVA/visible fluorescence

Specular light

Raking light

Fibre identification

Herzberg | Lofton Merritt | Graff C

SEM

Composition

XRF:
Elements identified: S, Ca, Sr, Ag, Ba, Fe (Kα), K

Bromide B.2. 33K Rough Lustre

Thickness: 0.31 ± 0.01 mm

Weight: 10.40 ± 0.01 g

Colourimetry:

Colour coordinates (SCE)	Recto	Verso
	L* 90.55 ± 0.04	**L*** 94.01 ± 0.03
	a* 0.04 ± 0.01	**a*** -0.73 ± 0.01
	b* 11.02 ± 0.01	**b*** 5.78 ± 0.03
ΔE (recto and verso)	6.33	
ΔSCI-SCE (recto)	1.15	

Photo-documentation

Normal light

UVA/visible fluorescence

Specular light

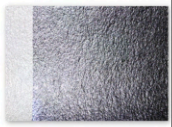

Raking light

Fibre identification

Herzberg | Lofton Merritt | Graff C

SEM

Composition

XRF:
Elements identified: S, Ca, Sr, Ag, Ba, Fe (Kα), K

Bromide B.2. 35K Rayon

Thickness: 0.26 ± 0.01 mm

Weight: 10.84 ± 0.01 g

Colourimetry:

Colour coordinates (SCE)	Recto	Verso
	L* 91.77 ± 0.12	**L*** 94.15 ± 0.01
	a* 0.16 ± 0	**a*** -0.43 ± 0.01
	b* 10.34 ± 0.02	**b*** 5.69 ± 0.01
ΔE (recto and verso)	5.26	
ΔSCI-SCE (recto)	0.92	

Photo-documentation

Normal light

UVA/visible fluorescence

Specular light

Raking light

Fibre identification

Herzberg | Lofton Merritt | Graff C

SEM

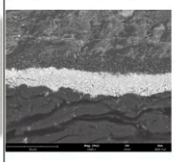

Composition

XRF:
Elements identified: S, Ca, Sr, Ag, Ba, Fe (Kα), K

SEM:
Top coat: Al, Si, S, Cl, Ca, Ag, Ba
Emulsion: Al, Si, S, Cl, Ca, Ag, Ba
Baryta layer: Ba, S, Sr, Ca
Paper: Al, Si, S

Bromide B.2. 55K Cream Matt

Thickness: 0.28 ± 0.01 mm

Weight: 10.65 ± 0.02 g

Colourimetry:

Colour coordinates (SCE)	Recto	Verso
	L* 89.74 ± 0.01	**L*** 91.11 ± 0.03
	a* 1.07 ± 0.01	**a*** 1.25 ± 0.01
	b* 18.81 ± 0.01	**b*** 15.06 ± 0.02
ΔE (recto and verso)	4	
ΔSCI-SCE (recto)	0.2	

Photo-documentation

Normal light

UVA/visible fluorescence

Specular light

Raking light

Fibre identification

Herzberg | Lofton Merritt | Graff C

SEM

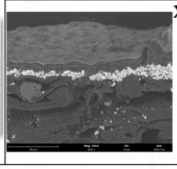

Composition

XRF:
Elements identified: S, Ca, Sr, Ag, Ba, Fe (Kα+ Kβ), K

SEM:
Top coat: Al, Si, S, Ca, Ag
Emulsion: Al, Si, S, Ag
Baryta layer: Ba, S, Sr
Paper: Al, Si, S

Bromide B.2. 61K Cream Smooth Lustre

Thickness: 0.29 ± 0.01 mm

Weight: 10.3 ± 0.01 g

Colourimetry:

Colour coordinates (SCE)	Recto	Verso
	L* 89.24 ± 0.04	**L*** 91.82 ± 0.03
	a* 1.98 ± 0.01	**a*** 1 ± 0.03
	b* 19.37 ± 0.04	**b*** 13.37 ± 0.02
ΔE (recto and verso)	6.6	
ΔSCI-SCE (recto)	0.55	

Photo-documentation

Normal light

UVA/visible fluorescence

Specular light

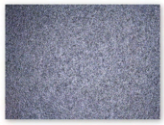

Raking light

Fibre identification: Softwood bleached sulfite pulp

Herzberg	Lofton Merritt	Graff C
	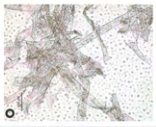	

SEM

Composition

XRF:
Elements identified: S, Ca, Sr, Ag, Ba, Fe (Kα+ Kβ), K

Bromide B.2. 76K Cream Velvet Stipple

Thickness: 0.29 ± 0.01 mm

Weight: 10.44 ± 0.01 g

Colourimetry:

Colour coordinates (SCE)	Recto	Verso
	L* 90.27 ± 0.28	**L*** 92 ± 0.05
	a* 2.09 ± 0.03	**a*** 0.82 ± 0.01
	b* 15.93 ± 0.01	**b*** 13.29 ± 0.07
ΔE (recto and verso)	3.41	
ΔSCI-SCE (recto)	0.38	

Photo-documentation

Normal light

UVA/visible fluorescence

Specular light

Raking light

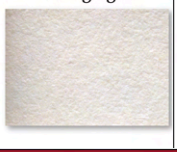

Fibre identification

Herzberg	Lofton Merritt	Graff C

SEM

Composition

XRF:
Elements identified: S, Ca, Sr, Ag, Ba, Fe (Kα+ Kβ), K

Raman:
Yellow particles: FeO(OH)

Bromide B.2. 83K Cream Rough Lustre

Thickness: 0.31 ± 0 mm

Weight: 10.25 ± 0.01 g

Colourimetry:

Colour coordinates (SCE)	Recto	Verso
	L* 88.43 ± 0.05	**L*** 91.31 ± 0.02
	a* 2.13 ± 0.01	**a*** 1.85 ± 0.01
	b* 19.09 ± 0.02	**b*** 14.93 ± 0.01
ΔE (recto and verso)	5.07	
ΔSCI-SCE (recto)	1.32	

Photo-documentation

Normal light

UVA/visible fluorescence

Specular light

Raking light

Fibre identification

Herzberg	Lofton Merritt	Graff C

SEM

Composition

XRF:
Elements identified: S, Ca, Sr, Ag, Ba, Fe (Kα+ Kβ), K

Raman:
Yellow particles: FeO(OH)

Bromide B.2. 85K Cream Rayon

Thickness: 0.26 ± 0.01 mm

Weight: 10.97 ± 0.01 g

Colourimetry:

Colour coordinates (SCE)	Recto	Verso
	L* 88.83 ± 0.04	**L*** 91.14 ± 0.02
	a* 3.04 ± 0.01	**a*** 1.08 ± 0.01
	b* 18.93 ± 0.07	**b*** 14.69 ± 0.02
ΔE (recto and verso)	5.72	
ΔSCI-SCE (recto)	0.76	

Photo-documentation

Normal light

UVA/visible fluorescence

Specular light

Raking light

Fibre identification

Herzberg	Lofton Merritt	Graff C

SEM

Composition

XRF:
Elements identified: S, Ca, Sr, Ag, Ba, Fe (Kα+ Kβ), K

Bromide B.2. 23P Light Weight Lustre

Thickness: 0.09 ± 0 mm

Weight: 3.28 ± 0.01 g

Colourimetry:

Colour coordinates (SCE)	Recto	Verso
	L* 94.27 ± 0.01	**L*** 95.02 ± 0.01
	a* -0.65 ± 0.01	**a*** -0.12 ± 0.01
	b* 7.35 ± 0.01	**b*** 5.35 ± 0.03
ΔE (recto and verso)	2.2	
ΔSCI-SCE (recto)	0.53	

Photo-documentation

Normal light

UVA / visible fluorescence

Specular light

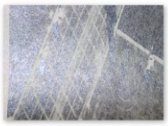

Raking light

Fibre identification: Softwood bleached sulfite pulp

Herzberg

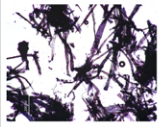

Lofton Merritt

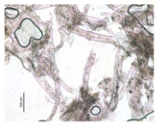

Graff C

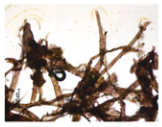

SEM

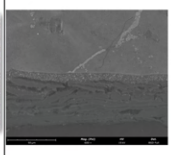

Composition

XRF:
Elements identified: S, Ca, Ag, Ti

Raman:
Anatase form of TiO_2

SEM:
Top coat: S, Ca, Ag
Emulsion: Al, Si, S, Ca, Ag
Paper: Al, Ti

Plastika A.2 Glossy

Thickness: 0.18 ± 0 mm

Weight: 7.78 ± 0.01 g

Colourimetry:

Colour coordinates (SCE)	Recto	Verso
	L* 88.4 ± 0.03	**L*** 92.71 ± 0.02
	a* 0.2 ± 0.01	**a*** -0.45 ± 0.01
	b* 5.29 ± 0.03	**b*** 3.37 ± 0.02
ΔE (recto and verso)	5.73	
ΔSCI-SCE (recto)	2.19	

Photo-documentation

Normal light

UVA / visible fluorescence

Specular light

Raking light

Fibre identification: Softwood bleached sulfite pulp

Herzberg

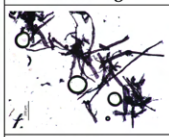

Lofton Merritt

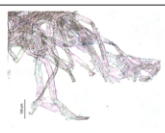

Graff C

SEM

Composition

XRF:
Elements identified: S, Ca, Sr, Ag, Ba, Fe (Kα), K

Plastika B.2 K Matt

Thickness: 0.30 ± 0.01 mm

Weight: 11.09 ± 0.01 g

Colourimetry:

Colour coordinates (SCE)	Recto	Verso
	L* 93.39 ± 0	**L*** 94.37 ± 0.01
	a* 0.17 ± 0.01	**a*** -0.44 ± 0.01
	b* 11.23 ± 0.01	**b*** 5.04 ± 0.01
ΔE (recto and verso)	6.29	
ΔSCI-SCE (recto)	0.24	

Photo-documentation

Normal light

UVA / visible fluorescence

Specular light

Raking light

Fibre identification

Herzberg

Lofton Merritt

Graff C

SEM

Composition

XRF:
Elements identified: S, Ca, Sr, Ag, Ba, Fe (Kα), K

Plastika D.2 K Semi Matt

Thickness: 0.29 ± 0.01 mm

Weight: 10.32 ± 0.01g

Colourimetry:

Colour coordinates (SCE)	Recto	Verso
	L* 93.05 ± 0	**L*** 93.88 ± 0.01
	a* 0.1 ± 0.01	**a*** -0.48 ± 0.01
	b* 11 ± 0.01	**b*** 5.72 ± 0.01
ΔE (recto and verso)	5.38	
ΔSCI-SCE (recto)	0.88	

Photo-documentation

Normal light

UVA / visible fluorescence

Specular light

Raking light

Fibre identification

Herzberg

Lofton Merritt

Graff C

SEM

Composition

XRF:
Elements identified: S, Ca, Sr, Ag, Ba, Fe (Kα), K

Plastika F.2 K Grained Half Matt

Thickness: 0.27 ± 0.01 mm

Weight: 10.44 ± 0.01 g

Colourimetry:

Colour coordinates (SCE)	Recto	Verso
	L* 93.63 ± 0.01	**L*** 93.89 ± 0.01
	a* 0.22 ± 0.01	**a*** -0.23 ± 0.02
	b* 10.69 ± 0.02	**b*** 6.31 ± 0.02
ΔE (recto and verso)	4.45	
ΔSCI-SCE (recto)	0.86	

Photo-documentation

Normal light

UVA / visible fluorescence

Specular light

Raking light

Fibre identification

Herzberg | Lofton Merritt | Graff C

SEM

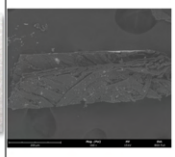

Composition

XRF:
Elements identified: S, Ca, Sr, Ag, Ba, Fe (Kα), K

SEM:
Topcoat: not analysed
Emulsion: not analysed
Baryta layer: Ba, S, Sr, Ca
Paper: Al, Si, S

Plastika G.2 K Rayon

Thickness: 0.28 ± 0.01 mm

Weight: 10.96 ± 0.01 g

Colourimetry:

Colour coordinates (SCE)	Recto	Verso
	L* 92.29 ± 0.01	**L*** 94.2 ± 0.01
	a* 0.21 ± 0	**a*** -0.36 ± 0.01
	b* 11.73 ± 0.02	**b*** 5.43 ± 0.01
ΔE (recto and verso)	6.61	
ΔSCI-SCE (recto)	0.83	

Photo-documentation

Normal light

UVA / visible fluorescence

Specular light

Raking light

Fibre identification

Herzberg | Lofton Merritt | Graff C

SEM

Composition

XRF:
Elements identified: S, Ca, Sr, Ag, Ba, Fe (Kα), K

Plastika P.2 K Cream Semi Matt

Thickness: 0.30 ± 0 mm

Weight: 11.01 ± 0.01 g

Colourimetry:

Colour coordinates (SCE)	Recto	Verso
	L* 88.78 ± 0.02	**L*** 92.07 ± 0.02
	a* 2.2 ± 0.02	**a*** 1.09 ± 0.01
	b* 19.51 ± 0.03	**b*** 13.32 ± 0.06
ΔE (recto and verso)	6.69	
ΔSCI-SCE (recto)	0.82	

Photo-documentation

Normal light

UVA / visible fluorescence

Specular light

Raking light

Fibre identification

Herzberg | Lofton Merritt | Graff C

SEM

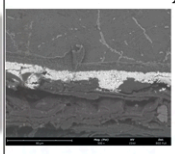

Composition

XRF:
Elements identified: S, Ca, Sr, Ag, Ba, Fe (Kα+ Kβ), K

SEM:
Top coat: Ag, S, Ca
Emulsion: Ag, S
Baryta layer: Ba, S, Sr
Paper: Al, Si

Plastika R.2 K Cream Matt

Thickness: 0.20 ± 0.01 mm

Weight: 11.59 ± 0.01 g

Colourimetry:

Colour coordinates (SCE)	Recto	Verso
	L* 90.99 ± 0.05	**L*** 91.89 ± 0.01
	a* 2.11 ± 0.01	**a*** 1.24 ± 0.01
	b* 16.37 ± 0.21	**b*** 14 ± 0.01
ΔE (recto and verso)	2.6	
ΔSCI-SCE (recto)	0.25	

Photo-documentation

Normal light

UVA / visible fluorescence

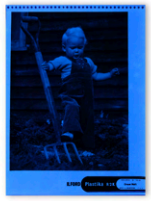

Specular light

Raking light

Fibre identification

Herzberg | Lofton Merritt | Graff C

SEM

Composition

XRF:
Elements identified: S, Ca, Sr, Ag, Ba, Fe (Kα+ Kβ), K

Plastika T.2 K Cream Grained Half Matt

Thickness: 0.29 ± 0.01 mm

Weight: 10.72 ± 0.01 g

Colourimetry:

Colour coordinates (SCE)	Recto	Verso
	L* 90.91 ± 0.01	**L*** 92.03 ± 0.03
	a* 2.08 ± 0.01	**a*** 0.87 ± 0.01
	b* 17.51 ± 0.06	**b*** 13.59 ± 0.03
ΔE (recto and verso)	4.25	
ΔSCI-SCE (recto)	0.49	

Photo-documentation

Normal light

UVA / visible fluorescence

Specular light

Raking light

Fibre identification

Herzberg | Lofton Merritt | Graff C

SEM

Composition

XRF:
Elements identified: S, Ca, Sr, Ag, Ba, Fe (Kα+ Kβ), K

Plastika V.2 K Cream Rayon

Thickness: 0.27 ± 0.01 mm

Weight: 11.63 ± 0.01 g

Colourimetry:

Colour coordinates (SCE)	Recto	Verso
	L* 88.85 ± 0.01	**L*** 91.18 ± 0.01
	a* 2.9 ± 0.02	**a*** 1.37 ± 0.01
	b* 17.74 ± 0.01	**b*** 16.65 ± 0.02
ΔE (recto and verso)	3	
ΔSCI-SCE (recto)	1.12	

Photo-documentation

Normal light

UVA / visible fluorescence

Specular light

Raking light

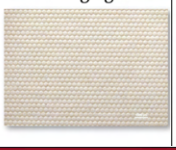

Fibre identification: Softwood bleached sulfite pulp

Herzberg | Lofton Merritt | Graff C

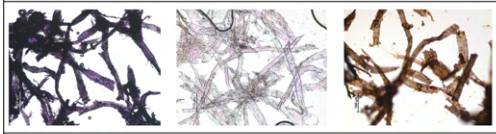

SEM

Composition

XRF:
Elements identified: S, Ca, Sr, Ag, Ba, Fe (Kα+ Kβ), K

Contact C.2. 1P Glossy

Thickness: 0.17 ± 0.01 mm

Weight: 7.67 ± 0.01 g

Colourimetry:

Colour coordinates (SCE)	Recto	Verso
	L* 88.94 ± 0.01	**L*** 93.84 ± 0.03
	a* 0.16 ± 0.01	**a*** -0.24 ± 0
	b* 4.01 ± 0.03	**b*** 4.35 ± 0.02
ΔE (recto and verso)	4.92	
ΔSCI-SCE (recto)	2.17	

Photo-documentation

Normal light

UVA / visible fluorescence

Specular light

Raking light

Fibre identification: Softwood bleached sulfite pulp

Herzberg | Lofton Merritt | Graff C

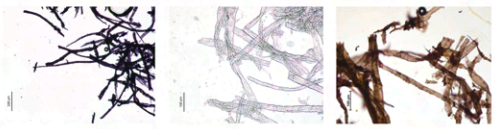

SEM

Composition

XRF:
Elements identified: S, Ca, Sr, Ag, Ba, Fe (Kα), K

Contact C.2. 51P Cream Glossy

Thickness: 0.17 ± 0.01 mm

Weight: 7.48 ± 0.01 g

Colourimetry:

Colour coordinates (SCE)	Recto	Verso
	L* 88.27 ± 0.02	**L*** 91.74 ± 0.03
	a* 3.2 ± 0.01	**a*** 2.36 ± 0.02
	b* 16.26 ± 0.03	**b*** 14.21 ± 0.05
ΔE (recto and verso)	4.11	
ΔSCI-SCE (recto)	2.2	

Photo-documentation

Normal light

UVA / visible fluorescence

Specular light

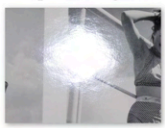

Raking light

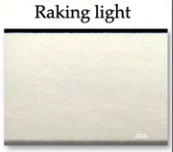

Fibre identification

Herzberg | Lofton Merritt | Graff C

SEM

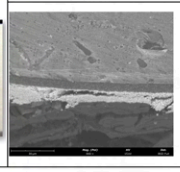

Composition

XRF:
Elements identified: S, Ca, Sr, Ag, Ba, Fe (Kα+ Kβ), K

SEM:
Topcoat: S, Ca, Ag
Emulsion: S, Ca, Ag, Ba
Baryta layer: Al, Si, S, Ag, Ba
Paper: Al, Si, S

Contact C.2. 25P Satin

Thickness: 0.20 ± 0.01 mm
Weight: 7.22 ± 0. g
Colourimetry:

Colour coordinates (SCE)	Recto	Verso
	L* 91.43 ± 0.02	**L*** 93.94 ± 0.01
	a* 0.05 ± 0.01	**a*** -0.22 ± 0.02
	b* 8.44 ± 0.06	**b*** 8.68 ± 0.03
ΔE (recto and verso)	2.53	
ΔSCI-SCE (recto)	1.05	

Photo-documentation

Normal light | UVA / visible fluorescence | Specular light | Raking light

Fibre identification: Softwood bleached sulfite pulp

Herzberg | Lofton Merritt | Graff C

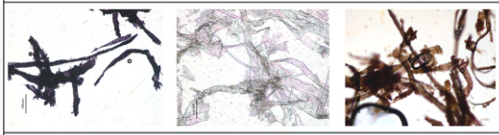

SEM | **Composition**

XRF:
Elements identified: S, Ca, Sr, Ag, Ba, Fe (Kα), K

Table B. 3 Multi-analytical characterisation results of the Kodak set

Polycontrast F (SW, White, Smooth, Glossy)

Thickness: 0.18 ± 0.01 mm
Weight: 2.09 ± 0.02 g
Colourimetry:

Colour coordinates (SCE)	Recto	Verso
	L* 91.75 ± 0.01	**L*** 93.67 ± 0.01
	a* -0.5 ± 0	**a*** -0.25 ± 0.01
	b* 6.22 ± 0.01	**b*** 7.35 ± 0.02
ΔE (recto and verso)	2.23	
ΔSCI-SCE (recto)	1.89	

Photo-documentation

Normal light | UVA / visible fluorescence | Specular light | Raking light

Fibre identification: Softwood bleached sulfite pulp mixed with hardwood bleached sulfite pulp

Herzberg | Lofton Merritt | Graff C

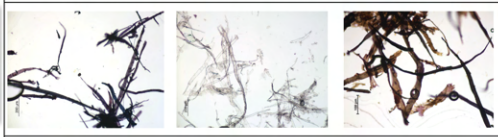

SEM | **Composition**

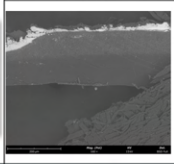

XRF:
Elements identified: S, Cl, Ca, Sr, Ag, Ba
SEM:
Top coat: Al, Si, S, Ag
Emulsion: not analysed
Baryta layer: Ba, S, Sr
Paper: -

Kodabormide A (LW, White, Smooth, Lustre)

Thickness: 0.12 ± 0.01 mm
Weight: 1.22 ± 0.01 g
Colourimetry:

Colour coordinates (SCE)	Recto	Verso
	L* 92.24 ± 0	**L*** 93.17 ± 0.03
	a* -0.63 ± 0.01	**a*** -0.15 ± 0
	b* 10.46 ± 0.01	**b*** 8.62 ± 0.04
ΔE (recto and verso)	2.11	
ΔSCI-SCE (recto)	0.86	

Photo-documentation

Normal light | UVA / visible fluorescence | Specular light | Raking light

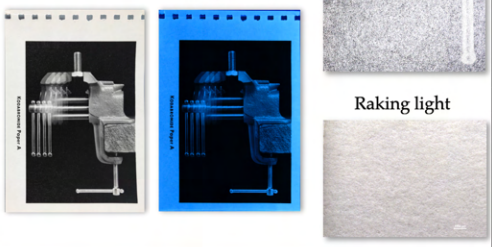

Fibre identification: Softwood bleached sulfite pulp

Herzberg | Lofton Merritt | Graff C

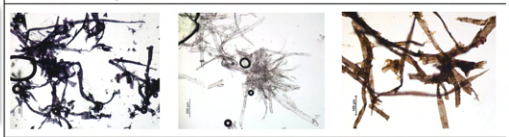

SEM | **Composition**

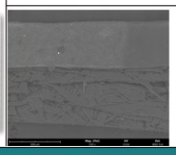

XRF:
Elements identified: S, Cl, Ca, Ag
SEM:
Top coat: Al, S, Ag
Emulsion: not analysed
Paper: -

Ektalure E (DW, Warm-white, Fine Grained, Lustre)

Thickness: 0.35 ± 0.01 mm
Weight: 3.52 ± 0.02 g
Colourimetry:

Colour coordinates (SCE)	Recto	Verso
	L* 93.3 ± 0.02	**L*** 94.7 ± 0.01
	a* -0.52 ± 0.01	**a*** -0.10 ± 0.01
	b* 8.29 ± 0.02	**b*** 7.77 ± 0.02
ΔE (recto and verso)	1.55	
ΔSCI-SCE (recto)	1.05	

Photo-documentation

Normal light | UVA / visible fluorescence | Specular light | Raking light

Fibre identification: Softwood bleached sulfite pulp

Herzberg | Lofton Merritt | Graff C

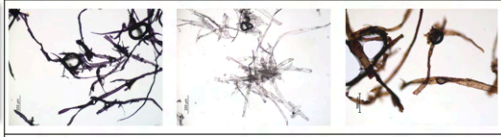

SEM | **Composition**

XRF:
Elements identified: S, Cl, Ca, Sr, Ag, Ba

Portalure G (DW, Warm-white, Fine Grained, Lustre)

Thickness: 0.35 ± 0.01 mm

Weight: 3.51 ± 0.01 g

Colourimetry:

Colour coordinates (SCE)	Recto	Verso
	L* 91.5 ± 0.02	**L*** 94.12 ± 0.01
	a* -0.64 ± 0.01	**a*** -0.08 ± 0.01
	b* 10.17 ± 0.02	**b*** 8.52 ± 0.05
ΔE (recto and verso)	3.15	
ΔSCI-SCE (recto)	0.93	

Photo-documentation

Normal light

UVA / visible fluorescence

Specular light

Raking light

Fibre identification: Softwood bleached sulfite pulp mixed with hardwood bleached sulfite pulp

Herzberg

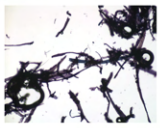

Lofton Merritt

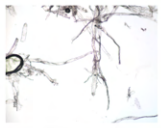

Graff C

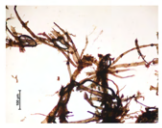

SEM

Composition

XRF:
Elements identified: S, Cl, Ca, Sr, Ag, Ba

Medalist J (DW, White, Smooth, High Lustre)

Thickness: 0.34 ± 0.01 mm

Weight: 3.49 ± 0 g

Colourimetry:

Colour coordinates (SCE)	Recto	Verso
	L* 91.03 ± 0.42	**L*** 93.18 ± 0.03
	a* -019 ± 0.07	**a*** 0.59 ± 0.01
	b* 6.19 ± 0.3	**b*** 9.47 ± 0.03
ΔE (recto and verso)	4	
ΔSCI-SCE (recto)	1.83	

Photo-documentation

Normal light

UVA / visible fluorescence

Specular light

Raking light

Fibre identification: Softwood bleached sulfite pulp

Herzberg

Lofton Merritt

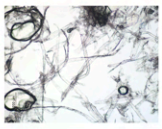

Graff C

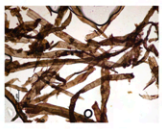

SEM

Composition

XRF:
Elements identified: S, Cl, Ca, Sr, Ag, Ba

Ektalure K (DW, Warm-white, Fine Grained, High Lustre)

Thickness: 0.35 ± 0.01 mm

Weight: 3.66 ± 0.01 g

Colourimetry:

Colour coordinates (SCE)	Recto	Verso
	L* 91.78 ± 0.02	**L*** 94.25 ± 0.01
	a* -0.53 ± 0	**a*** 0.06 ± 0.01
	b* 10.2 ± 0.03	**b*** 8.13 ± 0.02
ΔE (recto and verso)	3.28	
ΔSCI-SCE (recto)	1.88	

Photo-documentation

Normal light

UVA / visible fluorescence

Specular light

Raking light

Fibre identification: Softwood bleached sulfite pulp

Herzberg

Lofton Merritt

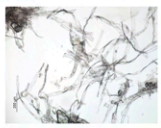

Graff C

SEM

Composition

XRF:
Elements identified: S, Cl, Ca, Sr, Ag, Ba

Portalure M (DW, Warm-white, Smooth, Matte)

Thickness: 0.31 ± 0.01 mm

Weight: 3.44 ± 0.02 g

Colourimetry:

Colour coordinates (SCE)	Recto	Verso
	L* 91.61 ± 0.03	**L*** 94.09 ± 0.01
	a* -0.4 ± 0	**a*** -0.15 ± 0.01
	b* 10.75 ± 0.01	**b*** 8.56 ± 0.01
ΔE (recto and verso)	3.31	
ΔSCI-SCE (recto)	0.21	

Photo-documentation

Normal light

UVA / visible fluorescence

Specular light

Raking light

Fibre identification: Softwood bleached sulfite pulp

Herzberg

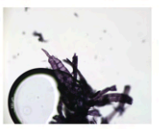

Lofton Merritt

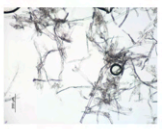

Graff C

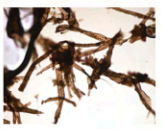

SEM

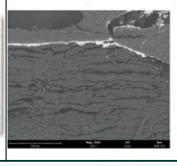

Composition

XRF:
Elements identified: Si, S, Cl, Ca, Sr, Ag, Ba

SEM:
Top coat: Al, Si, Ag, S
Emulsion: Al, Si, Ca, S, Ag, Ba
Baryta layer: Al, Si, Ba, S, Sr
Paper: -

Polycontrast Rapid N (SW, White, Smooth, Lustre)

Thickness: 0.17 ± 0.01 mm

Weight: 1.95 ± 0.02 g

Colourimetry:

Colour coordinates (SCE)	Recto	Verso
	L* 92.93 ± 0	**L*** 93.32 ± 0.04
	a* -0.36 ± 0.01	**a*** -018 ± 0.01
	b* 6.47 ± 0	**b*** 8.13 ± 0.01
ΔE (recto and verso)	1.72	
ΔSCI-SCE (recto)	0.5	

Photo-documentation

Normal light

UVA / visible fluorescence

Specular light

Raking light

Fibre identification: Softwood bleached sulfite pulp mixed with hardwood bleached sulfite pulp

Herzberg

Lofton Merritt

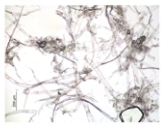

Graff C

SEM

Composition

XRF:
Elements identified: S, Cl, Ca, Sr, Ag, Ba

Mural R (SW, Cream, Tweed, Lustre)

Thickness: 0.2 ± 0.01 mm

Weight: 1.56 ± 0.02 g

Colourimetry:

Colour coordinates (SCE)	Recto	Verso
	L* 91.77 ± 0.02	**L*** 93.66 ± 0
	a* -0.52 ± 0	**a*** -0.37 ± 0.01
	b* 10.41 ± 0.02	**b*** 7.83 ± 0.01
ΔE (recto and verso)	3.2	
ΔSCI-SCE (recto)	0.45	

Photo-documentation

Normal light

UVA / visible fluorescence

Specular light

Raking light

Fibre identification: Softwood bleached sulfite pulp mixed with hardwood bleached sulfite pulp

Herzberg

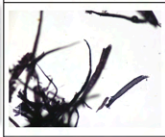

Lofton Merritt

Graff C

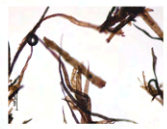

SEM

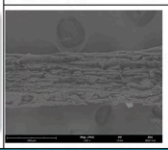

Composition

XRF:
Elements identified: S, Cl, Ca, Ag

SEM:
Top coat: not analysed
Emulsion: Al, S, Ca, Ag
Paper: -

Ektalure X (DW, Cream, Tapestry, Lustre)

Thickness: 0.34 ± 0.01 mm

Weight: 3.16 ± 0 g

Colourimetry:

Colour coordinates (SCE)	Recto	Verso
	L* 93.01 ± 0.03	**L*** 93.99 ± 0.01
	a* 0.15 ± 0.01	**a*** 0.46 ± 0
	b* 10.95 ± 0.05	**b*** 10.48 ± 0.02
ΔE (recto and verso)	1.13	
ΔSCI-SCE (recto)	0.5	

Photo-documentation

Normal light

UVA / visible fluorescence

Specular light

Raking light

Fibre identification: Softwood bleached sulfite pulp mixed with hardwood bleached sulfite pulp

Herzberg

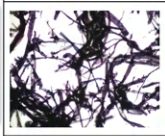

Lofton Merritt

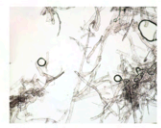

Graff C

SEM

Composition

XRF:
Elements identified: S, Cl, Ca, Sr, Ag, Ba

Portalure Y (DW, Warm-white, Silk, High Lustre)

Thickness: 0.3 ± 0.01 mm

Weight: 3.8 ± 0.01 g

Colourimetry:

Colour coordinates (SCE)	Recto	Verso
	L* 92.23 ± 0.01	**L*** 93.92 ± 0.02
	a* -0.6 ± 0	**a*** -0.04 ± 0
	b* 9.37 ± 0.02	**b*** 9.10 ± 0.05
ΔE (recto and verso)	1.8	
ΔSCI-SCE (recto)	1.06	

Photo-documentation

Normal light

UVA / visible fluorescence

Specular light

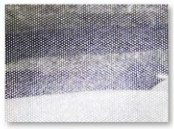

Raking light

Fibre identification: Softwood bleached sulfite pulp

Herzberg

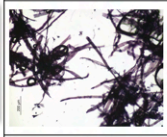

Lofton Merritt

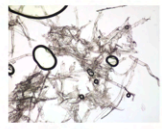

Graff C

SEM

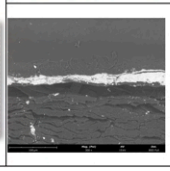

Composition

XRF:
Elements identified: S, Cl, Ca, Sr, Ag, Ba

SEM:
Top coat: Al, S, Ag
Emulsion: Ag, S
Baryta layer: Al, S, Sr, Ba
Paper: -

B.3 UV-induced visible fluorescence - verso

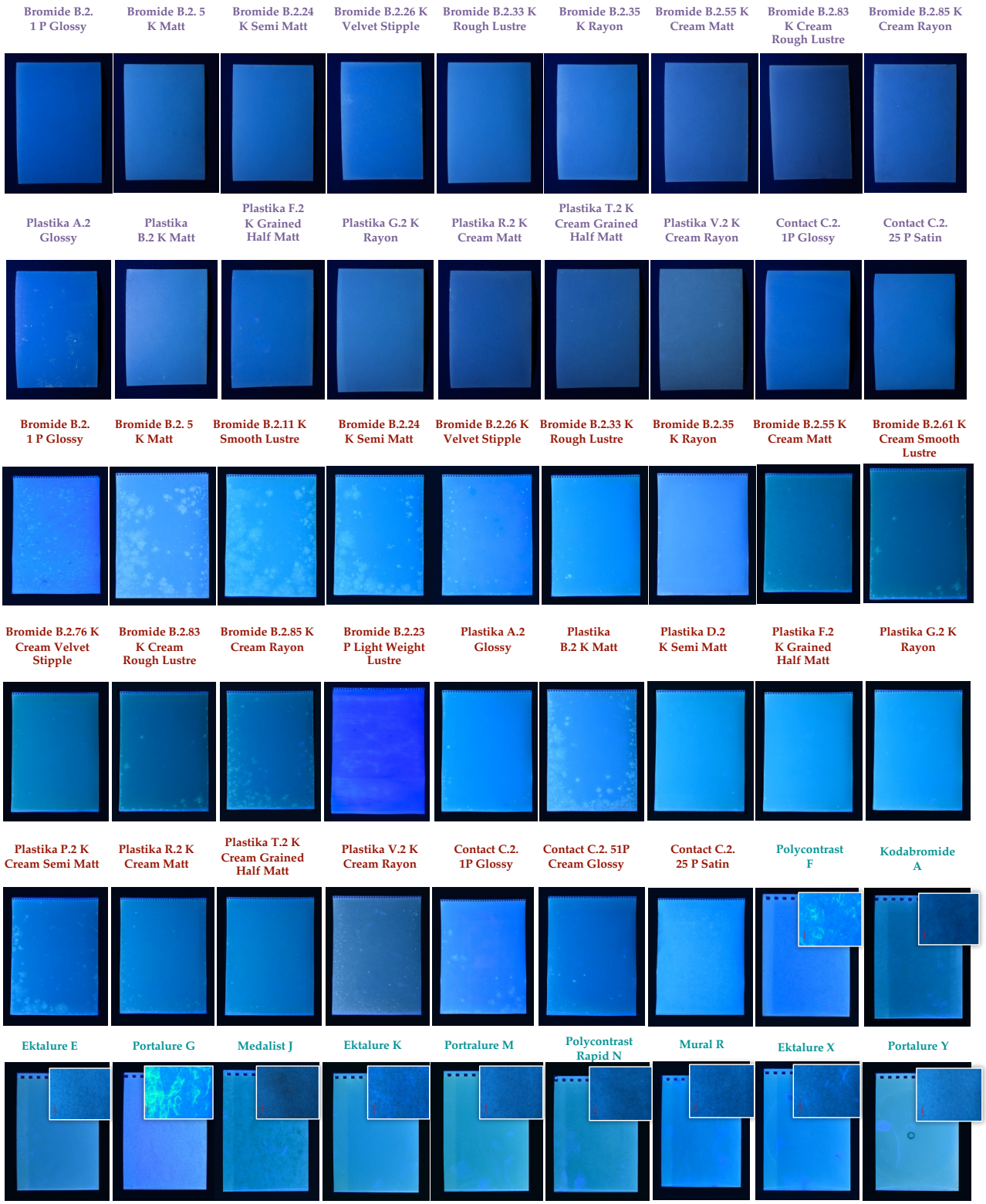

Figure B. 5 UV-induced visible fluorescence photo-documentation of prints' verso